Title
Selection Rules for the Nonlinear Interactions of Internal Gravity Waves and Inertia-Gravity Waves

Author
Jiang, Chung-Hsiang

Publication Date
2010

Peer reviewed|Thesis/dissertation

Selection Rules for the Nonlinear Interactions of Internal Gravity Waves and Inertia-Gravity Waves

by

Chung-Hsiang Jiang

A dissertation submitted in partial satisfaction of the
requirements for the degree of
Doctor of Philosophy

in

Engineering - Mechanical Engineering

in the

Graduate Division
of the
University of California, Berkeley

Committee in charge:
Professor Philip S. Marcus, Chair
Professor Ömer Savaş
Professor Mark Stacey

Fall 2010

Selection Rules for the Nonlinear Interactions of Internal Gravity Waves and Inertia-Gravity Waves

Abstract

Selection Rules for the Nonlinear Interactions of Internal Gravity Waves and Inertia-Gravity Waves

by

Chung-Hsiang Jiang
Doctor of Philosophy in Engineering - Mechanical Engineering

University of California, Berkeley

Professor Philip S. Marcus, Chair

Perturbation methods are used to calculate nonlinear interaction of waves, however most analyses skip the question as to whether the zeroth order solutions exist. The dispersion relation for internal gravity waves does *not* relate the magnitude of the wave vector and its frequency, rather it relates the frequency and *direction* of the wave vector. Thus, spatially columnated beams of internal waves are made of a continuum of plane waves with different wavelengths, but the same magnitude of frequency. For two parent beams to create a daughter, the plane waves within the parent and daughter beams must obey the triad condition (the spatial wave vector of the daughter equals the sum of the parents' vectors, and temporal frequency of the daughter equals the sum of the parents' frequencies) and the dispersion relation. Contrary to what is assumed implicitly, these conditions cannot always be satisfied. If they could, then the interaction of two beams of gravity waves would produce 8 daughter beams, consisting of two St. Andrew's crosses (each with 4 beams). The beams in one cross have a frequency equal to the sum of the frequencies of the parents and the beams in the other have a frequency equal to the difference. At least two daughter beams cannot exist for each cross according to the selection rules derived in this work.

Similar selection rules are obtained for the interaction among inertia-gravity conical waves. When two parent conical waves intersect, unlike the two-dimensional beams, the interaction area is not a single point. The intersection produces spatial continuous curves and there are no more than two intersection points in any horizontal plane with a normal vector parallel to gravity direction. Each intersection point is acted like the collision point of two-dimensional beam-beam interaction. As a result, *at most two harmonic beams* with a frequency either equal to the sum of the frequencies of the parents or to the difference, *not a conical wave*, are produced from the nonlinear interaction.

This work is dedicated to my parents and my sister.

Contents

List of Figures

List of Tables

Acknowledgments

I am not good at writing emotional stuff so this page would be pretty short. Thank you to my family especially my brother-in-law who takes care of my parents when I was absent. Thank you to my friends and labmates like Chunyi Liu, Jia-Long Wu, Yao-Jung Wen, Ming-Tsang Lee, Wei-Chun Kuo, Shiang-Lung Koo, Kang Li, Xylar Asay-Davis, Sushil Shetty, Jean Toilliez and Joseph Barranco. Just to name a few because there really are too many to name. And thank you to Profs. Philip S. Marcus, Ömer Savaş and Mark Stacey for approving this dissertation.

Chapter 1

Introduction

The internal gravity wave or inertia-gravity wave (IGW, in short) research can be traced back to the 1890s (Love, 1891). The early theoretical studies are summarized in Lamb's famous 1932 book. In (Mowbray and Rarity, 1967), the oscillating bar experiments were conducted to show four, columnated outgoing internal gravity wave beams in an "X" pattern a.k.a. the St. Andrew's cross and to test the linear theory of the internal gravity waves in a stably stratified background fluid. The oceanographers are more interested in the creation and reflection of the internal gravity wave from sloping topography since it provides, at least theoretically, a way to transfer energy and to possibly increase the mixing efficiency near the seabed. (Alford, 2003) states that in order to trigger the Earth's meridional overturning circulation (MOC), order of 2 TW (an arguable number) of power is needed to turbulently warm the abyssal waters and IGW could offer about 0.7 TW. Together with other energy sources, wind input ($\sim$ 1 TW available) and near-inertial waves (estimated to be $\sim$ 0.5 TW), it seems to be enough to start MOC. (Alford, 2003) and papers cited in it revived the interest of IGW in oceanography. Studies about the creation and reflection of internal gravity waves from complex bottom topography in the ocean and reflection from a flat bottom seafloor (Lamb, 2004; Gerkema et al., 2006) show that it is fairly easy to generate internal gravity waves from the tidal flow with M2 frequency passing through topography. The higher harmonics that their frequency is the multiple of the tidal frequency are also observed in these studies. From FIG. 2(b) in (Lamb, 2004) and FIG. 1 and FIG. 2(b) in (Gerkema et al., 2006), the numerical simulations show that the reflection from the flat ocean floor also generates beams with frequency M4 (M4 equals to twice the M2 frequency) or even higher harmonics (triple or quadruple of M2 frequency). The reflection is found to be asymmetric since the harmonic beams prefer certain direction (on the same side of the reflected beam) instead of emitting on both incoming and reflected beam side to form the top half of the St. Andrew's cross. Similarly, an asymmetry is also found in the super- or sub-critical reflection from a constant slope experiments, (Peacock and Tabaei, 2005; Zhang et al., 2008). The second-harmonic waves (twice the oscillating object frequency) are spotted only in the super-critical reflection experiments, see FIG. 2 in (Peacock and Tabaei, 2005) but are missing in the sub-critical case, see also FIG. 4 in (Peacock and Tabaei, 2005). Another

example shows the asymmetry is the permitted and forbidden formation of second-harmonic waves from colliding beams with identical properties except the relative position difference with respect to the collision region, see (Fig. 4.1(a)) and (Fig. 4.1(b)). In (van Haren and Millot, 2004; van Haren, 2005, 2006), the authors pointed out enhanced poleward diurnal (or local inertial frequency) energy transfer in $28 - 30^\circ$ north and a drop of semidiurnal energy in $25 - 27^\circ$ north where the latitude is around the diurnal critical latitude (local Coriolis parameter equals to diurnal tidal frequency).

In general, the methodologies in current studies of internal gravity or inertia-gravity waves in the ocean are divided into two categories. One is to use numerical simulations. Either plug in the real bathymetry, real buoyancy frequency profile and modelling tidal currents into the GCM (General Circulation Model) with lower spatial resolution or have a modelling two-dimensional topography but with higher resolution to emulate the IGW generated from tidal current passing through topography. And the other one is to analyze the observation data from moorings, topography arrays or satellite altimetry to obtain spectral information, sea surface height (SSH) and depth-integrated energy flux. Both approaches show their own complexities and hide the fundamental properties of the nonlinear interactions of internal gravity or inertia-gravity waves.

In (Tabaei et al., 2005), the authors noticed this lacking of fundamentals drawback and tried to resolve it by using the small amplitude perturbation analysis to solve the reflecting and colliding internal gravity wave beams problem. They pointed out the higher harmonic beams are generated from the nonlinear interactions in the vicinity of interaction region. The asymmetry seemed to be noticed by the authors but the prediction of the asymmetry is not correct in several different configurations in colliding beams problem probably due to the distraction of the complicated perturbation analysis. And the perturbation analysis is probably way too difficult and tedious to extend to solve three-dimensional inertia-gravity waves.

The idea that "the higher harmonic beams are generated from the nonlinear interactions of two colliding beams" leads to famous nonlinear constraints:

$$\mathbf{k}_1 \pm \mathbf{k}_2 = \mathbf{k}^{\mathrm{H}},$$
$$\omega_1 \pm \omega_2 = \omega^{\mathrm{H}},$$

where the first beam has frequency ω_1, wavevector $\mathbf{k}_1$, the second beam has frequency ω_2, wavevector $\mathbf{k}_2$ and the harmonic has frequency ω^{H}, wavevector $\mathbf{k}^{\mathrm{H}}$. The nonlinear constraints are formally the same as equations imposed by "resonant triad interaction" which have been studied in numerous articles, e.g. (Phillips, 1967). Actually, it is the lack of using geometric form of the dispersion relation to connect components of individual wave vectors (i.e. extra constraint) delays the discovery of selection rules derived in this work. Also in (Phillips, 1967), the author pointed out that "... the resonant interactions occurs at the third order, and only among components whose wavenumbers form a quadrilateral ...". This implies that the interaction between three wave vectors is "forbidden" and actually can be treated as an example of selection rule.

Based on the knowledge that the higher harmonic beams are generated from the nonlinear interactions, (Jiang and Marcus, 2009) used the geometry (orientations of incoming beams), linear dispersion relations for individual incoming and outgoing beams, radiation conditions for outgoing beams and nonlinear interactions as constraints to show that there are selection rules determining the permitted or forbidden generations of harmonic beams for two colliding internal gravity wave beams with no rotational effect. The selection rules are derived in a clever way without solving any partial differential equations and therefore are easier to extend to three-dimensions or including Coriolis effect. In this dissertation, the same methodology, geometry and algebra only and no PDE solving, is extended to cover quasi-two-dimensional and three-dimensional inertia-gravity waves, too. In chapter 2, the general equation of motion of a three-dimensional Boussinesq flow is specified with a general Coriolis parameter, $\mathbf{f} = f_x\mathbf{x} + f_y\mathbf{y} + f_z\mathbf{z}$. In chapter 3, the simplest two-dimensional without any rotational effect case, i.e. internal gravity waves discussed in (Jiang and Marcus, 2009), is briefly reviewed. In chapter 4, a simple Coriolis parameter, $\mathbf{f} = f_z\mathbf{z}$ is added but the flow is kept quasi-two-dimensional, $k_y = 0$. The nonlinear interaction of two inertia-gravity wave beams is studied. In chapter 5, the quasi-two-dimensional constraint is relaxed. The collision of two conical inertia-gravity waves is being studied. In chapter 6, another quasi-two-dimensional inertia-gravity waves problem is studied but this time with a general $\mathbf{f}$.

Chapter 2

Governing Equations for Internal Gravity and Inertia-Gravity Waves

In order to analyze the interactions among internal gravity, inertia-gravity wave beams or more general conical, three-dimensional internal gravity, inertia-gravity waves, consider the inviscid, constant Brunt-Väisälä frequency, Boussinesq flow. The stratification is chosen to be in the simplest form because the focus is on the rotational effect side. The Coriolis parameter therefore ranges from simplest form $\mathbf{f} = f_z\mathbf{z}$ to more general $\mathbf{f} = f_x\mathbf{x} + f_y\mathbf{y} + f_z\mathbf{z}$ where all the components of $\mathbf{f}$ are constant.

The governing equations written in primitive variables form are

$$\begin{aligned}
\frac{\partial \mathbf{v}}{\partial t} &= -\mathbf{v}\cdot\nabla\mathbf{v} - \frac{\nabla\tilde{P}}{\rho_0} - \frac{\tilde{\rho}}{\rho_0}g\hat{\mathbf{z}} + \mathbf{v}\times\mathbf{f}, \\
\frac{\partial \tilde{\rho}}{\partial t} &= -\mathbf{v}\cdot\nabla\tilde{\rho} - v_z\frac{d\bar{\rho}(z)}{dz}, \\
\nabla\cdot\mathbf{v} &= 0,
\end{aligned}$$

where ρ_0 is a constant referential density, e.g. $(\int_{-L_z}^{L_z}\bar{\rho}(z')dz')/2L_z$ or $\bar{\rho}(z=0)$. The base state of the Boussinesq approximation is $\bar{\mathbf{v}} = \mathbf{0}$, $\bar{\rho} = \bar{\rho}(z)$ and $\bar{P} = \bar{P}(z)$ which is in hydrostatic equilibrium, $d\bar{P}(z)/dz = -\bar{\rho}(z)g$.

The linear plane wave dispersion relation is derived by using the linearized version of

the Boussinesq flow written in component form,

$$\begin{aligned}
\frac{\partial v_x}{\partial t} &= (f_z\, v_y - f_y\, v_z) - \frac{\partial h}{\partial x}, \\
\frac{\partial v_y}{\partial t} &= (f_x\, v_z - f_z\, v_x) - \frac{\partial h}{\partial y}, \\
\frac{\partial v_z}{\partial t} &= (f_y\, v_x - f_x\, v_y) - \frac{\partial h}{\partial z} - \frac{\tilde{\rho}}{\rho_0} g, \\
\frac{\partial \tilde{\rho}}{\partial t} &= -v_z \frac{d\bar{\rho}(z)}{dz}, \\
0 &= \frac{\partial v_x}{\partial x} + \frac{\partial v_y}{\partial y} + \frac{\partial v_z}{\partial z},
\end{aligned}$$

where $h \equiv \tilde{P}/\rho_0$.

Assume each variable, $\tilde{\rho}$, $\mathbf{v}$ and h, can be written in the following form for specific $\mathbf{k}_\perp \equiv (k_x, k_y)$ and frequency ω,

$$\begin{aligned}
\tilde{\rho} &\to \hat{\rho}(z)\; e^{ik_x x}\; e^{ik_y y}\; e^{-i\omega t}, \\
\mathbf{v} &\to \hat{\mathbf{v}}(z)\; e^{ik_x x}\; e^{ik_y y}\; e^{-i\omega t}, \\
h &\to \hat{h}(z)\; e^{ik_x x}\; e^{ik_y y}\; e^{-i\omega t}.
\end{aligned}$$

The flow is doubly periodic in the horizontal directions but in vertical direction either slip (rigid-lid, free surface) or periodic boundary conditions are valid. Substituting above variables into the linearized governing equations leads to the following equation set,

$$\begin{aligned}
-i\omega \hat{v}_x &= f_z\, \hat{v}_y - f_y\, \hat{v}_z - ik_x\, \hat{h}, \\
-i\omega \hat{v}_y &= f_x\, \hat{v}_z - f_z\, \hat{v}_x - ik_y\, \hat{h}, \\
-i\omega \hat{v}_z &= f_y\, \hat{v}_x - f_x\, \hat{v}_y - \frac{d\hat{h}}{dz} - \frac{\hat{\rho}}{\rho_0} g, \\
-i\omega \hat{\rho} &= -\frac{d\bar{\rho}}{dz} \hat{v}_z, \\
0 &= ik_x \hat{v}_x + ik_y \hat{v}_y + \frac{d\hat{v}_z}{dz}.
\end{aligned}$$

$\hat{v}_x$, $\hat{v}_y$ and $\hat{v}_z$ can be expressed in terms of $\hat{h}$ and $d\hat{h}/dz$ only and the incompressible flow constraint therefore turns out to be a second order ordinary differential equation of variable $\hat{h}$,

$$\begin{aligned}
\left(\omega^2 - f_z^2\right) \frac{d^2\hat{h}}{dz^2} &- 2\, f_z \left(ik_x\, f_x + ik_y\, f_y\right) \frac{d\hat{h}}{dz} \\
&+ \left\{ \left(k_x^2 + k_y^2\right) \left(N^2 - \omega^2\right) + \left(k_x\, f_x + k_y\, f_y\right)^2 \right\} \hat{h},
\end{aligned}$$

where Brunt-Väisälä frequency is defined as $N^2 \equiv (-g/\rho_0)\,(d\bar{\rho}/dz)$.

If $\hat{h}$ has eigenfunctions with eigenvalues k_z's, the linear dispersion relation for three-dimensional inertia-gravity wave is

$$\omega^2 = \frac{k_\perp^2}{k^2} N^2 + \frac{(\mathbf{k}\cdot\mathbf{f})^2}{k^2}, \tag{2.1}$$

where $\mathbf{k}_\perp \equiv k_x\,\mathbf{x} + k_y\mathbf{y}$, $\mathbf{k} \equiv \mathbf{k}_\perp + k_z\,\mathbf{z}$, $k_\perp^2 = \mathbf{k}_\perp \cdot \mathbf{k}_\perp$ and $k^2 = \mathbf{k}\cdot\mathbf{k} = k_\perp^2 + k_z^2$.

If the Coriolis parameter is in the simplest form, $\mathbf{f} = f_z\mathbf{z} = f\mathbf{z}$, the dispersion relation reduces to

$$\omega^2 = \frac{k_\perp^2}{k^2} N^2 + \frac{k_z^2}{k^2} f^2. \tag{2.2}$$

For the three-dimensional internal gravity waves, the dispersion relation can be simplified furthermore since $f_z = 0$

$$\omega^2 = \frac{k_\perp^2}{k^2} N^2, \tag{2.3}$$

and the dispersion relation for the special case two-dimensional internal gravity wave,

$$\omega^2 = \frac{k_x^2}{k^2} N^2, \tag{2.4}$$

where $k^2 = k_x^2 + k_z^2$.

Chapter 3

Selection Rules for Quasi-Two-Dimensional Internal Gravity Waves

3.1 Introduction

The internal gravity wave (IGW, in short) research can be traced back to the 1890s (Love, 1891). The early theoretical studies are summarized in Lamb's famous 1932 book. In (Mowbray and Rarity, 1967), the oscillating bar experiments were conducted to show four, columnated outgoing internal gravity wave beams in an "X" pattern a.k.a. the St. Andrew's cross and to test the linear theory of the internal gravity waves in a stably stratified background fluid. The oceanographers are more interested in the creation and reflection of the internal gravity wave from sloping topography since it provides, at least theoretically, a way to transfer energy away from the generation sites [in $\mathcal{O}(1000$ km)] and to possibly increase the mixing efficiency in the deep sea. (Alford, 2003) states that in order to trigger the Earth's meridional overturning circulation (MOC), order of 2 TW (an arguable number) of power is needed to turbulently warm the abyssal waters and IGW could offer about 0.7 TW. Together with other energy sources, wind input ($\sim$ 1 TW available) and near-inertial waves (estimated to be $\sim$ 0.5 TW), it seems to be enough to start MOC. (Alford, 2003) and papers cited in it revived the interest of IGW in oceanography. Studies about the creation and reflection of internal gravity waves from complex bottom topography in the ocean and reflection from a flat bottom seafloor (Lamb, 2004; Gerkema et al., 2006) show that it is fairly easy to generate internal gravity waves from the tidal flow with M2 frequency passing through topography. The higher harmonics that their frequency is the multiple of the tidal frequency are also observed in these studies. From FIG. 2(b) in (Lamb, 2004) and FIG. 1 and FIG. 2(b) in (Gerkema et al., 2006), the two-dimensional or quasi-two-dimensional numerical simulations show that the reflection from the flat ocean floor also generates beams with frequency M4 (M4 equals to twice the M2 frequency) or even higher harmonics (triple or quadruple of M2

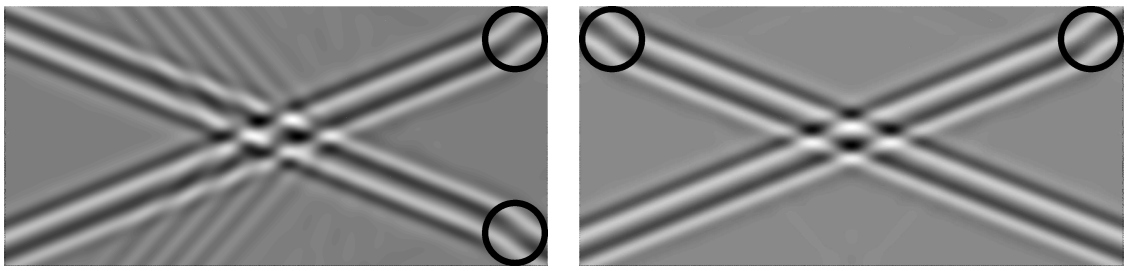

(a) (b)

Figure 3.1 Numerical simulations of physical beams, shown by the magnitude of their vertical velocities. Each primary beam has frequencies of $\pm\omega$ with $|\omega|/N = 0.3746 < 1/2$. (a) (left) The primary beam sources lie within the circles in the corners on the right side of the panel. Both primary beams propagate to the left, interact, and create two harmonic beams or "legs" with frequencies $\pm 2\omega$. (b) (right) As in (a), but with sources at the top. No harmonic beams are produced.

frequency). The reflection is found to be asymmetric since the harmonic beams prefer certain directions (on the same side of the reflected beam) instead of emanating on both incident and reflected beam side to form the top half of the St. Andrew's cross. Similarly, the asymmetry has also been found in the super- or sub-critical reflection from a slope, (Peacock and Tabaei, 2005; Zhang et al., 2008). The second-harmonic waves (twice the oscillating object frequency) are spotted only in the super-critical reflection experiments, see FIG. 2 in (Peacock and Tabaei, 2005) but are missing in the sub-critical case, see also FIG. 4 in (Peacock and Tabaei, 2005). Another example shows the asymmetry is the permitted and forbidden formation of second-harmonic waves from two-dimensional or quasi-two-dimensional colliding beams with identical properties except the relative position difference with respect to the collision region, see two-dimensional example (Fig. 3.1) and quasi-two-dimensional example (Fig. 4.1) in Chapter 4. In (Tabaei et al., 2005), the authors used the small amplitude perturbation analysis to solve the reflecting and colliding beams problem and pointed out the higher-harmonic beams are generated from the nonlinear interactions in the vicinity of interaction region. The asymmetry seemed to be noticed by the authors but the predictions of the asymmetry are not correct in several different colliding configurations probably due to the distraction of the complicated perturbation analysis. The selection rules introduced in this and next chapter are able to explain the asymmetry without actually solving the partial differential equations and show that geometry plus dispersion relation of IGW are enough to identify the asymmetry found in two-dimensional or quasi-two-dimensional problems.

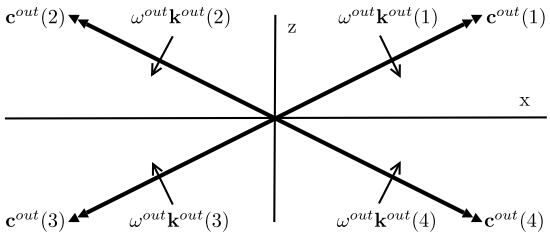

Figure 3.2 In each quadrant, the phase velocity and group velocity need to pair up in specific orientations in order to satisfy [Eqs. (3.1) and (3.2)].

3.2 Nonlinear Interaction of Internal Gravity Waves

A 2-dimensional, compact source of gravity waves oscillating at frequency $\pm\omega$ creates four, columnated outgoing beams in an "X" pattern, as in (Fig. 3.2), known as a "St. Andrew's cross" (Kundu and Cohen, 2004). There are four beams because the angle θ of each beam with respect to the positive x-axis (horizontal) obeys the dispersion relation, written in geometrical form, as

$$\frac{|\omega|}{N} = |\sin\theta|\,, \tag{3.1}$$

where $N \equiv \sqrt{-g(d\bar{\rho}/dz)/\rho_0}$ is the Brunt-Väisälä frequency, $d\bar{\rho}/dz$ is the horizontally-averaged vertical (z) density gradient of the unperturbed fluid, g is the acceleration of gravity, and ρ_0 is the average density.

A wave beam consists of a packet of complex conjugate pairs of plane waves $e^{i(k_x x + k_z z + \omega t)}$ with a continuum of wave numbers constrained such that all of the waves' group velocity vectors $\mathbf{c}$ are parallel and point in the same direction. From [Eq. (3.1)] the absolute value of the frequencies of all plane waves in a beam must be the same. To derive selection rules it is important to understand the relative directions of the group velocity vector $\mathbf{c}$ and wave vector $\mathbf{k}$. For internal gravity waves:

$$\text{sgn}\,\{c_x\} = \text{sgn}\,\{\omega\, k_x\}, \tag{3.2a}$$

$$\text{sgn}\,\{c_z\} = -\,\text{sgn}\,\{\omega\, k_z\}. \tag{3.2b}$$

To prove [Eq. (3.2)], note that the dispersion relation written in its traditional form is (Kundu and Cohen, 2004)

$$\omega = \pm N\frac{k_x}{k}. \tag{3.3}$$

This dispersion relation and the definition $\mathbf{c} \equiv \nabla_{\mathbf{k}}\omega$ show

$$\omega\, k_x = c_x k^2 \left(\frac{k_x}{k_z}\right)^2, \tag{3.4a}$$

$$\omega\, k_z = -c_z k^2. \tag{3.4b}$$

which proves $\mathbf{k}\cdot\mathbf{c} = 0$ and relations (3.2a) and (3.2b). The definition of θ and [Eq. (3.4)] show that for all beams:

$$\cot\theta \equiv \frac{c_x}{c_z} = -\frac{k_z}{k_x}. \tag{3.5}$$

Note that [Eq. (3.1)] follows from Eqs. (3.3) and (3.5). Eqs. (3.3) and (3.4) show that we must exclude the case when $\omega = 0$ (i.e. $\theta = 0$, or π) because no plane waves exist and also the case when $|\omega| = N$ (i.e., $\theta = \pm\pi/2$) because $\mathbf{c} = \mathbf{0}$, and we are only interested in propagating beams.

Although a beam of waves consists of complex conjugate pairs of plane waves, so both positive and negative frequencies are present, here we begin a thought experiment in which the waves in a beam have only a positive or a negative frequency. Consider the interaction of two of these beams. Because the linearized equations of motion for stratified gravity waves (Kundu and Cohen, 2004) are reflection-symmetric about both the x and z axes, we let one beam, labeled as the 0^{th} beam, approach the origin from the first quadrant. We use the notation that it has frequency $\omega^{in}(0)$, wave vector $\mathbf{k}^{in}(0)$, angle $\theta^{in}(0)$, and group velocity $\mathbf{c}^{in}(0)$ pointing toward the origin. At the origin this beam intersects a second beam, also pointing toward the origin, with frequency $\omega^{in}(j)$, wave vector $\mathbf{k}^{in}(j)$, group velocity $\mathbf{c}^{in}(j)$, and angle $\theta^{in}(j)$ with $j = 1$, 2, 3, or 4. We use the notation that j is the quadrant that contains the source of the second beam. Due to the fact that the inviscid, linearized equations of motion for gravity waves are reversible in time, without loss of generality, we let $\omega^{in}(0)$ be positive, and by using the reflection symmetries we can require that $\omega^{in}(0) \geq |\omega^{in}(j)|$ for $j = 1, \ldots, 4$.

Similarly, the four harmonic outgoing beams generated at the origin ((Fig. 3.2)) have frequency ω^{out}, wave vector $\mathbf{k}^{out}(n)$, group velocity, $\mathbf{c}^{out}(n)$, and angle $\theta^{out}(n)$, where n is the quadrant that the beam propagates into, and $n = 1, \ldots, 4$. Because the outgoing waves in the n^{th} beam are generated from the waves in the incoming 0^{th} and j^{th} beams by quadratic nonlinearities:

$$\omega^{out} = \omega^{in}(0) + \omega^{in}(j), \tag{3.6a}$$

$$\mathbf{k}^{out}(n) = \mathbf{k}^{in}(0) + \mathbf{k}^{in}(j). \tag{3.6b}$$

Note that ω^{out} is independent of the quadrant n of the outgoing beam.

Using Eqs. (3.1) and (3.6a), we obtain

$$\cot[\theta^{out}(n)] = (-1)^{n+1}\sqrt{(N/\omega^{out})^2 - 1}. \tag{3.7}$$

The sign in [Eq. (3.7)] is obtained from geometry, which requires $\text{sgn}\{\cot[\theta^{out}(n)]\} = (-1)^{n+1}$.

From Eqs. (3.5) and (3.6b):

$$k_z^{in}(0) + k_z^{in}(j) = -\cot[\theta^{out}(n)]\left(k_x^{in}(0) + k_x^{in}(j)\right). \tag{3.8}$$

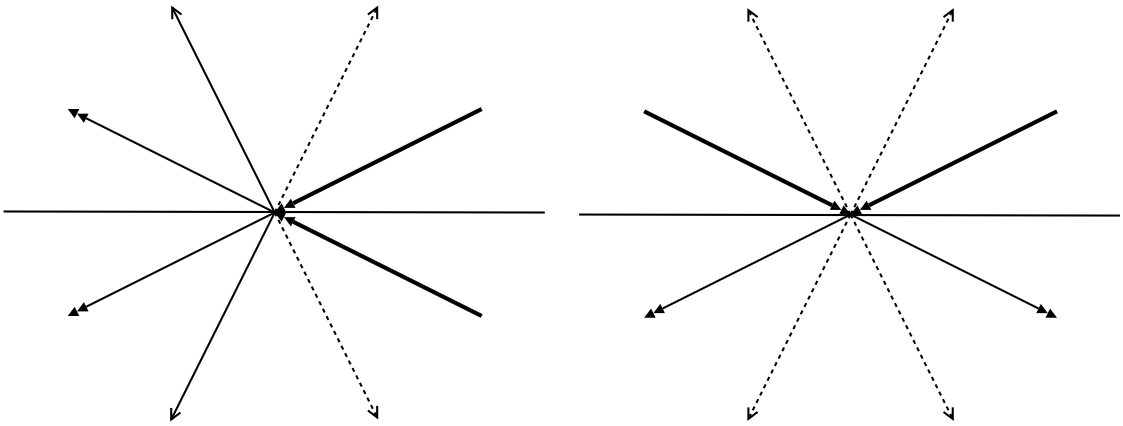

Figure 3.3 Schematic of permitted and forbidden formation of primary beams forcing at single frequency: The thick double-headed arrows represent colliding primary beams before collision, thin double-headed arrows represent colliding primary beams after collision, thin solid single-headed arrows represent permitted secondary harmonic beams and dotted single-headed arrows represent forbidden secondary harmonic beams. (a) (left) Permitted formation. Two harmonic beams with frequencies $\pm 2\omega$ are created. (b) (right) Forbidden formation. No harmonic beams are produced.

3.2.1 Two Simple Examples to Illustrate the Methodology

We would like to explain the methodology by using two examples, (Fig. 3.1(a)) and (Fig. 3.1(b)), first. In both examples, the two incoming beams are forced at the same frequency ω^{in} such that the $\omega^{out}(n)$ is twice the ω^{in}. The case that $\omega^{in}(0) = -\omega^{in}(j)$ produces $\omega^{out} \equiv 0$ which is not a propagating wave and hence it is not being considered here. In both examples, we only need to consider the formation of one St. Andrew's cross.

In the first example, the two beams collide and form a configuration that one of the incoming beams propagates upward ($j = 4$) and the other downward ($j = 0$). Thus we simplify the notations using $\omega^{in}(0) = \omega^{in}(4) = \omega^{in}$ and $\omega^{out} = 2\omega^{in}$. See the schematic, (Fig. 3.3(a)), for illustration.

Using [Eq. (3.5)] to relate the x-components of $\mathbf{k}^{in}(0)$ and $\mathbf{k}^{in}(4)$ in terms of their z-components in [Eq. (3.6b)] and vice versa. Then multiplying both sides of [Eq. (3.8)] with

ω^{in} leads to

$$\underbrace{\underbrace{[\omega^{in}\,k_z^{in}(0)]}_{>0}\,\underbrace{\frac{1-\cot[\theta^{out}(n)]\tan[\theta^{in}(0)]}{1-\cot[\theta^{out}(n)]\tan[\theta^{in}(4)]}}_{>0}}_{>0} = \underbrace{-\underbrace{[\omega^{in}\,k_z^{in}(4)]}_{<0}}_{>0},$$

$$\underbrace{\underbrace{[\omega^{in}\,k_x^{in}(0)]}_{<0}\,\underbrace{\frac{1-\tan[\theta^{out}(n)]\cot[\theta^{in}(0)]}{1-\tan[\theta^{out}(n)]\cot[\theta^{in}(4)]}}_{<0}}_{>0} = \underbrace{-\underbrace{[\omega^{in}\,k_x^{in}(4)]}_{<0}}_{>0}.$$

The sign of $\omega^{in}\,\mathbf{k}^{in}(0)$ or $\omega^{in}\,\mathbf{k}^{in}(4)$ is determined by applying [Eq. (3.2)] to satisfy the radiation condition of the incoming beam. The coefficient on the left-hand side of the first equation is > 0 by inspection since both $|\cot[\theta^{out}(n)]\tan[\theta^{in}(0)]|$ and $|\cot[\theta^{out}(n)]\tan[\theta^{in}(4)]|$ are less than one for all n. For the same reason, the coefficient on the left-hand side of the second equation is < 0. This is how "first selection rule" works. In deriving the first selection rule, the dispersion relations and radiation conditions of the incoming beams, the quadratic nonlinearities and the dispersion relations of the harmonics have been applied. In this special case, it does not rule out any possible outgoing harmonic beams.

Multiplying [Eq. (3.6b)] by ω^{in}, we obtain

$$[\omega^{out}\,k_z^{out}(n)] = 2\left(\underbrace{[\omega^{in}\,k_z^{in}(0)]}_{>0} + \underbrace{[\omega^{in}\,k_z^{in}(4)]}_{<0}\right) \lessgtr 0,$$

$$[\omega^{out}\,k_x^{out}(n)] = 2\left(\underbrace{[\omega^{in}\,k_x^{in}(0)]}_{<0} + \underbrace{[\omega^{in}\,k_x^{in}(4)]}_{<0}\right) < 0.$$

From the radiation conditions of the outgoing beams: $[\omega^{out}\,k_x^{out}(n)] < 0$ only if $n = 2$ or 3. This is how the "second selection rule" works and can be used to explain the asymmetry found in (Fig. 3.1(a)). In deriving the second selection rule, the quadratic nonlinearities and the radiation conditions of possible outgoing beams are used.

In the second example, the two beams collide and form another configuration that both the incoming beams propagate downward. Thus we simplify the notations using $\omega^{in}(0) = \omega^{in}(2) = \omega^{in}$ and $\omega^{out} = 2\omega^{in}$. See also the schematic, (Fig. 3.3(b)), for illustration.

Using [Eq. (3.5)] to relate the x-components of $\mathbf{k}^{in}(0)$ and $\mathbf{k}^{in}(2)$ in terms of their z-components in [Eq. (3.6b)] and vice versa. Then multiplying both sides of [Eq. (3.8)] with

ω^{in} leads to

$$\underbrace{\underbrace{[\omega^{in}\,k_z^{in}(0)]}_{>0}\,\underbrace{\frac{1-\cot[\theta^{out}(n)]\tan[\theta^{in}(0)]}{1-\cot[\theta^{out}(n)]\tan[\theta^{in}(2)]}}_{>0}}_{>0} = \underbrace{-\underbrace{[\omega^{in}\,k_z^{in}(2)]}_{>0}}_{<0},$$

$$\underbrace{\underbrace{[\omega^{in}\,k_x^{in}(0)]}_{<0}\,\underbrace{\frac{1-\tan[\theta^{out}(n)]\cot[\theta^{in}(0)]}{1-\tan[\theta^{out}(n)]\cot[\theta^{in}(2)]}}_{<0}}_{>0} = \underbrace{-\underbrace{[\omega^{in}\,k_x^{in}(2)]}_{>0}}_{<0}.$$

The sign of $\omega^{in}\,\mathbf{k}^{in}(0)$ or $\omega^{in}\,\mathbf{k}^{in}(2)$ is determined by applying [Eq. (3.2)] to satisfy the radiation condition of the incoming beam. The coefficient on the left-hand side of the first equation is > 0 by inspection since both $|\cot[\theta^{out}(n)]\tan[\theta^{in}(0)]|$ and $|\cot[\theta^{out}(n)]\tan[\theta^{in}(2)]|$ are less than one for all n. Similarly, the coefficient on the left-hand side of the second equation is < 0. Again, this is how the first selection rule works. In this case, the left-hand side of both equations are always greater than zero but the right-hand side are always less than zero. So it rules out all the possible formation of second harmonic beams and explains the asymmetry found in (Fig. 3.1(b)).

To clarify the methodology, we multiply [Eq. (3.6b)] by ω^{in} to proceed the derivation of the second selection rule:

$$[\omega^{out}\,k_z^{out}(n)] = 2\left(\underbrace{[\omega^{in}\,k_z^{in}(0)]}_{>0} + \underbrace{[\omega^{in}\,k_z^{in}(2)]}_{>0}\right) > 0,$$

$$[\omega^{out}\,k_x^{out}(n)] = 2\left(\underbrace{[\omega^{in}\,k_x^{in}(0)]}_{<0} + \underbrace{[\omega^{in}\,k_x^{in}(2)]}_{>0}\right) \lesseqgtr 0.$$

From the radiation conditions of the outgoing beams: $[\omega^{out}\,k_z^{out}(n)] > 0$ only if $n = 3$ or 4. No constraint is imposed by "second selection rule".

3.3 Conclusions

The selection rules for two colliding beams at individual frequencies are obtained in (Jiang and Marcus, 2009), the final results are summarized in Table 3.1. The methodology used in (Jiang and Marcus, 2009) is the same as in the two examples: to derive the first selection rule, the dispersion relations and radiation conditions of the incoming beams, the quadratic nonlinearities and the dispersion relations of the harmonics are the constraints on the possible outgoing beams; on the other hand, the quadratic nonlinearities and the radiation conditions of possible outgoing beams are used as constraints to obtain second

Table 3.1 Selection rules for creating harmonic beams from two primary beams intersecting at the origin. One incoming beam, labeled as the 0^{th} lies in the first quadrant with frequency $\omega^{in}(0)$. The second incoming beam lies in the j^{th} quadrant with frequency $\omega^{in}(j)$. Depending on the value of $\chi \equiv \omega^{in}(j)/\omega^{in}(0)$, there are four possible scenarios, indicated by each of the four rows of the table. The first two columns specify χ. (Without loss of generality, $|\chi| \leq 1$.) For each row, the quadrant numbers n of the allowable outgoing beams are listed as a function of j (column). *Solvability* requires $|\omega^{in}(j) + \omega^{in}(0)| < N$. This table uses both the first and second selection rules. For a harmonic beam to exist, it must satisfy both rules. When $\text{sgn}\{\chi\} = +1$ and $j = 3$, no harmonic beams are produced if $\omega^{in}(3) = \omega^{in}(0)$.

$\text{sgn}\{\chi\}$	range of $\lvert\chi\rvert$	$j=1$	$j=2$	$j=3$	$j=4$
$+1$		none	none	2, 3	2, 3
-1	$\lvert\chi\rvert < 1/2$	2	2	3	3
-1	$\lvert\chi\rvert = 1/2$	2	none	none	3
-1	$1/2 < \lvert\chi\rvert \leq 1$	1, 2	none	none	3, 4

selection rule. Although it might look quite different in (Jiang and Marcus, 2009) at first sight.

This formulation seems to be counter-intuitive and sophisticated and also not easy to extend to three-dimensional problem. Another methodology is introduced in next chapter and would be used repeatedly in the next three chapters.

Chapter 4

Selection Rules for Quasi-Two-Dimensional Inertia-Gravity Waves

4.1 Two dimensional inertia-gravity wave physics

A quasi-two-dimensional, compact source of inertia-gravity waves oscillating at frequency $\pm\omega$ in a rotating stratified fluid also creates four, columnated outgoing beams in an "X" pattern. There are four beams, or "legs", because the angle θ of each beam with respect to the closest horizontal x-axis obeys the linear dispersion relation

$$\frac{\omega^2 - f^2}{N^2 - f^2} = \sin^2\theta, \tag{4.1}$$

where $0 < \theta < \pi/2$, f is the constant Coriolis parameter, $N \equiv \sqrt{-g(d\bar{\rho}/dz)/\rho_0}$ is the buoyancy frequency or Brunt-Väisälä frequency, $d\bar{\rho}/dz$ is the vertical (z) density gradient of the unperturbed fluid, g is the acceleration of gravity, and ρ_0 is the average density. Intersecting beams can produce harmonics with frequencies ω equal to the sum or difference of the frequencies of the interacting beams, subject to the *solvability condition* imposed by [Eq. (4.1)]: either $f^2 < \omega^2 < N^2$ or $N^2 < \omega^2 < f^2$. Thus, two interacting beams should be able to produce at most two St. Andrew's crosses, one with a "low frequency" equal to the difference of the absolute values of the frequencies of the interacting beams and another St. Andrew's cross with a "high frequency" equal to the sum of the absolute values of the frequencies of the interacting beams if the solvability condition is satisfied. Therefore, one expects either four or eight harmonic beams or "legs". However, in many simulations and experiments of interacting beams of internal gravity waves (e.g., FIGs. 2(a),(b) in (Lamb, 2004); FIG. 2(b) in (Gerkema et al., 2006); and FIG. 3(a) in (Teoh et al., 1997)), one or more "legs" are missing. (Fig. 4.1) shows another example of missing beams: the two primary beams have the same frequencies, $\pm\omega$, so the "low frequency" St. Andrew's cross

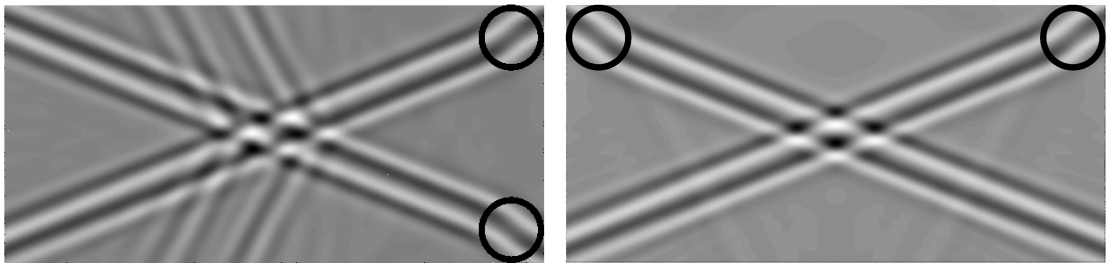

(a) (b)

Figure 4.1 Numerical simulations of physical beams, shown by the magnitude of their vertical velocities. Each primary beam has frequencies of $\pm\omega$ with $N = 1.5394$ rad/s $> |\omega| = 0.6781$ rad/s $> f = 0.3848$ rad/s. And the "high frequency" harmonics have frequencies, $\pm 2\omega$, with $N > |2\omega| > f$. (a) (left) The primary beam sources lie within the circles in the corners on the left side of the panel. Both primary beams propagate to the left, interact, and create two harmonic beams or "legs" with frequencies $\pm 2\omega$. (b) (right) As in panel (a), but with sources at the top. No harmonic beams are produced.

cannot form. However, one would expect the beams to pass through each other, interact and create a "high frequency" cross because $f^2 < (2\omega)^2 < N^2$. In (Fig. 4.1(a)) the sources of the primary beams are located at the right-side corners, and only two of the four expected "legs" are created. In (Fig. 4.1(b)) the sources of the primary beams are at the top, and *no* "legs" are created. Tabaei et al. (Tabaei et al., 2005) found selection rules governing the creation of harmonic "legs" that correctly predicted that the interaction in (Fig. 4.1(a)) creates only two, of the possible four, "legs". However, their rules are incomplete; they also predicted that the interaction in (Fig. 4.1(b)) would create all four "legs" (FIG. 6(b) and Table 1 in (Tabaei et al., 2005)).

Similarly and not surprisingly, the "non-traditional" branch $N^2 < \omega^2 < f^2$ also has this missing "legs" mystery. This time, in (Fig. 4.2(a)) the sources of the primary beams are at the right-side corner, and *no* "legs" are created. In (Fig. 4.2(b)) the sources of the primary beams are located at the top corners, and only two of the four expected "legs" are created.

4.2 Selection Rules

A beam consists of a packet of complex conjugate pairs of plane waves $e^{i(k_x x + k_z z + \omega t)}$ with a continuum of wave numbers constrained such that all of the plane waves' group velocity vectors $\mathbf{c}$ point in the same direction. From [Eq. (4.1)], the absolute value of the frequencies of all plane waves in a beam must be the same. It is important to understand the relative directions of the group velocity vector $\mathbf{c}$ and wave vector $\mathbf{k}$. First define a utility variable,

Ψ,

$$\Psi \equiv \mathrm{sgn}\{N^2 - f^2\} = \begin{cases} +1 & \text{if } f^2 < \omega^2 < N^2 \\ -1 & \text{if } N^2 < \omega^2 < f^2 \end{cases},$$

which distinguish the traditional ($\Psi = +1$) and non-traditional ($\Psi = -1$) branch. For internal gravity waves:

$$\mathrm{sgn}\{c_x\} = \mathrm{sgn}\{\omega\, k_x\}\, \Psi, \tag{4.2}$$
$$\mathrm{sgn}\{c_z\} = -\mathrm{sgn}\{\omega\, k_z\}\, \Psi. \tag{4.3}$$

To prove the above equations, note that the dispersion relation written in its traditional form is

$$\omega^2 = N^2 \left(k_x^2/k^2\right) + f^2 \left(k_z^2/k^2\right), \tag{4.4}$$

or

$$\omega^2 = N^2 \sin^2\theta + f^2 \cos^2\theta.$$

This dispersion relation and the definition $\mathbf{c} \equiv \nabla_{\mathbf{k}}\, \omega$ show

$$\begin{aligned} \omega\, k_x \left(N^2 - f^2\right) &= c_x\, k^2 \left[f^2 \left(k_z^2/k_x^2\right) + N^2\right] \left(k_x^2/k_z^2\right), \\ \omega\, k_z \left(N^2 - f^2\right) &= -c_z\, k^2 \left[f^2 \left(k_z^2/k_x^2\right) + N^2\right], \end{aligned} \tag{4.5}$$

which proves $(\mathbf{k} \cdot \mathbf{c}) = 0$ and relations (4.2) to (4.3). The definition of θ and [Eq. (4.5)] show that for all beams:

$$\left(\frac{c_x}{c_z}\right) = -\left(\frac{\omega\, k_z}{\omega\, k_x}\right), \tag{4.6}$$

and

$$\tan^2\,\theta = \left(\frac{\omega\, k_x}{\omega\, k_z}\right)^2 = \frac{\omega^2 - f^2}{N^2 - \omega^2}. \tag{4.7}$$

Although a beam consists of complex conjugate pairs of waves, consider a thought experiment in which each beam has only a positive *or* a negative frequency. Because the linearized equations for gravity waves are reflection-symmetric about the x and z axes, let one beam, labeled as the first beam, approach the origin from the first quadrant. The notation that it has frequency ω_1, wave vector $\mathbf{k}_1$, angle θ_1, and group velocity $\mathbf{c}_1$ pointing toward the origin. At the origin this beam intersects a second beam, also pointing toward the origin, with frequency ω_2, wave vector $\mathbf{k}_2$, group velocity $\mathbf{c}_2$, and angle θ_2. The inviscid, linearized equations for gravity waves are reversible in time and by using the reflection symmetries, the only assumption requires is that $|\omega_1| \geq |\omega_2|$. Further, define another utility function $F(\gamma) \equiv (\gamma - f^2)/(N^2 - \gamma) > 0$. If $\gamma > 0$ satisfies the solvability condition,

$$\frac{dF(\gamma)}{d\gamma} = \frac{N^2 - f^2}{(N^2 - \gamma)^2}.$$

Thus,

$$\mathrm{sgn}\left\{\frac{dF(\gamma)}{d\gamma}\right\} = \Psi,$$

Table 4.1 Signs of frequency modified wave vector of the second incoming beam, $\omega_2\,\mathbf{k}_2$, in component form. Quadrant number indicates from where the IGW beam propagates.

Quadrant	I	II	III	IV
$\mathrm{sgn}\{\omega_2\,k_{x,2}\}\,\Psi$	-1	$+1$	$+1$	-1
$\mathrm{sgn}\{\omega_2\,k_{z,2}\}\,\Psi$	$+1$	$+1$	-1	-1

Table 4.2 Signs of frequency modified wave vector of the outgoing beam, $\omega^{\mathrm{H}}\,\mathbf{k}^{\mathrm{H}}$, in component form. Quadrant number indicates where the IGW beam propagates into.

Quadrant	I	II	III	IV
$\mathrm{sgn}\{\omega^{\mathrm{H}}\,k_x^{\mathrm{H}}\}\,\Psi$	$+1$	-1	-1	$+1$
$\mathrm{sgn}\{\omega^{\mathrm{H}}\,k_z^{\mathrm{H}}\}\,\Psi$	-1	-1	$+1$	$+1$

which shows F is monotonically increasing when γ increases for traditional branch but F is monotonically decreasing when γ increases for non-traditional branch. Therefore,

$$\omega_1^2 > \omega_2^2 \;\;\Rightarrow\;\; \tan^2\theta_1 > \tan^2\theta_2 \;\;\text{for}\; f^2 < \omega_1^2, \omega_2^2 < N^2, \tag{4.8}$$
$$\omega_1^2 > \omega_2^2 \;\;\Rightarrow\;\; \tan^2\theta_1 < \tan^2\theta_2 \;\;\text{for}\; N^2 < \omega_1^2, \omega_2^2 < f^2. \tag{4.9}$$

Since both incoming beams are propagating toward the origin, use [Eq. (4.2)] and [Eq. (4.3)] to show:

$$\begin{aligned} \mathrm{sgn}\{\omega_1\,k_{x,1}\}\,\Psi &= -1, \\ \mathrm{sgn}\{\omega_1\,k_{z,1}\}\,\Psi &= +1. \end{aligned}$$

And the results for the second incoming beam are listed in Table 4.1.

By rearranging [Eq. (4.7)], the relation between $\omega\,k_x$ and $\omega\,k_z$ is obtained

$$\omega\,k_x = \mathrm{sgn}\{\omega\,k_x\}\,\tan\theta\,|\omega\,k_z|.$$

The frequency modified wave vector, $\omega\,\mathbf{k}$, can be expressed in terms of the absolute value of vertical wave number only. For each incoming beam,

$$\omega_1\,k_{x,1} = \mathrm{sgn}\{\omega_1\,k_{x,1}\}\,|\omega_1\,k_{z,1}|\,\tan\theta_1, \tag{4.10}$$
$$\omega_2\,k_{x,2} = \mathrm{sgn}\{\omega_2\,k_{x,2}\}\,|\omega_2\,k_{z,2}|\,\tan\theta_2, \tag{4.11}$$
$$\omega_1\,k_{z,1} = \mathrm{sgn}\{\omega_1\,k_{z,1}\}\,|\omega_1\,k_{z,1}|, \tag{4.12}$$
$$\omega_2\,k_{z,2} = \mathrm{sgn}\{\omega_2\,k_{z,2}\}\,|\omega_2\,k_{z,2}|. \tag{4.13}$$

Similarly, the four outgoing harmonics generated at the origin have frequency ω^{H}, wave vector $\mathbf{k}^{\mathrm{H}}$, group velocity $\mathbf{c}^{\mathrm{H}}$, and angle θ^{H} where "H" denotes "Harmonics". Because the outgoing waves are generated from the waves in the incoming beams by quadratic nonlinearities:

$$\begin{aligned} \omega^{\mathrm{H}} &= \omega_1 + \omega_2, && (4.14)\\ \mathbf{k}^{\mathrm{H}} &= \mathbf{k}_1 + \mathbf{k}_2. && (4.15) \end{aligned}$$

The "high frequency" harmonics have frequencies of $\pm\omega_{\mathrm{sum}}$ and the "low frequency" harmonics are forcing at $\pm\omega_{\mathrm{diff}}$ where

$$\begin{aligned} \omega_{\mathrm{sum}} &\equiv |\omega_1| + |\omega_2| > 0, && (4.16)\\ \omega_{\mathrm{diff}} &\equiv |\omega_1| - |\omega_2| > 0. && (4.17) \end{aligned}$$

The variable χ is useful in the comparison of ω_{diff} and $|\omega_2|$ for "low frequency" harmonics and R is used to determine the selection rules:

$$\begin{aligned} \chi &\equiv \frac{\omega_2}{\omega_1}, && (4.18)\\ R &\equiv \frac{|k_{z,1}|}{|k_{z,2}|} > 0. && (4.19) \end{aligned}$$

The frequency modified wave vectors of any outgoing beams written in component form are:

$$\begin{aligned} \omega^{\mathrm{H}}\, k_x^{\mathrm{H}} &= \omega^{\mathrm{H}} \left(\mathrm{sgn}\{\omega_1\, k_{x,1}\}\, |\omega_1\, k_{z,1}|\, \tan\theta_1 \,/\, \omega_1 \right.\\ &+ \qquad \left. \mathrm{sgn}\{\omega_2\, k_{x,2}\}\, |\omega_2\, k_{z,2}|\, \tan\theta_2 \,/\, \omega_2 \right),\\ \omega^{\mathrm{H}}\, k_z^{\mathrm{H}} &= \omega^{\mathrm{H}} \left(\mathrm{sgn}\{\omega_1\, k_{z,1}\}\, |\omega_1\, k_{z,1}| \,/\, \omega_1 \right.\\ &+ \qquad \left. \mathrm{sgn}\{\omega_2\, k_{z,2}\}\, |\omega_2\, k_{z,2}| \,/\, \omega_2 \right). \end{aligned}$$

Now, put every piece together, if $\omega_1\, \omega_2 > 0$, this corresponds to generation of "high frequency" harmonics,

$$\begin{aligned} \omega^{\mathrm{H}}\, k_x^{\mathrm{H}} &= \mathcal{K}_x^{\mathrm{S}} \left(\omega_{\mathrm{sum}}\, |k_{z,2}|\, \Psi\right), && (4.20)\\ \omega^{\mathrm{H}}\, k_z^{\mathrm{H}} &= \mathcal{K}_z^{\mathrm{S}} \left(\omega_{\mathrm{sum}}\, |k_{z,2}|\, \Psi\right), && (4.21) \end{aligned}$$

and

$$\begin{aligned} \mathcal{K}_x^{\mathrm{S}} &\equiv \left(\Psi\, \mathrm{sgn}\{\omega_1\, k_{x,1}\} \tan\theta_1\, R + \Psi\, \mathrm{sgn}\{\omega_2\, k_{x,2}\} \tan\theta_2\right), && (4.22)\\ \mathcal{K}_z^{\mathrm{S}} &\equiv \left(\Psi\, \mathrm{sgn}\{\omega_1\, k_{z,1}\}\, R + \Psi\, \mathrm{sgn}\{\omega_2\, k_{x,2}\}\right), && (4.23) \end{aligned}$$

where the superscript "S" denotes "Sum" and $\omega^{\mathrm{H}} = \pm\,\omega_{\mathrm{sum}}$. Moreover, if $\omega_1\, \omega_2 < 0$, this corresponds to "low frequency" harmonics generation,

$$\begin{aligned} \omega^{\mathrm{H}}\, k_x^{\mathrm{H}} &= \mathcal{K}_x^{\mathrm{D}} \left(\omega_{\mathrm{diff}}\, |k_{z,2}|\, \Psi\right), && (4.24)\\ \omega^{\mathrm{H}}\, k_z^{\mathrm{H}} &= \mathcal{K}_z^{\mathrm{D}} \left(\omega_{\mathrm{diff}}\, |k_{z,2}|\, \Psi\right), && (4.25) \end{aligned}$$

and

$$\mathcal{K}_x^{\mathrm{D}} \equiv (\Psi\,\mathrm{sgn}\{\omega_1\,k_{x,1}\}\tan\theta_1\,R - \Psi\,\mathrm{sgn}\{\omega_2\,k_{x,2}\}\tan\theta_2)\,, \tag{4.26}$$

$$\mathcal{K}_z^{\mathrm{D}} \equiv (\Psi\,\mathrm{sgn}\{\omega_1\,k_{z,1}\}\,R - \Psi\,\mathrm{sgn}\{\omega_2\,k_{x,2}\})\,, \tag{4.27}$$

where the superscript "D" refers to "Difference" and $\omega^{\mathrm{H}} = \pm\,\omega_{\mathrm{diff}}$.

Therefore, the direction of the outgoing beam group velocity can be determined by calculating $\mathcal{K}$'s:

$$\mathrm{sgn}\{c_x^{\mathrm{H}}\} = \mathrm{sgn}\{\mathcal{K}_x^{\mathrm{H}}\}, \tag{4.28}$$

$$\mathrm{sgn}\{c_z^{\mathrm{H}}\} = -\mathrm{sgn}\{\mathcal{K}_z^{\mathrm{H}}\}, \tag{4.29}$$

because from definition $\Psi^2 = 1$ and

$$\mathrm{sgn}\{c_x^{\mathrm{H}}\} = \mathrm{sgn}\{\omega^{\mathrm{H}}\,k_x^{\mathrm{H}}\}\,\Psi = \mathrm{sgn}\{\mathcal{K}_x^{\mathrm{H}}\,\Psi\}\,\Psi = \mathrm{sgn}\{\mathcal{K}_x^{\mathrm{H}}\}\,\Psi^2,$$
$$\mathrm{sgn}\{c_z^{\mathrm{H}}\} = -\mathrm{sgn}\{\omega^{\mathrm{H}}\,k_z^{\mathrm{H}}\}\,\Psi = -\mathrm{sgn}\{\mathcal{K}_z^{\mathrm{H}}\,\Psi\}\,\Psi = -\mathrm{sgn}\{\mathcal{K}_z^{\mathrm{H}}\}\,\Psi^2.$$

The frequency modified wave vector of a harmonic beam also needs to satisfy its own dispersion relation in geometrical form, [Eq. (4.7)],

$$\tan^2\theta^{\mathrm{H}} = \frac{(\mathcal{K}_x^{\mathrm{H}})^2}{(\mathcal{K}_z^{\mathrm{H}})^2},$$

and the dispersion relation leads to a quadratic equation in R:

$$\mathrm{A}^{\mathrm{H}}\,R^2 - 2\,\mathrm{B}^{\mathrm{H}}\,R + \mathrm{C}^{\mathrm{H}} = 0. \tag{4.30}$$

Define the discriminant in the following form:

$$\Delta^{\mathrm{H}} \equiv (\mathrm{B}^{\mathrm{H}})^2 - \mathrm{A}^{\mathrm{H}}\,\mathrm{B}^{\mathrm{C}},$$

then with the aid of the quadratic formula

$$R^{\mathrm{H},\pm} = \frac{\mathrm{B}^{\mathrm{H}} \pm \sqrt{\Delta^{\mathrm{H}}}}{\mathrm{A}^{\mathrm{H}}}, \tag{4.31}$$

where "H" could refer to either "S" or "D". The roots $R^{\mathrm{H},\pm}$ must be real (therefore $\Delta^{\mathrm{H}} \geq 0$) and positive otherwise violate the definition, [Eq. (4.19)], that $R > 0$.

Lemma 1 *[Eqs. (4.28), (4.29) and (4.31)] lead to a drastic conclusion that at most there are only* TWO, NOT FOUR, *"legs" permitted for each St. Andrew's cross (with either "high frequency" or "low frequency") since the direction of a harmonic beam and the value of R is a one-to-one mapping once the relative positions of the incoming beams have been designated.*

Table 4.3 The exact forms of $\mathcal{K}_x^{\rm H}$ and $\mathcal{K}_z^{\rm H}$ in terms of the quadrant from where the second incoming beam is approaching. Define shorthand notations using in this table: $\mathcal{K}_x^+ \equiv -\tan\theta_1\, R + \tan\theta_2$ and $\mathcal{K}_x^- \equiv -\tan\theta_1\, R - \tan\theta_2$. By inspection, since the definition requires $R > 0$, $\mathcal{K}_x^- < 0$ and $R + 1 > 0$. Recall that $\mathrm{sgn}\{c_x^{\rm H}\} = \mathrm{sgn}\{\mathcal{K}_x^{\rm H}\}$ and $\mathrm{sgn}\{c_z^{\rm H}\} = -\mathrm{sgn}\{\mathcal{K}_z^{\rm H}\}$. If $\mathcal{K}_x^{\rm H}$ equals to $\mathcal{K}_x^-$, the corresponding beam must be propagating to the left. And if $\mathcal{K}_z^{\rm H}$ equals to $R+1$, the corresponding beam must be propagating downward.

Quadrant	I	II	III	IV
$\mathcal{K}_x^{\rm S}$	$\mathcal{K}_x^-$	$\mathcal{K}_x^+$	$\mathcal{K}_x^+$	$\mathcal{K}_x^-$
$\mathcal{K}_z^{\rm S}$	$R+1$	$R+1$	$R-1$	$R-1$
$\mathcal{K}_x^{\rm D}$	$\mathcal{K}_x^+$	$\mathcal{K}_x^-$	$\mathcal{K}_x^-$	$\mathcal{K}_x^+$
$\mathcal{K}_z^{\rm D}$	$R-1$	$R-1$	$R+1$	$R+1$

Table 4.4 The value of $\mathrm{B}^{\rm S}$ in terms of the quadrant from where the second incoming beam is approaching.

Quadrant	$\mathrm{B}^{\rm S}$	$\mathrm{sgn}\{\mathrm{B}^{\rm S}\}$
I	$\Psi\,(\ \ \tan\theta_1\tan\theta_2 - \tan^2\theta^{\rm S})$	-1
II	$\Psi\,(-\tan\theta_1\tan\theta_2 - \tan^2\theta^{\rm S})$	$-\Psi$
III	$\Psi\,(-\tan\theta_1\tan\theta_2 + \tan^2\theta^{\rm S})$	$+1$
IV	$\Psi\,(\ \ \tan\theta_1\tan\theta_2 + \tan^2\theta^{\rm S})$	$+\Psi$

The functional forms of $\mathcal{K}_x^{\rm H}$, $\mathcal{K}_z^{\rm H}$ and $\mathrm{B}^{\rm H}$ are dependent on the quadrant where the second incoming beam approaches and the exact formulas are listed in Table 4.3, Table 4.4 and 4.5. But $\mathrm{A}^{\rm H}$ and $\mathrm{C}^{\rm H}$ are the same in every quadrant,

$$\begin{aligned} \mathrm{A}^{\rm S} &\equiv \Psi\,(\tan^2\theta^{\rm S} - \tan^2\theta_1) > 0, \\ \mathrm{C}^{\rm S} &\equiv \Psi\,(\tan^2\theta^{\rm S} - \tan^2\theta_2) > 0, \end{aligned}$$

and

$$\begin{aligned} \mathrm{A}^{\rm D} &\equiv \Psi\,(\tan^2\theta_1 - \tan^2\theta^{\rm D}) > 0, \\ \mathrm{C}^{\rm D} &\equiv \Psi\,(\tan^2\theta_2 - \tan^2\theta^{\rm D}) \begin{cases} < 0, & |\chi| < 1/2 \\ = 0, & |\chi| = 1/2 \\ > 0, & |\chi| > 1/2 \end{cases} . \end{aligned}$$

There are only two functional forms of $\Delta^{\rm H}$: for second incoming beam coming from first or third quadrant,

$$\Delta^{\rm H} = \tan^2\theta^{\rm H}\,(\tan\theta_1 - \tan\theta_2)^2 > 0, \tag{4.32}$$

Table 4.5 The value of $\mathrm{B^D}$ in terms of the quadrant from where the second incoming beam is approaching.

Quadrant	$\mathrm{B^D}$	$\mathrm{sgn}\{\mathrm{B^D}\}$	
I	$\Psi\,(\quad \tan\theta_1\tan\theta_2 - \tan^2\theta^{\mathrm{D}})$	$+1$	$\lvert\chi\rvert \geq 1/2$
		?	$\lvert\chi\rvert < 1/2$
II	$\Psi\,(-\tan\theta_1\tan\theta_2 - \tan^2\theta^{\mathrm{D}})$	$-\Psi$	
III	$\Psi\,(-\tan\theta_1\tan\theta_2 + \tan^2\theta^{\mathrm{D}})$	-1	$\lvert\chi\rvert \geq 1/2$
		?	$\lvert\chi\rvert < 1/2$
IV	$\Psi\,(\quad \tan\theta_1\tan\theta_2 + \tan^2\theta^{\mathrm{D}})$	$+\Psi$	

and for second incoming beam coming from second or fourth quadrant,

$$\Delta^{\mathrm{H}} = \tan^2\theta^{\mathrm{H}}\,(\tan\theta_1 + \tan\theta_2)^2 > 0. \tag{4.33}$$

Because the discriminants are always greater than zero, both $R^{\mathrm{H},\pm}$ are real but not necessary to be positive. After substituting the exact formulas of Δ^{H}, the analytical form for R's where the second incoming beam is from first quadrant is

$$R^{\mathrm{S},\pm} = -\frac{\tan\theta^{\mathrm{S}} \pm \tan\theta_2}{\tan\theta^{\mathrm{S}} \pm \tan\theta_1}, \tag{4.34}$$

$$R^{\mathrm{D},\pm} = \frac{\tan\theta^{\mathrm{D}} \pm \tan\theta_2}{\tan\theta^{\mathrm{D}} \pm \tan\theta_1}; \tag{4.35}$$

from second quadrant

$$R^{\mathrm{S},\pm} = -\frac{\tan\theta^{\mathrm{S}} \mp \Psi\tan\theta_2}{\tan\theta^{\mathrm{S}} \pm \Psi\tan\theta_1}, \tag{4.36}$$

$$R^{\mathrm{D},\pm} = \frac{\tan\theta^{\mathrm{D}} \mp \Psi\tan\theta_2}{\tan\theta^{\mathrm{D}} \pm \Psi\tan\theta_1}; \tag{4.37}$$

from third quadrant

$$R^{\mathrm{S},\pm} = \frac{\tan\theta^{\mathrm{S}} \mp \tan\theta_2}{\tan\theta^{\mathrm{S}} \mp \tan\theta_1}, \tag{4.38}$$

$$R^{\mathrm{D},\pm} = -\frac{\tan\theta^{\mathrm{D}} \mp \tan\theta_2}{\tan\theta^{\mathrm{D}} \mp \tan\theta_1}; \tag{4.39}$$

and from fourth quadrant

$$R^{\mathrm{S},\pm} = \frac{\tan\theta^{\mathrm{S}} \pm \Psi\tan\theta_2}{\tan\theta^{\mathrm{S}} \mp \Psi\tan\theta_1}, \tag{4.40}$$

$$R^{\mathrm{D},\pm} = -\frac{\tan\theta^{\mathrm{D}} \pm \Psi\tan\theta_2}{\tan\theta^{\mathrm{D}} \mp \Psi\tan\theta_1}. \tag{4.41}$$

R's are determined to be positive or negative in a case by case sense (governed by Ψ and χ) as follows.

4.2.1 $\Psi = +1$ and "high frequency" harmonics ($\chi > 0$)

In this case, $(\omega^{\rm H} = \pm\omega_{\rm sum})^2 > \omega_1^2 \geq \omega_2^2$, from [Eq. (4.8)]:

$$\tan\theta^{\rm S} > \tan\theta_1 \geq \tan\theta_2.$$

This relation is used to determine $R^{\rm S,\pm}$.

When the second incoming beam is from first quadrant:

$$R^{\rm S,\pm} = -\frac{\overbrace{\tan\theta^{\rm S} \pm \tan\theta_2}^{>0}}{\underbrace{\tan\theta^{\rm S} \pm \tan\theta_1}_{>0}} < 0;$$

from second quadrant

$$R^{\rm S,\pm} = -\frac{\overbrace{\tan\theta^{\rm S} \mp \tan\theta_2}^{>0}}{\underbrace{\tan\theta^{\rm S} \pm \tan\theta_1}_{>0}} < 0;$$

from third quadrant

$$\begin{aligned} R^{\rm S,+} &= \frac{\overbrace{\tan\theta^{\rm S} - \tan\theta_2}^{>0}}{\underbrace{\tan\theta^{\rm S} - \tan\theta_1}_{>0}} > 1, \\ R^{\rm S,-} &= \frac{\overbrace{\tan\theta^{\rm S} + \tan\theta_2}^{>0}}{\underbrace{\tan\theta^{\rm S} + \tan\theta_1}_{>0}} > 0, < 1; \end{aligned}$$

and from fourth quadrant

$$\begin{aligned} R^{\rm S,+} &= \frac{\overbrace{\tan\theta^{\rm S} + \tan\theta_2}^{>0}}{\underbrace{\tan\theta^{\rm S} - \tan\theta_1}_{>0}} > 1, \\ R^{\rm S,-} &= \frac{\overbrace{\tan\theta^{\rm S} - \tan\theta_2}^{>0}}{\underbrace{\tan\theta^{\rm S} + \tan\theta_1}_{>0}} > 0, < 1. \end{aligned}$$

$R^{\mathrm{S},\pm} < 0$ if the second incoming beam is from top half plane and $R^{\mathrm{S},+} > 1, 0 < R^{\mathrm{S},-} < 1$ if the second incoming beam is from bottom half plane. $R \leq 0$ contradicts the definition of R and thus violates the dispersion relation. Therefore, there is no harmonic beam generated if both incoming beams are from the top. Use Table 4.3 and [Eqs. (4.28) and (4.29)]:

$$\begin{aligned} \mathcal{K}_x^{\mathrm{S}} &= -\tan\theta_1 R^{\mathrm{S},\pm} + \tan\theta_2 = \frac{\tan\theta^{\mathrm{S}}(\tan\theta_2 - \tan\theta_1)}{\tan\theta^{\mathrm{S}} \mp \tan\theta_2} < 0, \\ \mathcal{K}_z^{\mathrm{S}} &= R^{\mathrm{S},\pm} - 1 \begin{cases} > 0 & \text{w.r.t. } R^{\mathrm{S},+} \\ < 0 & \text{w.r.t. } R^{\mathrm{S},-} \end{cases}, \end{aligned}$$

for the second incoming beam from third quadrant. The same procedures can be applied to incoming beam from quadrant IV. Therefore,

$$\begin{aligned} (c_x)^{\mathrm{S},\pm} &< 0, \\ (c_z)^{\mathrm{S},+} &< 0, \\ (c_z)^{\mathrm{S},-} &> 0, \end{aligned}$$

for the second incoming beam from quadrant III or IV. Or the outgoing "high frequency" harmonics are propagating into second and third quadrant. Using reflection symmetries, these statements can be generalized so that no beam needs to be in the first quadrant: a high frequency cross is produced only if one of the incoming beams propagates upward and the other downward. The cross has only two outgoing beams – one propagates upward and the other downward. Both outgoing beams propagate horizontally in the same direction as the incoming beam with the higher absolute value of its frequency. There is an exception that the incoming beams have the same frequency and heading in opposite directions such that $R^{\mathrm{S},\pm} = 1$ and the corresponding group velocity is zero. This is not qualified to be a wave.

4.2.2 $\Psi = -1$ and "high frequency" harmonics ($\chi > 0$)

Similar procedures like in 4.2.1 are used to determine R again.But in this case, based on [Eq. (4.9)]: $\tan\theta^{\mathrm{S}} < \tan\theta_1 \leq \tan\theta_2$. $R^{\mathrm{S},\pm} < 0$ if the second incoming beam is propagating from right half plane, $R^{\mathrm{S},\pm} > 0$ if that is from second quadrant and $R^{\mathrm{S},\pm} > 1$ if that is from quadrant III. By using Table 4.3 and [Eqs. (4.28) and (4.29)]:

$$\begin{aligned} (c_x)^{\mathrm{S},+} &< 0, \\ (c_x)^{\mathrm{S},-} &> 0, \\ (c_z)^{\mathrm{S},\pm} &< 0, \end{aligned}$$

for the second incoming beam is from left half plane. The outgoing "high frequency" harmonics are propagating into third and fourth quadrant. Using reflection symmetries again, these statements can be generalized so that no beam needs to be in the first quadrant: a

high frequency cross is produced only if one of the incoming beams propagates leftward and the other rightward. The cross has only two outgoing beams – one propagates rightward and the other leftward. Both outgoing beams propagate vertically in the same direction as the incoming beam with the higher absolute value of its frequency. The incoming beams have the same frequency and propagate in the opposite directions is also an exception such that $R^{\mathrm{S},\pm} = 1$ and the corresponding group velocity is zero. Like in 4.2.1, this is not considered to be a wave, either.

4.2.3 $\Psi = +1$ and "low frequency" harmonics ($\chi < 0$)

(i) $|\chi| < 1/2$

Since $|\chi| < 1/2$ and therefore $\omega_1^2 > (\omega^{\mathrm{H}} = \pm\omega_{\mathrm{diff}})^2 > \omega_2^2$, from [Eq. (4.8)]: $\tan\theta_1 > \tan\theta^{\mathrm{D}} > \tan\theta_2$. Similar procedures like in 4.2.1 are used to determine R. $0 < R^{\mathrm{D},+} < 1, R^{\mathrm{D},-} < 0$ if the second incoming beam is from quadrant I or II and $R^{\mathrm{D},+} > 0, R^{\mathrm{D},-} < 0$ if that is from quadrant III or IV. By using Table 4.3 and [Eqs. (4.28) and (4.29)]:

$$\begin{aligned} (c_x)^{\mathrm{D},+} &< 0, \\ (c_z)^{\mathrm{D},+} &> 0, \end{aligned}$$

for the second incoming beam from first and second quadrant and

$$\begin{aligned} (c_x)^{\mathrm{D},+} &< 0, \\ (c_z)^{\mathrm{D},+} &< 0, \end{aligned}$$

for the second incoming beam from third and fourth quadrant. The single, outgoing "low frequency" harmonic is propagating into second quadrant if the second incoming beam is from the top and into the third quadrant if that is from the bottom. In general, a low frequency cross with only one "leg" is always generated. This is because in the quadratic formula, $\sqrt{\Delta^{\mathrm{D}}}$ is always greater than $\left|\mathrm{B}^{\mathrm{D}}\right|$, thus no matter what the numerator, $\mathrm{B}^{\mathrm{D}} + \sqrt{\Delta^{\mathrm{D}}}$, is always positive and $\mathrm{B}^{\mathrm{D}} - \sqrt{\Delta^{\mathrm{D}}} < 0$. Therefore, one root is always positive and another one is always negative. The outgoing beam propagates in the same horizontal direction as the incoming beam with higher frequency. The outgoing beam propagates vertically in the direction opposite that of the vertical direction of the incoming beam with lower frequency.

(ii) $|\chi| = 1/2$

Since $\omega_1^2 > \omega_2^2 = (\omega^{\mathrm{H}} = \pm\omega_{\mathrm{diff}})^2$, by using [Eq. (4.8)]:

$$\tan\theta_1 > \tan\theta_2 = \tan\theta^{\mathrm{D}}.$$

$0 < R^{\mathrm{D},+} < 1, R^{\mathrm{D},-} = 0$ if the second incoming beam is from first quadrant, $R^{\mathrm{D},+} = 0, R^{\mathrm{D},-} < 0$ for that from the left half plane and $R^{\mathrm{D},+} > 0, R^{\mathrm{D},-} = 0$ if the second incoming

beam is from fourth quadrant. Based on Table 4.3 and [Eqs. (4.28) and (4.29)]:

$$\begin{aligned}(c_x)^{\mathrm{D},+} &< 0,\\ (c_z)^{\mathrm{D},+} &> 0,\end{aligned}$$

for the second incoming beam from first quadrant and

$$\begin{aligned}(c_x)^{\mathrm{D},+} &< 0,\\ (c_z)^{\mathrm{D},+} &< 0,\end{aligned}$$

for the second incoming beam from fourth quadrant. The outgoing "low frequency" harmonic is propagating into second quadrant if the second incoming beam is from the first quadrant and into the third quadrant if that is from the fourth quadrant. Extend this to general case, a low frequency cross is created only when both incoming beams propagate in the same horizontal direction. The cross has only one beam. It propagates horizontally in the direction of the incoming beams. The outgoing beam propagates vertically in a direction opposite that of the incoming beam with lower frequency.

(iii) $|\chi| > 1/2$

Because $\omega_1^2 > \omega_2^2 > (\omega^{\mathrm{H}} = \pm\omega_{\mathrm{diff}})^2$, [Eq. (4.8)] shows

$$\tan\theta_1 > \tan\theta_2 > \tan\theta^{\mathrm{D}}.$$

$0 < R^{\mathrm{D},\pm} < 1$ if the second incoming beam is from first quadrant, $R^{\mathrm{D},\pm} < 0$ for that is from the left half plane and $R^{\mathrm{D},+} > 0, 0 < R^{\mathrm{D},-} < 1$ if that is from fourth quadrant. By using Table 4.3 and [Eqs. (4.28) and (4.29)]:

$$\begin{aligned}(c_x)^{\mathrm{D},+} &< 0,\\ (c_x)^{\mathrm{D},-} &> 0,\\ (c_z)^{\mathrm{D},\pm} &> 0,\end{aligned}$$

for the second incoming beam from first quadrant and

$$\begin{aligned}(c_x)^{\mathrm{D},+} &< 0,\\ (c_x)^{\mathrm{D},-} &> 0,\\ (c_z)^{\mathrm{D},\pm} &< 0,\end{aligned}$$

for the second incoming beam from fourth quadrant. The outgoing "low frequency" harmonics are propagating into first and second quadrant if the second incoming beam is from the first quadrant and into the third and fourth quadrant if that is from the fourth quadrant. In this case, a low frequency cross is generated only when the two incoming beams propagate in the same horizontal direction. The cross has two "legs". They propagate vertically in the direction opposite that of the incoming beam with lower frequency. The two outgoing "legs" propagate horizontally in opposite directions.

4.2.4 $\Psi = -1$ and "low frequency" harmonics ($\chi < 0$)

(i) $|\chi| < 1/2$

Since $\omega_1^2 > (\omega^{\mathrm{H}} = \pm\omega_{\mathrm{diff}})^2 > \omega_2^2$, from [Eq. (4.9)]:

$$\tan\theta_1 < \tan\theta^{\mathrm{D}} < \tan\theta_2.$$

Similar procedures like in 4.2.1 are used again to determine R. $R^{\mathrm{D},+} > 1, R^{\mathrm{D},-} < 0$ if the second incoming beam is from top half plane, $R^{\mathrm{D},+} > 0, R^{\mathrm{D},-} < 0$ if that is from the bottom half. Based on Table 4.3 and [Eqs. (4.28) and (4.29)]:

$$\begin{aligned}(c_x)^{\mathrm{D},+} &> 0,\\ (c_z)^{\mathrm{D},+} &< 0,\end{aligned}$$

for the second incoming beam from first and fourth quadrant and

$$\begin{aligned}(c_x)^{\mathrm{D},+} &< 0,\\ (c_z)^{\mathrm{D},+} &< 0,\end{aligned}$$

for the second incoming beam from second and third quadrant. The outgoing "low frequency" harmonic is propagating into fourth quadrant if the second incoming beam is from the right and into the third quadrant if that is from the left. A low frequency cross with only one "leg" is always generated for the same reason $\Psi = +1$ counter-part has. The outgoing beam propagates in the same vertical direction as the incoming beam with higher frequency. The outgoing beam propagates horizontally in the direction opposite that of the horizontal direction of the incoming beam with lower frequency.

(ii) $|\chi| = 1/2$

Because $\omega_1^2 > \omega_2^2 = (\omega^{\mathrm{H}} = \pm\omega_{\mathrm{diff}})^2$, [Eq. (4.9)] leads to $\tan\theta_1 < \tan\theta_2 = \tan\theta^{\mathrm{D}}$. $R^{\mathrm{D},+} > 1, R^{\mathrm{D},-} = 0$ if the second incoming beam is from the top half plane and $R^{\mathrm{D},+} = 0, R^{\mathrm{D},-} < 0$ if that is from bottom half plane. By using Table 4.3 and [Eqs. (4.28) and (4.29)]:

$$\begin{aligned}(c_x)^{\mathrm{D},+} &> 0,\\ (c_z)^{\mathrm{D},+} &< 0,\end{aligned}$$

for the second incoming beam from quadrant I and

$$\begin{aligned}(c_x)^{\mathrm{D},+} &< 0,\\ (c_z)^{\mathrm{D},+} &< 0,\end{aligned}$$

for the second incoming beam from quadrant II. The outgoing "low frequency" harmonic is propagating into fourth quadrant if the second incoming beam is from the first quadrant and into the third quadrant if that is from the second quadrant. Extend this to general case by using reflection symmetries, a low frequency cross is created only when both incoming beams propagate in the same vertical direction. The cross has only one beam. It propagates vertically in the direction of the incoming beams. The outgoing beam propagates horizontally in a direction opposite that of the incoming beam with lower frequency.

(iii) $|\chi| > 1/2$

$\omega_1^2 > \omega_2^2 > (\omega^{\mathrm{H}} = \pm\omega_{\mathrm{diff}})^2$ in this case therefore [Eq. (4.9)] shows:

$$\tan\theta_1 < \tan\theta_2 < \tan\theta^{\mathrm{D}}.$$

$R^{\mathrm{D},+} > 1, 0 < R^{\mathrm{D},-} < 1$ if the second incoming beam is from top half plane and $R^{\mathrm{D},\pm} < 0$ if the second incoming beam is from the bottom half plane. Based on Table 4.3 and [Eqs. (4.28) and (4.29)]:

$$\begin{aligned}(c_x)^{\mathrm{D},\pm} &> 0,\\ (c_z)^{\mathrm{D},+} &< 0,\\ (c_z)^{\mathrm{D},-} &> 0,\end{aligned}$$

for the second incoming beam from first quadrant and

$$\begin{aligned}(c_x)^{\mathrm{D},\pm} &< 0,\\ (c_z)^{\mathrm{D},+} &< 0,\\ (c_z)^{\mathrm{D},-} &> 0,\end{aligned}$$

for the second incoming beam from second quadrant. The outgoing "low frequency" harmonics are propagating into first and fourth quadrant if the second incoming beam is from the first quadrant and into the second and third quadrant if that is from the second quadrant. In this case, a low frequency cross is generated only when the two incoming beams propagate in the same vertical direction. The cross has two "legs". They propagate horizontally in the direction opposite that of the incoming beam with lower frequency. The two outgoing "legs" emit vertically in opposite directions.

4.2.5 Conclusion

The results are summarized in Table 4.6 for traditional branch and Table 4.7 for non-traditional branch.

All selection rules for both traditional and non-traditional branch have been verified by numerical simulations, e.g. see (Figs. 4.1,4.2 and 4.3). The selection rules derived in this chapter are sufficient because no harmonic beams allowed by Tables 4.6 and 4.7 are missing from numerical simulations (all the possibilities have been tested).

4.3 Reflection from a Sloping Boundary in Traditional Branch

Here the selection rules are applied to explain the fundamental difference between the super- and sub-critical reflection from a sloping topography. The slope angle γ is measured from the horizontal and the incident gravity wave beam inclination relative to the horizontal is θ.

Table 4.6 Selection rules for creating harmonic beams from two primary beams intersecting at the origin. One incoming beam, labeled as source 1, lies in the first quadrant with frequency ω_1. The second incoming beam can probably from any quadrant with frequency ω_2. Depending on the value of $\chi \equiv \omega_2/\omega_1$, there are four possible scenarios, indicated by each of the four rows of the table. The first two columns specify χ. (Without loss of generality, $|\chi| \leq 1$.) For each row, the quadrant numbers n of the allowable outgoing beams are listed as a function of quadrant in which second incoming beam lies. *Solvability* requires $f^2 < (\omega^{\mathrm{H}})^2 < N^2$.

$\mathrm{sgn}\{\chi\}$	range of $\lvert\chi\rvert$	I	II	III	IV
$+1$		none	none	2, 3	2, 3
-1	$\lvert\chi\rvert < 1/2$	2	2	3	3
-1	$\lvert\chi\rvert = 1/2$	2	none	none	3
-1	$1/2 < \lvert\chi\rvert < 1$	1, 2	none	none	3, 4

Table 4.7 As in Table 4.6 but *solvability* requires $N^2 < (\omega^{\mathrm{H}})^2 < f^2$.

$\mathrm{sgn}\{\chi\}$	range of $\lvert\chi\rvert$	I	II	III	IV
$+1$		none	3, 4	3, 4	none
-1	$\lvert\chi\rvert < 1/2$	4	3	3	4
-1	$\lvert\chi\rvert = 1/2$	4	3	none	none
-1	$1/2 < \lvert\chi\rvert < 1$	1, 4	2, 3	none	none

4.3.1 Super-critical Reflection from a Slope

In this case, $\theta > \gamma$, the reflection is called super-critical. The reflected beam and the observed second-harmonic beam would both go up-slope.

The flow of reflection from the slope can be emulated from the colliding of the incident primary beam and an image beam coming from lower-right, as depicted in (Fig. 4.4). In the inviscid limit, the normal velocity on the slope is zero:

$$(\mathbf{v}^{(\mathrm{i})} + \mathbf{v}^{(\mathrm{I})}) \cdot \hat{\mathbf{n}} = 0,$$

where

$$\begin{aligned} \mathbf{n} &= (-\sin\gamma\hat{\mathbf{x}} + \cos\gamma\hat{\mathbf{z}}), \\ v_z^{(\mathrm{i})} &= -v_x^{(\mathrm{i})}\tan\theta, \\ v_z^{(\mathrm{I})} &= v_x^{(\mathrm{I})}\tan\theta, \end{aligned}$$

and "i" denotes incident beam and "I" refers to image beam.

The strength of the image gravity wave beam can be determined by combining the above equations,

$$v_x^{(\mathrm{I})} = \underbrace{\frac{\tan\theta + \tan\gamma}{\tan\theta - \tan\gamma}}_{>0} v_x^{(\mathrm{i})} = \underbrace{\frac{\sin(\theta+\gamma)}{\sin(\theta-\gamma)}}_{>0} v_x^{(\mathrm{i})}. \tag{4.42}$$

The incident beam and image beam collide in the sense like the colliding beams are from quadrant I and IV. The outgoing second harmonic beam propagates horizontally in the same direction as the incident primary beam but vertically in the opposite direction according to the first row and quadrant IV of Table 4.6.

4.3.2 Sub-critical Reflection from a Slope

When $\theta < \gamma$, the flow is called sub-critical. The reflected beam would go down-slope and the second-harmonic beam, if exists, would only allow to go up-slope. Similar to super-critical case but the image beam is coming from upper-left, as depicted in (Fig. 4.5). In the inviscid limit, the normal velocity on the slope is zero:

$$v_x^{(\mathrm{I})} = \underbrace{-\frac{\tan\theta + \tan\gamma}{\tan\gamma - \tan\theta}}_{<0} v_x^{(\mathrm{i})} = \underbrace{-\frac{\sin(\theta+\gamma)}{\sin(\gamma-\theta)}}_{<0} v_x^{(\mathrm{i})}.$$

The incident beam and image beam collide in the sense like the colliding beams are from quadrant I and II. According to first row and quadrant II of Table 4.6, the second harmonics are forbidden. The result is confirmed by experiments (e.g. (Peacock and Tabaei, 2005)) and numerical simulations, see (Fig. 4.5(b)).

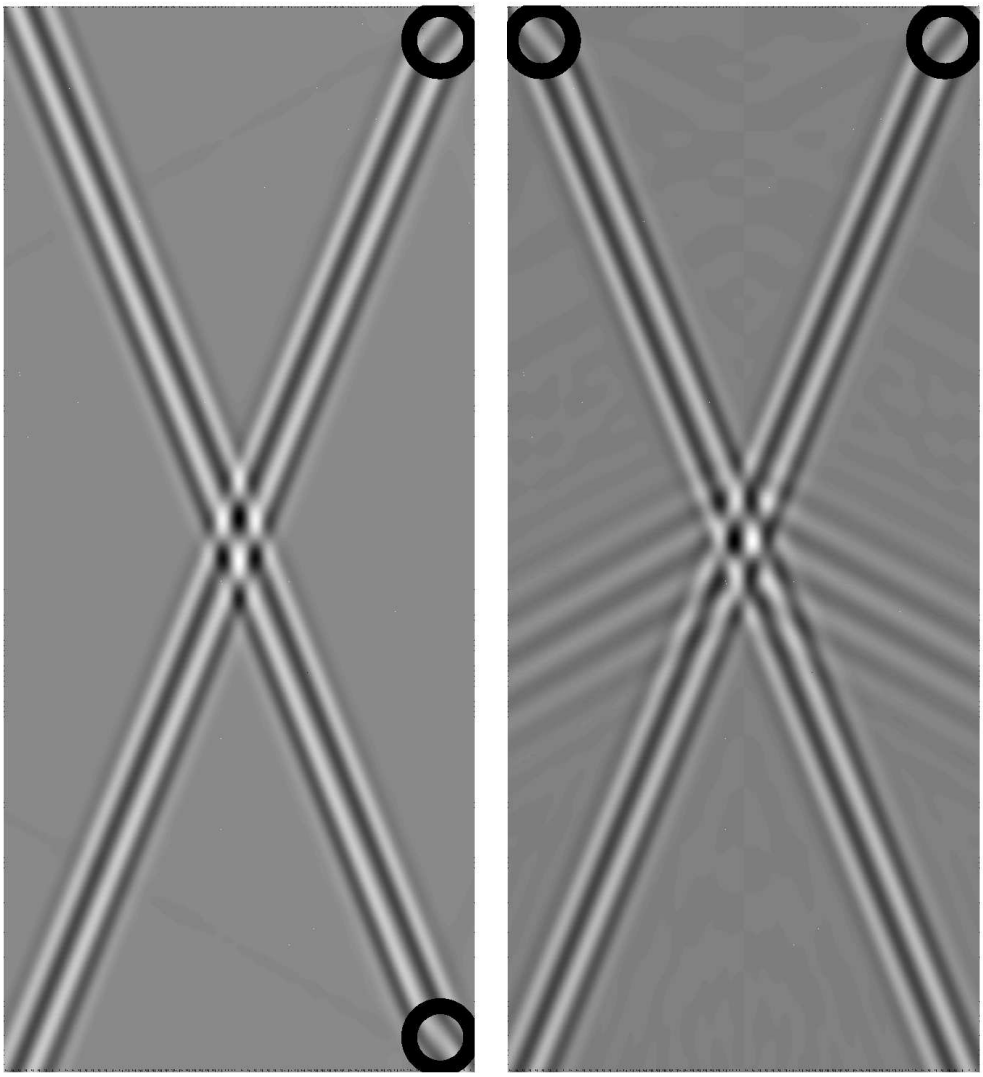

(a) (b)

Figure 4.2 Numerical simulations of physical beams, shown by the magnitude of their horizontal velocities. Each primary beam has frequencies of $\pm\omega$ with $N = 1.5394$ rad/s $< |\omega| = 2.7125$ rad/s $< f = 6.1575$ rad/s. And the "high frequency" harmonics have frequencies, $\pm 2\omega$, with $N < |2\omega| < f$. (a) (left) The primary beam sources lie within the circles in the corners on the right side of the panel. Both primary beams propagate to the left, interact, and no harmonic beams are produced. (b) (right) As in panel (a), but with sources at the top and create two harmonic beams or "legs" with frequencies $\pm 2\omega$.

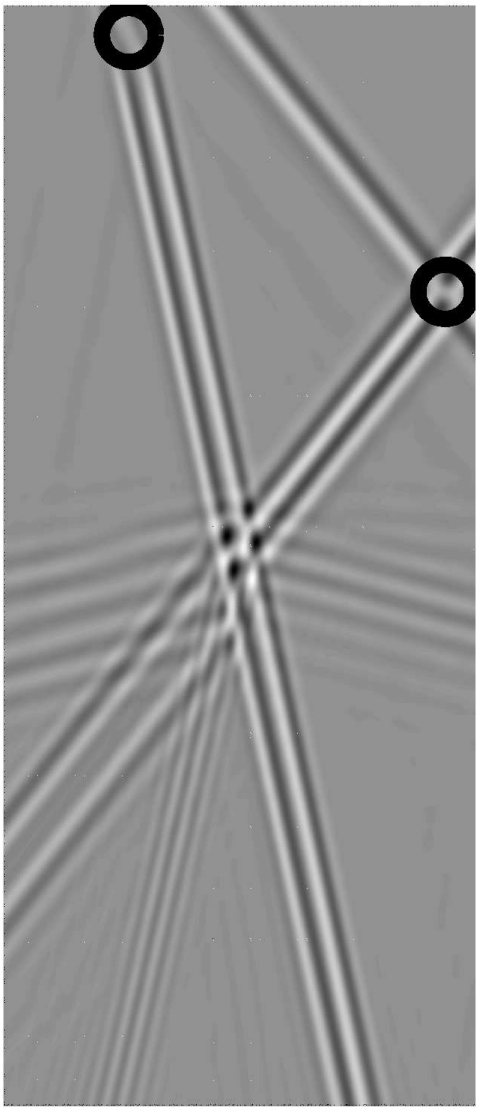

Figure 4.3 Numerical simulations of physical beams, shown by the magnitude of their horizontal velocities, ω_y. The primary beam sources lie within the circles approaching the origin from quadrant I (labelled 0) and II (labelled 2). Each primary beam has its own frequencies of $\pm\omega^{in}$ with $N = 1.5394$ rad/s $< |\omega^{in}(2)| = 1.9764$ rad/s $< |\omega^{in}(0)| = 3.9803$ rad/s $< f = 6.1575$ rad/s and $|\chi| = 0.4965 < 1/2$. From Table 4.7, the "high frequency" harmonics should propagate into quadrant III and IV and the "low frequency" harmonics should only emanate into quadrant III. The numerical simulation verifies the theoretical selection rules.

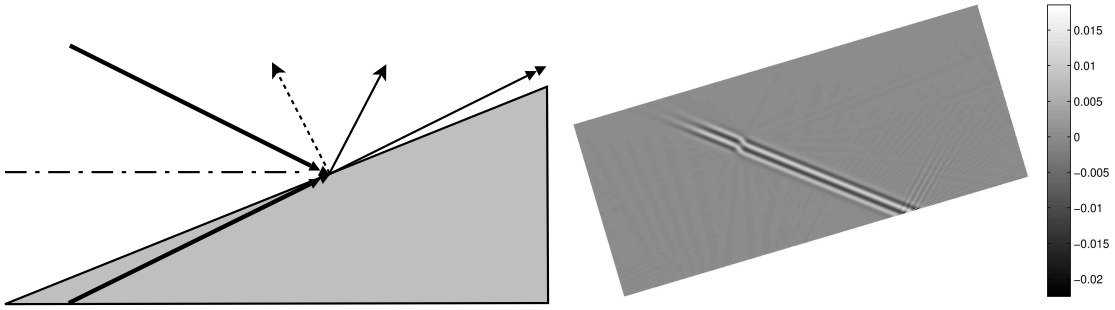

(a) (b)

Figure 4.4 Schematic (not to scale) and numerical simulation of physical beams, shown by the magnitude of their vertical velocities of super-critical reflection. In the numerical simulation, the incoming beam has frequency of $\pm\omega$ with $N = 1.5394$ rad/s $> |\omega| = 0.6781$ rad/s $> f = 0.3848$ rad/s. The incoming beam angle is 22° and the slope angle is 16.5° measured from the nearest horizontal axis. The slope is shaded in gray in the schematic. (a) (left) Schematic of supercritical reflection: The thick, double-headed arrow outside the slope is the primary incoming beam and that lies inside the slope is the image beam. The thin, double-headed arrow represents the primary reflected beam. The thin, single-headed arrow shows the only one second harmonic beam allowed and the dashed, single-headed arrow shows the non-existed second harmonic beam. (b) (right) The numerical simulation confirms that only one harmonic beam is produced.

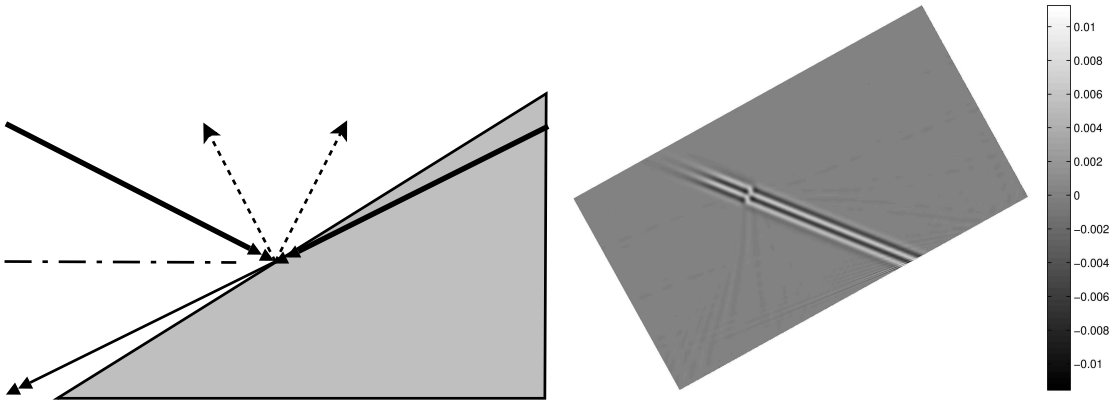

(a) (b)

Figure 4.5 Schematic (not to scale) and numerical simulation of physical beams, shown by the magnitude of their vertical velocities of sub-critical reflection. In the numerical simulation, the incoming beam has frequency of $\pm\omega$ with $N = 1.5394$ rad/s $> |\omega| = 0.6781$ rad/s $> f = 0.3848$ rad/s. The incoming beam angle is 22° and the slope angle is 29° measured from the nearest horizontal axis. The slope is shaded in gray in the schematic. (a) (left) Schematic of subcritical reflection: The thick, double-headed arrow outside the slope is the primary incoming beam and that lies inside the slope is the image beam. The thin, double-headed arrow represents the primary reflected beam. The dashed, single-headed arrows show the non-existed second harmonic beam. (b) (right) The numerical simulation confirms that no harmonics are produced.

Chapter 5

Selection Rules for Three-Dimensional Inertia-Gravity Waves

5.1 Introduction

The observation of the low-mode internal tides (internal waves at tidal frequency) is complicated by the interactions of waves produced by multiple generation sites, e.g. (Zhao and Alford, 2009) and (Rainville et al., 2010). In (Rainville et al., 2010), the authors pointed out that although wave interference is not a new concept in oceanography and physics but there is little documentation advocated to interference of internal tides. This chapter is devoted to fill a gap in the fundamental research of the nonlinear interaction of internal waves.

5.2 Three dimensional inertia-gravity wave physics

The dispersion relation for three-dimensional internal gravity wave with rotational effect can be written in the form, recall [Eq. (2.2)],

$$\omega^2 = \frac{k_\perp^2}{k^2} N^2 + \frac{k_z^2}{k^2} f^2 \tag{5.1}$$

where ω is the forcing frequency, N is the Brunt-Väisälä frequency or the buoyancy frequency and f is the Coriolis parameter or the inertial frequency ($\mathbf{f} = f\,\mathbf{z}$). $k_\perp \equiv \sqrt{k_x^2 + k_y^2}$ and k_z is the horizontal and vertical wave number respectively and $k^2 \equiv k_\perp^2 + k_z^2$. The Cartesian coordinate system is chosen in the way that the apex of the conical wave is the origin and the vertical axis is parallel to the gravity. θ is the angle between the conical wave and the horizontal plane passing through the apex such that $0 < \theta < \pi/2$. The geometric form of the

dispersion relation which is more useful in deriving the selection rules is defined as follows,

$$\cos^2\theta = \frac{k_z^2}{k^2} = \frac{N^2-\omega^2}{N^2-f^2}, \tag{5.2a}$$

$$\sin^2\theta = \frac{k_\perp^2}{k^2} = \frac{\omega^2-f^2}{N^2-f^2}, \tag{5.2b}$$

$$\tan^2\theta = \frac{k_\perp^2}{k_z^2} = \frac{\omega^2-f^2}{N^2-\omega^2}. \tag{5.2c}$$

The phase velocity $\mathbf{c}_\mathrm{p}$ and group velocity $\mathbf{c} \equiv \nabla_\mathbf{k}\,\omega = c_x\,\mathbf{x} + c_y\,\mathbf{y} + c_z\,\mathbf{z}$ obeying the dispersion relation are

$$\mathbf{c}_\mathrm{p} = \frac{1}{k^2}(\omega\,k_x\,\mathbf{x} + \omega\,k_y\,\mathbf{y} + \omega\,k_z\,\mathbf{z}), \tag{5.3}$$

and

$$\mathbf{c} = \frac{N^2-f^2}{\omega^2\,k^2}(\cos^2\theta\,\omega\,k_x\,\mathbf{x} + \cos^2\theta\,\omega\,k_y\,\mathbf{y} - \sin^2\theta\,\omega\,k_z\,\mathbf{z}) \tag{5.4}$$

$$= \frac{N^2-\omega^2}{\omega^2\,k^2}(\omega\,k_x\,\mathbf{x} + \omega\,k_y\,\mathbf{y} - \tan^2\theta\,\omega\,k_z\,\mathbf{z}). \tag{5.5}$$

Also the ratio between the components of group velocity is:

$$c_x : c_y : c_z = k_x : k_y : -\tan^2\theta\,k_z = \omega\,k_x : \omega\,k_y : -\tan^2\theta\,\omega\,k_z. \tag{5.6}$$

It is straightforward to show that the phase velocity is orthogonal to the group velocity since $\mathbf{c}_\mathrm{p}\cdot\mathbf{c} = 0$. The dispersion relation actually allows two branches of inertia-gravity waves. The first branch which is the most-studied, traditional branch has $f^2 < N^2$. A well-known example of this branch is the IGW propagating in the deep ocean. Another branch which is the less-studied, non-traditional branch has $N^2 < f^2$. The "non-traditional" branch (Gerkema and Exarchou, 2008; van Haren and Millot, 2004; van Haren, 2006) pretty much is ignored in oceanography since it requires very weak stratification which is not valid in most of the ocean on earth (one counter-example, see (van Haren and Millot, 2004), is the Algerian Basin of the Western Mediterranean Sea). But it is important in astrophysics that IGW, which has been shown in numerical simulations, is able to transfer angular momentum effectively radially outward and create vortices far away from the protoplanetary disk in the planet formation process.

Recall $\Psi \equiv \mathrm{sgn}\{N^2-f^2\}$, the signum function of N^2-f^2, such that the traditional branch is with $\Psi = +1$ and the non-traditional branch corresponds to $\Psi = -1$. $\tan\theta$ is a monotonically increasing (decreasing) function of the absolute value of forcing frequency, $|\omega|$, for traditional (non-traditional) branch:

$$\tan\theta_1 > \tan\theta_2 \text{ if } |\omega_1| > |\omega_2| \text{ and } \Psi = +1, \tag{5.7}$$

$$\tan\theta_1 < \tan\theta_2 \text{ if } |\omega_1| > |\omega_2| \text{ and } \Psi = -1, \tag{5.8}$$

because

$$\frac{d\tan^2\theta}{d\omega} = \frac{2\omega\,(N^2 - f^2)}{(N^2 - \omega^2)^2}.$$

According to [Eqs. (5.3) and (5.5)], the group velocity and "frequency modified wave vector", $\omega\,\mathbf{k}$, have the following relations:

$$\begin{aligned} \mathrm{sgn}\{c_x\}\,\mathrm{sgn}\{\omega\,k_x\} &= +\Psi, \\ \mathrm{sgn}\{c_y\}\,\mathrm{sgn}\{\omega\,k_y\} &= +\Psi, \\ \mathrm{sgn}\{c_z\}\,\mathrm{sgn}\{\omega\,k_z\} &= -\Psi. \end{aligned}$$

By using dispersion relation [Eq. (5.2c)], group velocity [Eq. (5.5)] is actually a function of $\omega\,k_z$ only because

$$\mathbf{c} = \frac{|N^2 - \omega^2|\,\Psi}{(\omega\,k_z)^2\,(\tan^2\theta + 1)}(|\omega\,k_z|\tan\theta\,\Psi\cos\phi\,\mathbf{x} + |\omega\,k_z|\tan\theta\,\Psi\sin\phi\,\mathbf{y} - \tan^2\theta\,(\omega\,k_z)\,\mathbf{z}), \quad (5.9)$$

where $\phi \in [0, 2\pi]$ is the azimuthal angle of the group velocity vector relative to the IGW source. And

$$\begin{aligned} \omega\,k_x &= |\omega\,k_z|\,\tan\theta\,\Psi\,\cos\phi, \\ \omega\,k_y &= |\omega\,k_z|\,\tan\theta\,\Psi\,\sin\phi, \end{aligned}$$

since $k_\perp^2 = k_z^2\tan^2\theta$, following [Eq. (5.2c)]. The key point is to recognize that the group velocity is parallel to the position vector measured from the IGW source. If the coordinates of the intersection points of two double conical waves are determined, the group velocities from two sources are known up to a constant (i.e. the magnitude of the group velocity vector) and the frequency modified wave vectors are also known.

The interference or interaction patterns of two intersecting IGWs located at $(0, 0, 0)$ and $(2H, 0, V)$ are observed analytically here. The origin of the coordinate system are chosen to be the apex of the first source. The x-coordinate is rotated to be parallel to the center line connecting the two sources. Without loss of generality, H and V are positive by definition and cannot be equal to zero at the same time. Also assume the magnitude of the forcing frequency of the first source is not less than that of the second source, i.e. $|\omega_1| \geq |\omega_2|$.

If the intersection point is at (x_I, y_I, z_I), the azimuthal angles, ϕ_1, ϕ_2, relative to the sources are

$$\cos\phi_1 = \frac{x_I}{r_1}, \sin\phi_1 = \frac{y_I}{r_1},$$

and

$$\cos\phi_2 = \frac{x_I - 2H}{r_2}, \sin\phi_2 = \frac{y_I}{r_2},$$

where $r_1 = \sqrt{x_I^2 + y_I^2} = |z_I|\cot\theta_1$ and $r_2 = \sqrt{(x_I - 2H)^2 + y_I^2} = |(z_I - V)|\cot\theta_2$ are the distances between the intersection point and sources. The three typical geometric patterns,

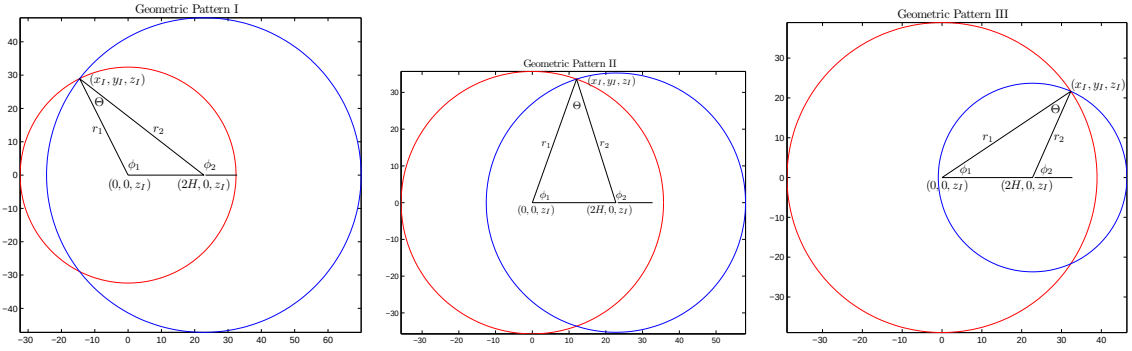

(a) (b) (c)

Figure 5.1 Three intersection patterns. (a) (left) Geometric pattern I. At certain z_I, the two conical internal gravity waves intersect at some $x_I < 0$. The red circle is the locus of internal gravity wave emitted from source number 1 located at $(0, 0, 0)$. The blue circle is the locus of internal gravity wave emitted from source number 2 located at $(2H = 22.7398 \text{ cm}, 0, V = 35.5325 \text{ cm})$. Brunt-Väisälä frequency is 1.5394 rad s^{-1} and Coriolis parameter equals to a quarter of Brunt-Väisälä frequency. Source number 1 is forced at frequency $\omega_1 = 0.9351$ rad s^{-1}. Forcing frequency of source number 2 is $\omega_1/2$. Under these settings, $\alpha_2 > \alpha_1 > 1$. For every pair of α_1 and α_2 that yields $x_I < 0$ (although $\alpha_2 > \alpha_1 > 1$ is used to generate this schematics), $\cos\Theta$ is always greater than zero because r_2 is always greater than $2H$ in this configuration. (b) (middle) Geometric pattern II. Parameters are the same as in Fig. 5.1(a). But at a different z_I, the two conical internal gravity waves intersect at $0 < x_I < 2H$. In this configuration, range of $\cos\Theta$ varies considerably from case to case. (c) (right) Geometric pattern III. Parameters are the same as in Fig. 5.1(a). But at another different z_I, the two conical internal gravity waves intersect at $x_I > 2H$. For every pair of α_1 and α_2 yields $x_I > 2H$, $\cos\Theta$ is always greater than zero because r_1 is always greater than $2H$ in this configuration.

(I) $x_I < 0$, (II) $0 < x_I < 2H$ and (III) $x_I > 2$, are illustrated in (Fig. 5.1(a), 5.1(b) and 5.1(c)).

With the knowledge of the coordinates of an intersection point, the frequency modified wave vectors of both IGWs, $\omega_1 \mathbf{k}_1$ and $\omega_2 \mathbf{k}_2$, can be expressed in terms of the azimuthal angles ϕ_1, ϕ_2, absolute values of the polar angles θ_1, θ_2, the vertical components of the wave vectors and the utility variable, Ψ:

$$\begin{aligned}
\omega_1 k_{x,1} &= \cos\phi_1 \tan\theta_1 |\omega_1 k_{z,1}| \Psi, \\
\omega_2 k_{x,2} &= \cos\phi_2 \tan\theta_2 |\omega_2 k_{z,2}| \Psi, \\
\omega_1 k_{y,1} &= \sin\phi_1 \tan\theta_1 |\omega_1 k_{z,1}| \Psi, \\
\omega_2 k_{y,2} &= \sin\phi_2 \tan\theta_2 |\omega_2 k_{z,2}| \Psi,
\end{aligned}$$

and

$$\begin{aligned}\omega_1\, k_{z,1} &= -\mathrm{sgn}\{z_I\}\,|\omega_1\, k_{z,1}|\,\Psi,\\ \omega_2\, k_{z,2} &= -\mathrm{sgn}\{z_I - V\}\,|\omega_2\, k_{z,2}|\,\Psi.\end{aligned}$$

The nonlinear interactions of the two sources would possibly generate harmonics at two frequencies. One would be the sum and the other would be the difference of the intersecting IGWs frequencies. The "high frequency" harmonics have frequencies with $\pm\omega_{\mathrm{sum}}$ and the "low frequency" harmonics are forcing at $\pm\omega_{\mathrm{diff}}$ where $\omega_{\mathrm{sum}} \equiv |\omega_1| + |\omega_2|$ and $\omega_{\mathrm{diff}} \equiv |\omega_1| - |\omega_2| > 0$. The quadratic nonlinearities require that the frequencies and wave vectors of harmonics being the sum of the frequencies and wave vectors of the incoming IGWs:

$$\omega^{\mathrm{H}} = \omega_1 + \omega_2, \tag{5.10}$$

$$\mathbf{k}^{\mathrm{H}} = \mathbf{k}_1 + \mathbf{k}_2, \tag{5.11}$$

where "H" stands for "Harmonics" and ω^{H} is either $\pm\omega_{\mathrm{sum}}$ or $\pm\omega_{\mathrm{diff}}$.

Rewrite [Eq. (5.11)] in component form:

$$\begin{aligned}k_x^{\mathrm{H}} &= k_{x,1} + k_{x,2} = (\omega_1\, k_{x,1})/\omega_1 + (\omega_2\, k_{x,2})/\omega_2,\\ k_y^{\mathrm{H}} &= k_{y,1} + k_{y,2} = (\omega_1\, k_{y,1})/\omega_1 + (\omega_2\, k_{y,2})/\omega_2,\\ k_z^{\mathrm{H}} &= k_{z,1} + k_{z,2} = (\omega_1\, k_{z,1})/\omega_1 + (\omega_2\, k_{z,2})/\omega_2,\end{aligned}$$

and therefore the frequency modified wave vectors for the harmonic waves written in terms of $k_{z,1}$, $k_{z,2}$ are

$$\begin{aligned}\omega^{\mathrm{H}}\, k_x^{\mathrm{H}} &= \omega^{\mathrm{H}} \left(\cos\phi_1\ \tan\theta_1 \tfrac{|\omega_1\, k_{z,1}|}{\omega_1} + \cos\phi_2\ \tan\theta_2 \tfrac{|\omega_2\, k_{z,2}|}{\omega_2}\right)\ \Psi,\\ \omega^{\mathrm{H}}\, k_y^{\mathrm{H}} &= \omega^{\mathrm{H}} \left(\sin\phi_1\ \tan\theta_1 \tfrac{|\omega_1\, k_{z,1}|}{\omega_1} + \sin\phi_2\ \tan\theta_2 \tfrac{|\omega_2\, k_{z,2}|}{\omega_2}\right)\ \Psi,\\ \omega^{\mathrm{H}}\, k_z^{\mathrm{H}} &= \omega^{\mathrm{H}} \left(-\mathrm{sgn}\{z_I\} \tfrac{|\omega_1\, k_{z,1}|}{\omega_1} - \mathrm{sgn}\{z_I - V\} \tfrac{|\omega_2\, k_{z,2}|}{\omega_2}\right)\ \Psi.\end{aligned} \tag{5.12}$$

Instead of working on $k_{z,1}$ and $k_{z,2}$ directly, it is more succinct to use $k_{z,2}$ and $R \equiv |k_{z,1}|/|k_{z,2}| > 0$, the ratio between vertical components of wave vectors of two intersecting double conical waves. It will be shown later that the dispersion relation is function of R only. The ratio between two forcing frequencies, $\chi \equiv \omega_2/\omega_1$, is proved to be useful later, too.

[Eq. (5.12)] can be simplified in accordance with $\omega_1\,\omega_2 > 0$ or $\omega_1\,\omega_2 < 0$ and by using the above definitions. For $\omega_1\,\omega_2 > 0$ or equivalently $\chi > 0$,

$$\begin{aligned}\mathcal{K}_x^{\mathrm{S}} &= (\cos\phi_1 \tan\theta_1 R + \cos\phi_2 \tan\theta_2),\\ \mathcal{K}_y^{\mathrm{S}} &= (\sin\phi_1 \tan\theta_1 R + \sin\phi_2 \tan\theta_2),\\ \mathcal{K}_z^{\mathrm{S}} &= (-\mathrm{sgn}\{z_I\} R - \mathrm{sgn}\{z_I - V\}),\\ \omega^{\mathrm{H}}\ (k_x^{\mathrm{H}},\ k_y^{\mathrm{H}},\ k_z^{\mathrm{H}}) &= (\mathcal{K}_x^{\mathrm{S}},\ \mathcal{K}_y^{\mathrm{S}},\ \mathcal{K}_z^{\mathrm{S}})\ (\Psi\ |k_{z,2}|\ \omega_{\mathrm{sum}}),\\ (c_x)^{\mathrm{S}} : (c_y)^{\mathrm{S}} : (c_z)^{\mathrm{S}} &= \mathcal{K}_x^{\mathrm{S}} : \mathcal{K}_y^{\mathrm{S}} : -\tan^2\theta^{\mathrm{S}}\, \mathcal{K}_z^{\mathrm{S}},\end{aligned}$$

and for $\omega_1\,\omega_2 < 0$ or equivalently $\chi < 0$,

$$\begin{aligned}
\mathcal{K}_x^{\mathrm{D}} &= (\cos\phi_1 \tan\theta_1 R - \cos\phi_2 \tan\theta_2),\\
\mathcal{K}_y^{\mathrm{D}} &= (\sin\phi_1 \tan\theta_1 R - \sin\phi_2 \tan\theta_2),\\
\mathcal{K}_z^{\mathrm{D}} &= (-\mathrm{sgn}\{z_I\} R + \mathrm{sgn}\{z_I - V\}),\\
\omega^{\mathrm{H}}\ (k_x^{\mathrm{H}},\ k_y^{\mathrm{H}},\ k_z^{\mathrm{H}}) &= (\mathcal{K}_x^{\mathrm{D}},\ \mathcal{K}_y^{\mathrm{D}},\ \mathcal{K}_z^{\mathrm{D}})\ (\Psi\ |k_{z,2}|\ \omega_{\mathrm{diff}}),\\
(c_x)^{\mathrm{D}} : (c_y)^{\mathrm{D}} : (c_z)^{\mathrm{D}} &= \mathcal{K}_x^{\mathrm{D}} : \mathcal{K}_y^{\mathrm{D}} : -\tan^2\theta^{\mathrm{D}}\,\mathcal{K}_z^{\mathrm{D}}.
\end{aligned}$$

The relation between $\mathcal{K}$'s and the group velocity which is a function of R only is very important:

$$\begin{aligned}
\mathrm{sgn}\{(c_x)^{\mathrm{H}}\} &= \mathrm{sgn}\{\mathcal{K}_x^{\mathrm{H}}\},\\
\mathrm{sgn}\{(c_y)^{\mathrm{H}}\} &= \mathrm{sgn}\{\mathcal{K}_y^{\mathrm{H}}\},\\
\mathrm{sgn}\{(c_z)^{\mathrm{H}}\} &= -\mathrm{sgn}\{\mathcal{K}_z^{\mathrm{H}}\},
\end{aligned} \tag{5.13}$$

where 'H' can be either 'S' or 'D'.

The harmonics are also required to satisfy their own dispersion relations in geometric form [Eq. (5.2c)] respectively so that lead to quadratic equations in R,

$$\tan^2\theta^{\mathrm{S}} = \frac{(\mathcal{K}_x^{\mathrm{S}})^2 + (\mathcal{K}_y^{\mathrm{S}})^2}{(\mathcal{K}_z^{\mathrm{S}})^2} \Rightarrow \mathrm{A}^{\mathrm{S}}\,R^2 - 2\,\mathrm{B}^{\mathrm{S}}\,R + \mathrm{C}^{\mathrm{S}} = 0, \tag{5.14}$$

if $\omega_1\,\omega_2 > 0$ or $\chi > 0$ and

$$\tan^2\theta^{\mathrm{D}} = \frac{(\mathcal{K}_x^{\mathrm{D}})^2 + (\mathcal{K}_y^{\mathrm{D}})^2}{(\mathcal{K}_z^{\mathrm{D}})^2} \Rightarrow \mathrm{A}^{\mathrm{D}}\,R^2 - 2\,\mathrm{B}^{\mathrm{D}}\,R + \mathrm{C}^{\mathrm{D}} = 0, \tag{5.15}$$

if $\omega_1\,\omega_2 < 0$ or $\chi < 0$. The exact definitions of B^{S}, B^{D}, $\mathcal{K}_z^{\mathrm{S}}$ and $\mathcal{K}_z^{\mathrm{D}}$ are listed in Table 5.1 because of their dependencies on z_I. But the formal definitions of A^{S}, A^{D}, C^{S}, C^{D} and $\cos\Theta$ are independent of z_I:

$$\begin{aligned}
\mathrm{A}^{\mathrm{S}} &\equiv \Psi\,(\tan^2\theta^{\mathrm{S}} - \tan^2\theta_1) > 0,\\
\mathrm{C}^{\mathrm{S}} &\equiv \Psi\,(\tan^2\theta^{\mathrm{S}} - \tan^2\theta_2) > 0,\\
\mathrm{A}^{\mathrm{D}} &\equiv \Psi\,(\tan^2\theta_1 - \tan^2\theta^{\mathrm{D}}) > 0,\\
\mathrm{C}^{\mathrm{D}} &\equiv \Psi\,(\tan^2\theta_2 - \tan^2\theta^{\mathrm{D}}) \begin{cases} < 0 & |\chi| < 1/2 \\ = 0 & |\chi| = 1/2 \\ > 0 & |\chi| > 1/2 \end{cases},\\
\cos\Theta &\equiv \cos\phi_1\cos\phi_2 + \sin\phi_1\sin\phi_2 = \cos\left(\phi_2 - \phi_1\right).
\end{aligned}$$

A quadratic equation has real roots if its discriminant is positive or zero. Accordingly, discriminants of [Eqs. (5.14) and (5.15)] are greater than or equal to zero is a necessary condition for R to be positive:

$$\Delta^{\mathrm{S}} = (\mathrm{B}^{\mathrm{S}})^2 - \mathrm{A}^{\mathrm{S}}\,\mathrm{C}^{\mathrm{S}} \geq 0, \Delta^{\mathrm{D}} = (\mathrm{B}^{\mathrm{D}})^2 - \mathrm{A}^{\mathrm{D}}\,\mathrm{C}^{\mathrm{D}} \geq 0.$$

Table 5.1 Definitions of $\mathcal{K}_z^{\rm S}$, $\mathcal{K}_z^{\rm D}$, $\mathrm{B}_z^{\rm S}$ and $\mathrm{B}_z^{\rm D}$ for z_I at different ranges. $0 < z_I < V$ collapses into empty set when $V \equiv 0$.

	$z_I > V, \eta > 1, \zeta > 0$ or $z_I, \eta, \zeta < 0$	$0 < z_I < V, 0 < \eta < 1$
$\mathcal{K}_z^{\rm S}$	$\mathrm{sgn}\{\eta \text{ or } \zeta\}\,(-R-1)$	$-R+1$
$\mathcal{K}_z^{\rm D}$	$\mathrm{sgn}\{\eta \text{ or } \zeta\}\,(-R+1)$	$-R-1$
$\mathrm{B}_z^{\rm S}$	$\Psi\,(\tan\theta_1\tan\theta_2\cos\Theta - \tan^2\theta^{\rm S})$	$\Psi\,(\tan\theta_1\tan\theta_2\cos\Theta + \tan^2\theta^{\rm S})$
$\mathrm{B}_z^{\rm D}$	$\Psi\,(\tan\theta_1\tan\theta_2\cos\Theta - \tan^2\theta^{\rm D})$	$\Psi\,(\tan\theta_1\tan\theta_2\cos\Theta + \tan^2\theta^{\rm D})$

The roots then are given by the quadratic formula:

$$R^{\rm S,\pm} = \frac{\mathrm{B}^{\rm S} \pm \sqrt{\Delta^{\rm S}}}{\mathrm{A}^{\rm S}}, R^{\rm D,\pm} = \frac{\mathrm{B}^{\rm D} \pm \sqrt{\Delta^{\rm D}}}{\mathrm{A}^{\rm D}}.$$

Both $R^{\rm S,\pm}$ and $R^{\rm D,\pm}$ are needed to be positive in order not to violate the definition of R. Each R corresponds to an internal gravity wave beam because frequency modified wave vector is a constant vector multiplied by $|\omega\, k_{z,2}|$ and the group velocity is another constant vector divided by $|\omega\, k_{z,2}|$ once R is fixed. In other words, the group velocities for different $k_{z,2}$'s with the same R are parallel to each other, i.e. forming a beam.

Lemma 2 *[Eqs. (5.14) and (5.15)] lead to another drastic conclusion that for each harmonic frequency ($\omega_1 + \omega_2$ or $\omega_1 - \omega_2$) at most there are only* TWO BEAMS*, not a double conical wave, generated from quadratic nonlinearities at each intersection point.*

The discriminants can be written in various equivalent forms (in the following formulas, 'H' can be either 'S' or 'D'):

$$\begin{aligned}
\Delta^{\rm H} &\equiv (\tan\theta_1\tan\theta_2\cos\Theta \pm \tan^2\theta^{\rm H})^2 \\
&- (\tan^2\theta^{\rm H} - \tan^2\theta_1)(\tan^2\theta^{\rm H} - \tan^2\theta_2) \qquad (5.16)\\
\Rightarrow \Delta^{\rm H} &= (\tan\theta_1\tan\theta_2\cos\Theta \pm \tan^2\theta^{\rm H})^2 \\
&- (\tan\theta_1\tan\theta_2 \quad - \tan^2\theta^{\rm H})^2 + \tan^2\theta^{\rm H}(\tan\theta_1 - \tan\theta_2)^2 \qquad (5.17)\\
\Rightarrow \Delta^{\rm H} &= (\tan\theta_1\tan\theta_2\cos\Theta \pm \tan^2\theta_1)^2 \\
&+ (\tan^2\theta^{\rm H} - \tan^2\theta_1)\underbrace{(\tan^2\theta_1 \pm 2\tan\theta_1\tan\theta_2 + \tan^2\theta_2)}_{>0}, \qquad (5.18)
\end{aligned}$$

where

$$\Delta^{\rm H} \begin{cases} > (\tan\theta_1\tan\theta_2\cos\Theta \pm \tan^2\theta_1)^2 & \text{if } \tan^2\theta^{\rm H} > \tan^2\theta_1 \\ < (\tan\theta_1\tan\theta_2\cos\Theta \pm \tan^2\theta_1)^2 & \text{if } \tan^2\theta^{\rm H} < \tan^2\theta_1 \end{cases}. \qquad (5.19)$$

Each form would be useful under different circumstances (e.g. to determine $\Delta^{\rm H} > 0$ or R is greater than unity or not which is used to determine the direction where the harmonics propagate into).

5.3 Selection rules, two sources forced at single frequency

As described before, the first source is always located at (0, 0, 0). But the position of the second source can be divided into three categories:

- Case I: $H = 0$, the horizontal distance between two sources is zero, the second source is located at (0, 0, V).
- Case II: $V = 0$, the vertical distance between two sources is zero, the second source is located at ($2H$, 0, 0).
- Case III: $H, V \neq 0$, most general case, the second source is located at ($2H$, 0, V).

Since the two sources are forced at single frequency, for simplicity set $\omega_1 = \omega_2 = \omega$ and $\theta_1 = \theta_2 = \theta$.

5.3.1 Case I: $H = 0$

The locus of the first IGW source in $z = z_I$ plane is

$$x_I^2 + y_I^2 = z_I^2 \cot^2\theta$$

and that of the second source is

$$x_I^2 + y_I^2 = (z_I - V)^2 \cot^2\theta.$$

The two double conical waves intersect only at $z_I = V/2$, thus $x_I^2 + y_I^2 = (V/2)^2 \cot^2\theta$. Therefore the locus of the intersection points is a circle in $z = V/2$ plane where $(x_I,\ y_I,\ z_I) = (V/2\cot\theta\cos\phi,\ V/2\cot\theta\sin\phi, V/2)$ and $\phi \in [0,\ 2\pi]$ is the azimuthal angle. $\cos\Theta$ can be determined easily since $\cos\phi_1 = \cos\phi_2 = \cos\phi$ and $\sin\phi_1 = \sin\phi_2 = \sin\phi$. This leads to $\cos\Theta = \cos^2\phi + \sin^2\phi = 1$. Each intersection point is acting like the collision point in two-dimensional colliding beams problem. The interaction scenario is analogous to $j = 4$ case studied in Chapter 4: both incoming beams are propagating horizontally in the same direction but vertically in opposite directions. From Tables 4.6 and 4.7, one would expect harmonics are produced for $\Psi = +1$ and harmonics are forbidden if $\Psi = -1$.

Since $0 < z_I < V$, it turns out that $\mathrm{B}^{\mathrm{S}} = \Psi\,(\tan^2\theta^{\mathrm{S}} + \tan^2\theta)$ and $\Delta^{\mathrm{S}} = 4\tan^2\theta^{\mathrm{S}}\tan^2\theta > 0$ by using Table 5.1 and assigning $\cos\Theta = 1$. Therefore,

$$R^{\mathrm{S},\pm} = \frac{(\tan\theta^{\mathrm{S}} \pm \Psi\tan\theta)^2}{\tan^2\theta^{\mathrm{S}} - \tan^2\theta}. \tag{5.20}$$

(A) $\Psi = +1$

From [Eq. (5.7)] and applying $|\omega^{\mathrm{H}}| = 2|\omega| > |\omega|$, $\tan\theta^{\mathrm{S}} > \tan\theta$ thus

$$\begin{aligned} R^{\mathrm{S},+} &= \frac{\tan\theta^{\mathrm{S}} + \tan\theta}{\tan\theta^{\mathrm{S}} - \tan\theta} > 1 \Rightarrow \mathcal{K}_z^{\mathrm{S}} < 0 \Rightarrow (c_z)^{\mathrm{S},+} > 0, \\ 0 < R^{\mathrm{S},-} &= \frac{\tan\theta^{\mathrm{S}} - \tan\theta}{\tan\theta^{\mathrm{S}} + \tan\theta} < 1 \Rightarrow \mathcal{K}_z^{\mathrm{S}} > 0 \Rightarrow (c_z)^{\mathrm{S},-} < 0. \end{aligned}$$

By using the facts that $\mathrm{sgn}\{\mathcal{K}_z^{\mathrm{S}}\} = \mathrm{sgn}\{-R+1\}$ from Table 5.1, $R^{\mathrm{S},+} > 1$ and $\mathrm{sgn}\{c_z\} = -\mathrm{sgn}\{\mathcal{K}_z^{\mathrm{S}}\}$ from [Eq. (5.13)], the corresponding vertical direction group velocity thus is greater than zero, i.e. the beam is propagating upward. On the other hand, the beam corresponds to $0 < R^{\mathrm{S},-} < 1$ is propagating downward using the same procedures. Since $\mathcal{K}_x^{\mathrm{S}} = \cos\phi\,\tan\theta\,(R+1) > 0$ and $\mathcal{K}_y^{\mathrm{S}} = \sin\phi\,\tan\theta\,(R+1) > 0$, $c_y/c_x = \sin\phi/\cos\phi$ by using [Eq. (5.6)]. Therefore the harmonics are going radially outward. *One of the two harmonic beams is propagating upward and radially outward. The other beam is propagating downward and radially outward.*

(B) $\Psi = -1$

In this case, $\tan\theta^{\mathrm{S}} < \tan\theta$ holds instead. The numerator of [Eq. (5.20)] is always positive but the denominator is less than zero so that $R < 0$ which violates the definition of $R > 0$. Therefore *no harmonics are generated if* $\Psi = -1$ *(non-traditional branch:* $f^2 > N^2$*).*

$$R^{\mathrm{S},\pm} = \frac{\overbrace{(\tan\theta^{\mathrm{S}} \mp \tan\theta)^2}^{>0}}{\underbrace{\tan^2\theta^{\mathrm{S}} - \tan^2\theta}_{<0}} < 0.$$

5.3.2 Case II: $V = 0$

The locus of the first IGW source in $z = z_I$ plane is $x_I^2 + y_I^2 = z_I^2\,\cot^2\theta$ and that of the second source is $(x_I - 2H)^2 + y_I^2 = z_I^2\,\cot^2\theta$. The two IGWs thus intersect if $z_I^2 \geq H^2\,\tan^2\theta$. The coordinates of intersection points are $(H, \pm W, z_I)$ where $W \equiv \sqrt{z_I^2\cot^2\theta - H^2}$. Because $W = 0$ when $z_I^2 = H^2\,\tan^2\theta$, the two double conical waves first come into contact in a single point. Since the coordinates are known, $\cos\phi_1 = H/r$, $\cos\phi_2 = -H/r$ and $\sin\phi_1 = \sin\phi_2 = \pm W/r$ where $r^2 \equiv H^2 + W^2$ are also determined. Therefore, the analytical form of $\cos\Theta$ can be obtained:

$$\cos\Theta = \frac{W^2 - H^2}{W^2 + H^2}.$$

When $z_I \to \pm H\tan\theta$, $\cos\Theta \to -1$ and $z_I \to \pm\infty$, $\cos\Theta \to 1$, the range of $\cos\Theta$ is $[-1, +1]$. Only the case that $y_I > 0$ and $z_I > 0$ is considered here since the selection rules can be derived using symmetric properties for all other intersection points with $y_I < 0$ or

$z_I < 0$. The intersection points that have $z_I = \pm H \tan\theta$ are analogous to $j = 2$ case in Chapter 4 (after applying reflection symmetry about the x-axis): both incoming beams are propagating vertically in the same direction but horizontally in opposite directions. But when z_I gradually moves away from $\pm H \tan\theta$, the interaction starts to deviate from the two-dimensional collision scenario. From Tables 4.6 and 4.7, one would expect harmonics are not produced for $\Psi = +1$ and harmonics are produced if $\Psi = -1$ and the intersection points are not too far away from $\pm H \tan\theta$.

Since $0 < z_I < V$, it turns out that $\mathrm{B}^{\mathrm{S}} = \Psi(\tan^2\theta\cos\Theta - \tan^2\theta^{\mathrm{S}})$ from Table 5.1 and the discriminant is

$$\begin{aligned}
\Delta^{\mathrm{S}} &= (\tan^2\theta\cos\Theta - \tan^2\theta^{\mathrm{S}})^2 - (\tan^2\theta^{\mathrm{S}} - \tan^2\theta)^2 \\
&< (\tan^2\theta\cos\Theta - \tan^2\theta^{\mathrm{S}})^2 = (\mathrm{B}^{\mathrm{S}})^2, \\
\Delta^{\mathrm{S}} &= [\tan^2\theta \underbrace{(\cos\Theta - 1)}_{\leq 0}][\tan^2\theta(\cos\Theta + 1) - 2\tan^2\theta^{\mathrm{S}}].
\end{aligned}$$

(A) $\Psi = +1$

Since $\tan\theta^{\mathrm{S}} > \tan\theta$ and accordingly $[\tan^2\theta(\cos\Theta + 1) - 2\tan^2\theta^{\mathrm{S}}] < 0$, Δ^{S} is always greater or equal to zero, $\Delta^{\mathrm{S}} \geq 0$.

Applying $\Delta^{\mathrm{S}} < \left(\mathrm{B}^{\mathrm{S}}\right)^2$ and $\mathrm{B}^{\mathrm{S}} < 0$ to calculate $R^{\mathrm{S},\pm}$ gives:

$$R^{\mathrm{S},\pm} = \frac{\overbrace{(\tan^2\theta\cos\Theta - \tan^2\theta^{\mathrm{S}})}^{\mathrm{B}^{\mathrm{S}}<0} \pm \overbrace{\sqrt{\Delta^{\mathrm{S}}}}^{<|\mathrm{B}^{\mathrm{S}}|}}{\underbrace{\tan^2\theta^{\mathrm{S}} - \tan^2\theta}_{>0}} < 0$$

because no matter what the numerator is always less than zero. This contradicts the definition that $R > 0$. Therefore *there is no harmonic beam generated.*

(B) $\Psi = -1$

Since $\tan\theta^{\mathrm{S}} < \tan\theta$, Δ^{S} is greater or equal to zero only if $[\tan^2\theta(\cos\Theta+1) - 2\tan^2\theta^{\mathrm{S}}] \leq 0$, i.e.

$$\cos\Theta \leq -1 + \frac{2\tan^2\theta^{\mathrm{S}}}{\tan^2\theta},$$

and after rearrangement, the above inequality and the roots, R, have the following forms:

$$\tan^2\theta^{\mathrm{S}} - \tan^2\theta\cos\Theta \geq \tan^2\theta - \tan^2\theta^{\mathrm{S}} > 0,$$

$$R^{\mathrm{S},\pm} = \frac{\overbrace{(\tan^2\theta^{\mathrm{S}} - \tan^2\theta\cos\Theta)}^{\mathrm{B}^{\mathrm{S}}>0} \pm \overbrace{\sqrt{\Delta^{\mathrm{S}}}}^{<|\mathrm{B}^{\mathrm{S}}|}}{\underbrace{\tan^2\theta - \tan^2\theta^{\mathrm{S}}}_{>0}} > 0.$$

Applying [Eq. (A.1)], $\cos\Theta \leq -1/2$ (a very crude and conservative estimate) or accordingly $z_I^2 \leq (2H)^2 \tan^2\theta/3$. This means harmonics are permitted to generate while $|z_I|$ is in the neighborhood of $H\tan\theta$ although the two conical IGWs intersect from $|z_I| = H\tan\theta$ to ∞. Rewriting R and $\Delta^{\rm S}$ to determine R's are greater than unity or not lead to

$$\begin{aligned} R^{\rm S,\pm} &= 1 + \frac{[2\tan^2\theta^{\rm S} - \tan^2\theta(1+\cos\Theta)] \pm \sqrt{\Delta^{\rm S}}}{\tan^2\theta - \tan^2\theta^{\rm S}}, \\ \Delta^{\rm S} &= \{[\tan^2\theta\,(\cos\Theta+1) - 2\tan^2\theta^{\rm S}] \\ &- \underbrace{2(\tan^2\theta - \tan^2\theta^{\rm S})}_{>0}\} [\tan^2\theta\,(\cos\Theta+1) - 2\tan^2\theta^{\rm S}] \\ &> [2\tan^2\theta^{\rm S} - \tan^2\theta\,(\cos\Theta+1)]^2. \end{aligned}$$

Consequently, $R^{\rm S,+} > 1$, $0 < R^{\rm S,-} < 1$. In order to determine the direction of the group velocity, $\mathcal{K}$'s are needed to be determined first:

$$\begin{aligned} \mathcal{K}_x^{\rm S} &= (H/r)\,\tan\theta\,(R-1) \Rightarrow \mathcal{K}_x^{\rm S,+} > 0, \mathcal{K}_x^{\rm S,-} < 0, \\ \mathcal{K}_y^{\rm S} &= (W/r)\,\tan\theta\,(R+1) \Rightarrow \mathcal{K}_y^{\rm S,\pm} > 0, \\ \mathcal{K}_z^{\rm S} &= -R-1 \Rightarrow \mathcal{K}_z^{\rm S,\pm} < 0. \end{aligned}$$

The direction of the corresponding group velocity is

$$\begin{aligned} {\rm sgn}\{c_x\} = \quad {\rm sgn}\{\mathcal{K}_x^{\rm S}\} \quad &\Rightarrow \quad (c_x)^{\rm S,+} > 0,\ (c_x)^{\rm S,-} < 0, \\ {\rm sgn}\{c_y\} = \quad {\rm sgn}\{\mathcal{K}_y^{\rm S}\} \quad &\Rightarrow \quad (c_y)^{\rm S,\pm} > 0, \\ {\rm sgn}\{c_z\} = -{\rm sgn}\{\mathcal{K}_z^{\rm S}\} \quad &\Rightarrow \quad (c_z)^{\rm S,\pm} > 0. \end{aligned}$$

Each intersection point satisfying $\cos\Theta \leq -1 + 2\tan^2\theta^{\rm S}/\tan^2\theta$ *is acting like an IGW source emanating TWO BEAMS (NOT a double conical wave!) propagating upward. An observer sitting at the intersection point and facing north would only see one beam emanating rightward and another leftward in this case.*

5.3.3 Case III: $H, V \neq 0$

The derivation would rely on a non-dimensional parameter α and two non-dimensional variables $\xi,\ \eta$ where

$$\begin{aligned} \alpha &\equiv \frac{V}{2H\tan\theta} > 0, \\ \xi &\equiv \frac{x_I}{H}, \\ \eta &\equiv \frac{z_I}{V}. \end{aligned}$$

The range of intersection points is dependent on α. If $\alpha > 1$, the η-coordinate of the intersection points must satisfy

$$0 < \frac{1-\alpha^{-1}}{2} \leq \eta \leq \frac{1+\alpha^{-1}}{2} < 1, \tag{5.21}$$

and $\cos\Theta$ in this region is:

$$\cos\Theta = -1 + \frac{\alpha^2 - 1}{2\alpha^2\eta(1-\eta)}.$$

Thus, the range of $\cos\Theta$ can be determined to be $+1 \geq \cos\Theta \geq -\alpha^{-2} = \cos\Theta(\eta = 1/2)$ where $\cos\Theta(\eta = [1 \pm \alpha^{-1}]/2) = +1$.

On the other hand, if $0 < \alpha < 1$, the intersection point is either in

$$0 > \frac{1-\alpha^{-1}}{2} \geq \eta, \text{ or } \eta \geq \frac{1+\alpha^{-1}}{2} > 1, \tag{5.22}$$

and $\cos\Theta$ is in the form:

$$\cos\Theta = 1 - \frac{1-\alpha^2}{2\alpha^2\eta(\eta-1)}.$$

$\cos\Theta$ is in $[-1, +1]$ where $\cos\Theta(\eta = [1 \pm \alpha^{-1}]/2) = -1$ and $\cos\Theta(\eta \to \pm\infty) = +1$.

The non-dimensional coordinates of intersection points obey the following relation:

$$\xi = 1 + \alpha^2(2\eta - 1). \tag{5.23}$$

(A) $\alpha > 1$

[Eq. (5.21)] shows the intersection region is in $0 < \eta < 1$. From Table 5.1, this leads to

$$\mathrm{B^S} = \Psi(\tan^2\theta\cos\Theta + \tan^2\theta^{\mathrm{S}}),$$

and $\Delta^{\mathrm{S}} < (\mathrm{B^S})^2$ is obtained:

$$\begin{aligned}
\Delta^{\mathrm{S}} &= (\tan^2\theta\cos\Theta + \tan^2\theta^{\mathrm{S}})^2 - (\tan^2\theta^{\mathrm{S}} + \tan^2\theta)^2 \\
&< (\tan^2\theta\cos\Theta - \tan^2\theta^{\mathrm{S}})^2 = (\mathrm{B^S})^2, \\
\Delta^{\mathrm{S}} &= [\tan^2\theta \underbrace{(\cos\Theta + 1)}_{\geq 0}][\tan^2\theta(\cos\Theta - 1) + 2\tan^2\theta^{\mathrm{S}}].
\end{aligned}$$

(A1) $\Psi = +1$

From [Eq. (5.7)], $\tan\theta^{\mathrm{S}} > \tan\theta$ is obtained and recall that $+1 \geq \cos\Theta \geq -\alpha^{-2}$, therefore

$$\mathrm{B^S} = \tan^2\theta\cos\Theta + \tan^2\theta^{\mathrm{S}} > \tan^2\theta^{\mathrm{S}} - \alpha^{-2}\tan^2\theta > 0.$$

And after rearrangement:

$$\tan^2\theta(\cos\Theta - 1) + 2\tan^2\theta^{\mathrm{S}} \geq 2\tan^2\theta^{\mathrm{S}} - (1 + \alpha^{-2})\tan^2\theta > 0$$

leads to $\Delta^{\rm S} > 0$ because $0 < \alpha^{-2} < 1$.

Accordingly, the two real roots given by quadratic formula are

$$R^{\rm S,\pm} = \frac{\overbrace{(\tan^2\theta^{\rm S} + \tan^2\theta\cos\Theta)}^{{\rm B^S}>0} \pm \overbrace{\sqrt{\Delta^{\rm S}}}^{<|{\rm B^S}|}}{\underbrace{\tan^2\theta^{\rm S} - \tan^2\theta}_{>0}} > 0.$$

The above equation can be rewritten in the following form to determine R is greater than unity or not:

$$R^{\rm S,\pm} = 1 + \frac{\overbrace{[\tan^2\theta(1+\cos\Theta)]}^{>0} \pm \sqrt{\Delta^{\rm S}}}{\tan^2\theta^{\rm S} - \tan^2\theta},$$

and $\Delta^{\rm S}$ is determined to be greater than $[\tan^2\theta\ (\cos\Theta + 1)]^2$,

$$\begin{aligned} \Delta^{\rm S} &= [\tan^2\theta\,(\cos\Theta+1)]\,[\tan^2\theta\,(\cos\Theta+1) + 2(\tan^2\theta^{\rm S} - \tan^2\theta)] \\ &> [\tan^2\theta\ (\cos\Theta+1)]^2. \end{aligned}$$

Therefore, $R^{\rm S,+} > 1$ and $0 < R^{\rm S,-} < 1$. From Table 5.1, $\mathcal{K}_z^{\rm S} = -R + 1.$. The corresponding vertical direction group velocity has

$$\mathrm{sgn}\{c_z\} = -\mathrm{sgn}\{\mathcal{K}_z^{\rm S}\} \Rightarrow (c_z)^{\rm S,+} > 0, (c_z)^{\rm S,-} < 0.$$

The nonlinear interference pattern would be at every intersection point one beam is emanating upward and another is traveling downward. The numerical simulation, see (Fig. 5.2 and 5.3), verifies the selection rules derived above.

(A2) $\Psi = -1$

[Eq. (5.8)] shows that $\tan\theta^{\rm S} < \tan\theta$. $\Delta^{\rm S} \geq 0$ if and only if $[\tan^2\theta\,(\cos\Theta - 1) + 2\tan^2\theta^{\rm S}] \geq 0$, i.e.

$$\cos\Theta \geq 1 - \frac{2\tan^2\theta^{\rm S}}{\tan^2\theta}.$$

But, by rearranging the above inequality, it turns out that

$$\tan^2\theta\ \cos\Theta + \tan^2\theta^{\rm S} \geq \tan^2\theta - \tan^2\theta^{\rm S} > 0,$$

and accordingly the roots given by the quadratic formula are less than zero,

$$R^{\rm S,\pm} = \frac{\overbrace{-(\tan^2\theta^{\rm S} + \tan^2\theta\cos\Theta)}^{{\rm B^S}<0} \pm \overbrace{\sqrt{\Delta^{\rm S}}}^{<|{\rm B^S}|}}{\underbrace{\tan^2\theta - \tan^2\theta^{\rm S}}_{>0}} < 0,$$

which violates the definition that $R > 0$.

In this case, *either there is no real root or the roots are negative. Harmonics are not allowed to generate.*

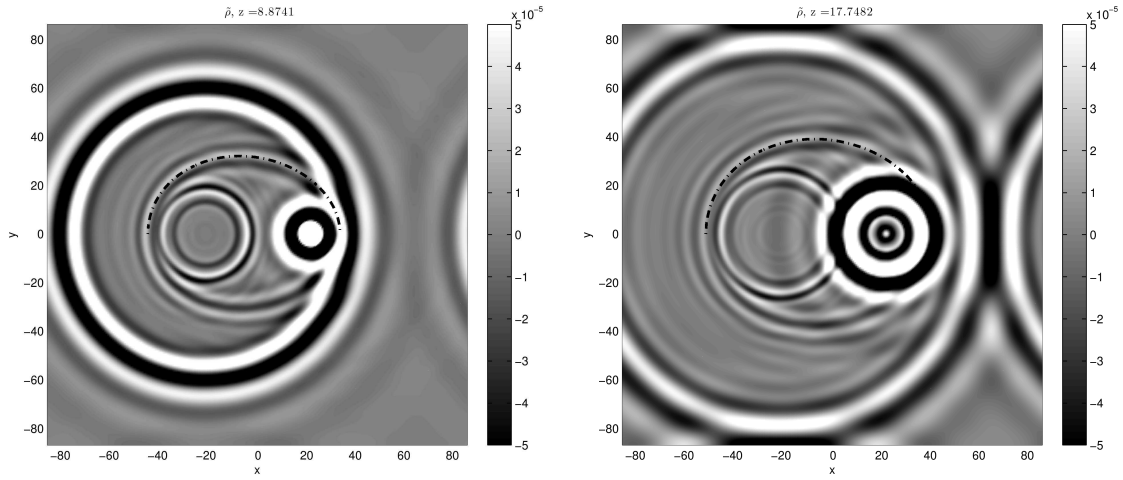

(a) (b)

Figure 5.2 In this numerical simulation, Brunt-Väisälä frequency, N, equals to 1.5394 rad s^{-1}, $f = N/4$ and forcing frequency is at $0.4\,N$. The figures are horizontal slices of the density field at $z = 0.4V, 0.8V$ where the two IGW sources located at $(-H, 0, -V/2)$ and $(H, 0, V/2)$. The colormap is chosen to emphasize the second harmonics. $\alpha = 1.5 > 1$ in this case. The long dotted curve is the theoretical locus of second harmonics propagating upward calculated by applying the selection rules. (a) (left) $z = 0.4V$. (b) (right) $z = 0.8V$.

(B) $0 < \alpha < 1$

The interaction pattern is exactly the same as in Case II. Although for non-traditional branch, $\Psi = -1$, the intersection region that allows to generate harmonics is $\cos\Theta \leq -1 + 2\tan^2\theta^{\mathrm{S}}\tan^{-2}\theta$. Using the estimate $\cos\Theta \leq -1/2$ shows that the harmonics are allowed in limited regions $(1+\alpha^{-1})/2 \leq \eta \leq (1+\sqrt{(4\alpha^{-2}-1)/3})/2$ (and the corresponding ξ: $1 < 1+\alpha \leq \xi \leq 1+\alpha^2\sqrt{(4\alpha^{-2}-1)/3} < 2$) and $(1-\alpha^{-1})/2 \geq \eta \geq (1-\sqrt{(4\alpha^{-2}-1)/3})/2$ (and the corresponding ξ: $1 > 1-\alpha \geq \xi \geq 1-\alpha^2\sqrt{(4\alpha^{-2}-1)/3} > 0$). This implies that the second harmonics are permitted to generate only in the neighborhoods of the IGW sources (slightly higher than the second source and lower than first source vertically and in between the two sources horizontally since $0 < \xi < 2$).

5.3.4 Rule of Thumb

In the traditional branch, $N^2 > f^2$, the high frequency harmonics are only allowed to generate if and only if one of the two interacting conical waves is travelling downward and the other upward. *This constraint is satisfied when there is no horizontal distance ($H = 0$) between two IGW sources or the nondimensional parameter* $\alpha \equiv V/(2H\tan\theta) > 1$. *The phase difference between two internal gravity waves is NOT AT ALL important in*

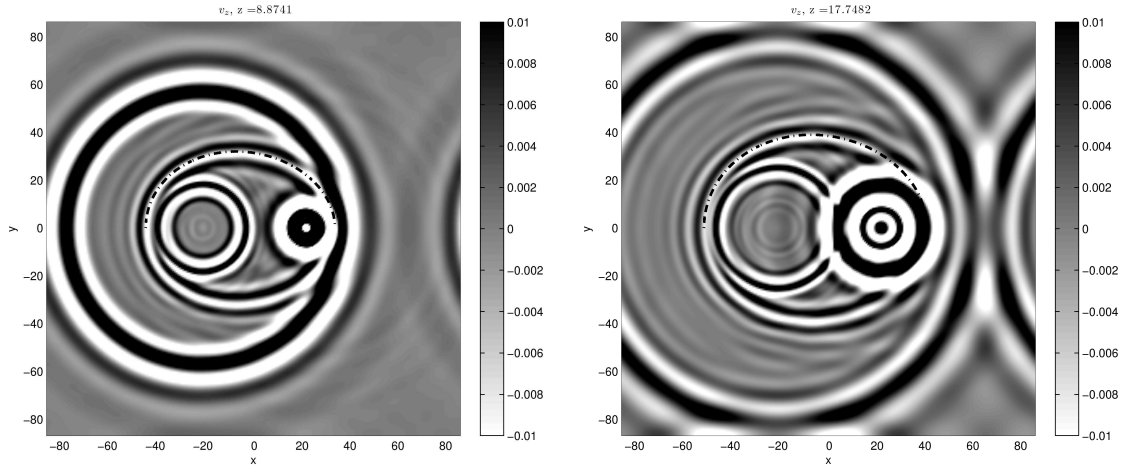

(a) (b)

Figure 5.3 As in (Fig. 5.2), but the field plotted is the vertical velocity.

determining interference pattern. This geometric constraint is not commonly satisfied in the ocean on earth since the ocean depth is typically pretty shallow compared to the horizontal extent. For example, if the horizontal and vertical distance between two sources is 100 km and 1 km (a very rough estimation for IGWs interacted near Hawaiian ridge), $\alpha \approx 0.17$ for IGWs forced at M_2 tidal frequency. In other words, if this geometric constraint is not met, the IGWs just nonlinearly interact locally without generating higher harmonics and losing energy. This is probably good since the IGW can thus propagate far away without feeding energy to the local nonlinear interactions with other IGW sources.

On the other hand, the high frequency harmonic beams are permitted when two IGWs both travelling upward or downward (no vertical distance between two IGW sources, $V = 0$, or more general case: $\alpha < 1$) in the non-traditional branch, $f^2 > N^2$. In addition, another geometric constraint, $\cos\Theta \leq -1 + 2\tan^2\theta^{\mathrm{S}}/\tan^2\theta$ where $\tan^2\theta^{\mathrm{S}}/\tan^2\theta$ is estimated to be less than one quarter, must also be satisfied. This requires the intersection point is not too far away from the sources. Consequently, the harmonic waves can only be detected in a confined space in the vicinity of the sources.

5.4 Selection rules, two sources forced at individual frequencies

Define "slope ratio" in the following way,

$$\mathrm{Sr} \equiv \frac{\tan\theta_2}{\tan\theta_1} \begin{cases} < 1, & \Psi = +1 \\ > 1, & \Psi = -1 \end{cases} . \tag{5.24}$$

Later on, it would be shown that Sr is critical in determining selection rules.

From [Eqs. (5.7) and (5.8)] and by definition $\left|\omega^{\mathrm{S}}\right| = |\omega_1| + |\omega_2| > |\omega_1| > |\omega_2|$, this leads to:

$$\text{for } \Psi = +1 \;\Rightarrow\; \theta^{\mathrm{S}} > \theta_1 > \theta_2,\ \tan\theta^{\mathrm{S}} > \tan\theta_1 > \tan\theta_2, \tag{5.25a}$$
$$\text{for } \Psi = -1 \;\Rightarrow\; \theta^{\mathrm{S}} < \theta_1 < \theta_2,\ \tan\theta^{\mathrm{S}} < \tan\theta_1 < \tan\theta_2. \tag{5.25b}$$

The relation between $\left|\omega^{\mathrm{D}}\right| = |\omega_1| - |\omega_2|$, $|\omega_1|$ and $|\omega_2|$ is a bit complicated. It is not only dependent on Ψ but also the absolute value of χ (recall that $\chi < 0$):

$$\begin{aligned}
\text{for } |\chi| < |1/2| \;&\Rightarrow\; |\omega_2| < |\omega^{\mathrm{D}}| < |\omega_1|, \\
\text{for } |\chi| = |1/2| \;&\Rightarrow\; |\omega^{\mathrm{D}}| = |\omega_2| < |\omega_1|, \\
\text{for } |\chi| > |1/2| \;&\Rightarrow\; |\omega^{\mathrm{D}}| < |\omega_2| < |\omega_1|.
\end{aligned}$$

Therefore, for different pairs of Ψ and $|\chi|$, there are six variations of the relation between θ^{D}, θ_1 and θ_2:

$$\text{for } \Psi = +1 \text{ and } |\chi| < 1/2 \Rightarrow \theta_1 > \theta^{\mathrm{D}} > \theta_2,\ \tan\theta_1 > \tan\theta^{\mathrm{D}} > \tan\theta_2, \tag{5.26a}$$
$$\text{for } \Psi = +1 \text{ and } |\chi| = 1/2 \Rightarrow \theta_1 > \theta_2 = \theta^{\mathrm{D}},\ \tan\theta_1 > \tan\theta_2 = \tan\theta^{\mathrm{D}}, \tag{5.26b}$$
$$\text{for } \Psi = +1 \text{ and } |\chi| > 1/2 \Rightarrow \theta_1 > \theta_2 > \theta^{\mathrm{D}},\ \tan\theta_1 > \tan\theta_2 > \tan\theta^{\mathrm{D}}, \tag{5.26c}$$

$$\text{for } \Psi = -1 \text{ and } |\chi| < 1/2 \Rightarrow \theta_1 < \theta^{\mathrm{D}} < \theta_2,\ \tan\theta_1 < \tan\theta^{\mathrm{D}} < \tan\theta_2, \tag{5.27a}$$
$$\text{for } \Psi = -1 \text{ and } |\chi| = 1/2 \Rightarrow \theta_1 < \theta_2 = \theta^{\mathrm{D}},\ \tan\theta_1 < \tan\theta_2 = \tan\theta^{\mathrm{D}}, \tag{5.27b}$$
$$\text{for } \Psi = -1 \text{ and } |\chi| > 1/2 \Rightarrow \theta_1 < \theta_2 < \theta^{\mathrm{D}},\ \tan\theta_1 < \tan\theta_2 < \tan\theta^{\mathrm{D}}. \tag{5.27c}$$

The first source is placed at the origin of the coordinate system. Then the position of the second source is divided into three categories like what have been done in the previous section:

- Case IV: $H = 0$, the second source is located at $(0,\, 0,\, V)$.
- Case V: $V = 0$, the second source is located at $(2H,\, 0,\, 0)$.
- Case VI: $H, V \neq 0$, the second source is located at $(2H,\, 0,\, V)$.

5.4.1 Case IV: $H = 0$

The locus of the first IGW source in $z = z_I$ plane is $x_I^2 + y_I^2 = z_I^2 \cot^2\theta_1$ and that of the second source is $x_I^2 + y_I^2 = (z_I - V)^2 \cot^2\theta_2$. The two double conical waves would intersect at two different vertical positions,

$$\eta = \frac{1}{1 - \mathrm{Sr}} \begin{cases} > 1, & \Psi = +1 \\ < 0, & \Psi = -1 \end{cases},$$

and

$$0 < \eta = \frac{1}{1+\mathrm{Sr}} < 1,$$

for both $\Psi = \pm 1$. The loci $x_I^2 + y_I^2 = [V/(1 \mp \mathrm{Sr})]^2 \cot^2\theta_1$ in $z = V/(1 \mp \mathrm{Sr})$ plane are circles. $(x_I,\, y_I,\, z_I) = (|V/(1 \mp \mathrm{Sr})| \cot\theta_1 \cos\phi,\, |V/(1 \mp \mathrm{Sr})| \cot\theta_1 \sin\phi, V/[1 \mp \mathrm{Sr}])$ where $\phi \in [0,\, 2\pi]$ is the azimuthal angle. Since $\cos\phi_1 = \cos\phi_2 = \cos\phi$ and $\sin\phi_1 = \sin\phi_2 = \sin\phi$, this leads to $\cos\Theta = \cos^2\phi + \sin^2\phi = 1$ for every intersection point.

(A) Intersection point: $\eta = (1 - \mathrm{Sr})^{-1}$

Similar to Case I, each intersection point is acting like the collision point in two-dimensional colliding beams problem. But the interaction scenario here is analogous to $j = 1$ case in Chapter 4 (after applying reflection symmetries): both incoming beams are propagating in the same direction vertically and horizontally. From Tables 4.6 and 4.7, one would expect high frequency harmonics are forbidden for both $\Psi = \pm 1$.

Although for $\Psi = +1$, z_I is higher than V and z_I is lower than zero for $\Psi = -1$, $\mathrm{B}^{\mathrm{S}} = \Psi\,(\tan\theta_1 \tan\theta_2 - \tan\theta^{\mathrm{S}})$ and $\mathrm{B}^{\mathrm{D}} = \Psi\ (\tan\theta_1 \tan\theta_2 - \tan\theta^{\mathrm{D}})$ are formally the same from Table 5.1. Because $\cos\Theta = 1$, Δ^{S} and Δ^{D} therefore are always greater than zero:

$$\Delta^{\mathrm{S}} = \tan^2\theta^{\mathrm{S}}\,(\tan\theta_1 - \tan\theta_2)^2 > 0, \Delta^{\mathrm{D}} = \tan^2\theta^{\mathrm{D}}\,(\tan\theta_1 - \tan\theta_2)^2 > 0.$$

After putting everything together, the quadratic formula gives the roots

$$R^{\mathrm{S},\pm} = \frac{\tan\theta_1 \tan\theta_2 - \tan^2\theta^{\mathrm{S}}}{\tan^2\theta^{\mathrm{S}} - \tan^2\theta_1} \pm \frac{\tan\theta^{\mathrm{S}}(\tan\theta_1 - \tan\theta_2)}{\tan^2\theta^{\mathrm{S}} - \tan^2\theta_1},$$

and

$$R^{\mathrm{D},\pm} = \frac{\tan\theta_1 \tan\theta_2 - \tan^2\theta^{\mathrm{D}}}{\tan^2\theta_1 - \tan^2\theta^{\mathrm{D}}} \pm \frac{\tan\theta^{\mathrm{D}}(\tan\theta_1 - \tan\theta_2)}{\tan^2\theta_1 - \tan^2\theta^{\mathrm{D}}}.$$

(A1) $\Psi = +1$

(i) $\chi > 0, \tan\theta^{\mathrm{S}} > \tan\theta_1 > \tan\theta_2$

The roots reduce to

$$R^{\mathrm{S},\pm} = -\frac{\overbrace{\tan\theta^{\mathrm{S}} \pm \tan\theta_2}^{>0}}{\underbrace{\tan\theta^{\mathrm{S}} \pm \tan\theta_1}_{>0}} < 0.$$

This violates the restriction that $R > 0$ so *no harmonics with frequencies* $\pm\omega_{\mathrm{sum}}$ *are permitted.*

(ii) $\chi < 0, |\chi| < 1/2, \tan\theta_1 > \tan\theta^{\mathrm{D}} > \tan\theta_2$

Again, the roots cab be simplified to

$$0 < R^{\mathrm{D},+} = \frac{\overbrace{\tan\theta_2 + \tan\theta^{\mathrm{D}}}^{>0}}{\underbrace{\tan\theta_1 + \tan\theta^{\mathrm{D}}}_{>0}} < 1, R^{\mathrm{D},-} = \frac{\overbrace{\tan\theta_2 - \tan\theta^{\mathrm{D}}}^{<0}}{\underbrace{\tan\theta_1 - \tan\theta^{\mathrm{D}}}_{>0}} < 0.$$

$R^{\mathrm{D},-} < 0$ does not satisfy the dispersion relation of the low frequency harmonics. The vertical direction group velocity with $R = R^{\mathrm{D},+}$, using the fact that $\mathcal{K}_z^{\mathrm{D},+} = -R^{\mathrm{D},+} + 1 > 0$ from Table 5.1, has

$$\mathrm{sgn}\{c_z\} = -\mathrm{sgn}\{\mathcal{K}_z^{\mathrm{D}}\} \Rightarrow (c_z)^{\mathrm{D},+} < 0.$$

Because the values of $\mathcal{K}_x^{\mathrm{D}}$ and $\mathcal{K}_y^{\mathrm{D}}$ can actually be determined, too:

$$\begin{aligned} \mathcal{K}_x^{\mathrm{D}} &= \cos\phi\,(\tan\theta_1\, R - \tan\theta_2), \\ \mathcal{K}_y^{\mathrm{D}} &= \sin\phi\,(\tan\theta_1\, R - \tan\theta_2). \end{aligned}$$

Thus $c_y/c_x = \sin\phi/\cos\phi$ and the group velocity is going radially. It is radially inward or outward can be determined by computing

$$\tan\theta_1\, R^{\mathrm{D},+} - \tan\theta_2 = \frac{\tan\theta^{\mathrm{D}}\,(\tan\theta_1 - \tan\theta_2)}{\tan\theta_1 + \tan\theta^{\mathrm{D}}} > 0.$$

Only one low frequency harmonic beam is produced with frequencies $\pm\omega_{\mathrm{diff}}$ from the intersection point and is emanating downward and radially outward.

(iii) $\chi < 0, |\chi| = 1/2, \tan\theta_1 > \tan\theta_2 = \tan\theta^{\mathrm{D}}$

$$0 < R^{\mathrm{D},+} = \frac{\overbrace{2\tan\theta_2}^{>0}}{\underbrace{\tan\theta_1 + \tan\theta_2}_{>0}} < 1, R^{\mathrm{D},-} = 0.$$

Similar to (ii), *only one low frequency harmonic beam is produced with frequencies $\pm\omega_{\mathrm{diff}}$ from the intersection point and is emanating downward and radially outward.*

(iv) $\chi < 0, |\chi| > 1/2, \tan\theta_1 > \tan\theta_2 > \tan\theta^{\mathrm{D}}$

$$0 < R^{\mathrm{D},\pm} = \frac{\overbrace{\tan\theta_2 \pm \tan\theta^{\mathrm{D}}}^{>0}}{\underbrace{\tan\theta_1 \pm \tan\theta^{\mathrm{D}}}_{>0}} < 1.$$

Both harmonic beams with frequencies $\pm\omega_{\text{diff}}$ are travelling downward at different azimuthal and polar angles if the origin is set to be the intersection point. The group velocity is radially inward or outward can be determined by computing

$$\begin{aligned}\tan\theta_1\, R^{\mathrm{D},+} - \tan\theta_2 &= \frac{\tan\theta^{\mathrm{D}}\,(\tan\theta_1 - \tan\theta_2)}{\tan\theta_1 + \tan\theta^{\mathrm{D}}} > 0,\\ \tan\theta_1\, R^{\mathrm{D},-} - \tan\theta_2 &= -\frac{\tan\theta^{\mathrm{D}}\,(\tan\theta_1 - \tan\theta_2)}{\tan\theta_1 - \tan\theta^{\mathrm{D}}} < 0.\end{aligned}$$

$R^{\mathrm{D},+}$ generates harmonic beam going radially outward and $R^{\mathrm{D},-}$ corresponds to harmonic beam emanating radially inward. Both beams are propagating downward but at different polar angles.

(A2) $\Psi = -1$

(i) $\chi > 0, \tan\theta^{\mathrm{S}} < \tan\theta_1 < \tan\theta_2$

$$R^{\mathrm{S},\pm} = -\frac{\overbrace{\tan\theta_2 \pm \tan\theta^{\mathrm{S}}}^{>0}}{\underbrace{\tan\theta_1 \pm \tan\theta^{\mathrm{S}}}_{>0}} < 0.$$

This violates the restriction that $R > 0$ so *no high frequency harmonics are permitted.*

(ii) $\chi < 0, |\chi| < 1/2, \tan\theta_1 < \tan\theta^{\mathrm{D}} < \tan\theta_2$

$$R^{\mathrm{D},+} = \frac{\overbrace{\tan\theta^{\mathrm{D}} + \tan\theta_2}^{>0}}{\underbrace{\tan\theta^{\mathrm{D}} + \tan\theta_1}_{>0}} > 1, R^{\mathrm{D},-} = \frac{\overbrace{\tan\theta^{\mathrm{D}} - \tan\theta_2}^{<0}}{\underbrace{\tan\theta^{\mathrm{D}} - \tan\theta_1}_{>0}} < 0.$$

The corresponding vertical direction group velocity with $R = R^{\mathrm{D},+}$, using the relation that $\mathcal{K}_z^{\mathrm{D}} = R - 1$, has

$$\mathrm{sgn}\{c_z\} = \mathrm{sgn}\{\mathcal{K}_z^{\mathrm{D}}\} \Rightarrow (c_z)^{\mathrm{D},+} < 0.$$

The group velocity is radially inward or outward can be determined by computing

$$\tan\theta_1\, R^{\mathrm{D},+} - \tan\theta_2 = \frac{\tan\theta^{\mathrm{D}}\,(\tan\theta_1 - \tan\theta_2)}{\tan\theta_1 + \tan\theta^{\mathrm{D}}} < 0.$$

Only one low frequency harmonic beam is produced with frequencies $\pm\omega_{\text{diff}}$ and emanating downward and radially inward.

(iii) $\chi < 0, |\chi| = 1/2, \tan\theta_1 < \tan\theta_2 = \tan\theta^{\mathrm{D}}$

$$R^{\mathrm{D},+} = \frac{\overbrace{2\tan\theta_2}^{>0}}{\underbrace{\tan\theta_1 + \tan\theta_2}_{>0}} > 1, R^{\mathrm{D},-} = 0.$$

Similarly to (ii), *only one low frequency harmonic beam is produced with frequencies* $\pm\omega_{\mathrm{diff}}$ *and emanating downward and radially inward.*

(iv) $\chi < 0, |\chi| > 1/2, \tan\theta_1 < \tan\theta_2 < \tan\theta^{\mathrm{D}}$

$$R^{\mathrm{D},+} = \frac{\overbrace{\tan\theta^{\mathrm{D}} + \tan\theta_2}^{>0}}{\underbrace{\tan\theta^{\mathrm{D}} + \tan\theta_1}_{>0}} > 1, 0 < R^{\mathrm{D},-} = \frac{\overbrace{\tan\theta^{\mathrm{D}} - \tan\theta_2}^{>0}}{\underbrace{\tan\theta^{\mathrm{D}} - \tan\theta_1}_{>0}} < 1.$$

$R^{\mathrm{D},+}$ corresponds to harmonic beam emitting downward and $R^{\mathrm{D},-}$ is the beam propagating upward. The group velocity is radially inward or outward can be determined by computing

$$\tan\theta_1\, R^{\mathrm{D},\pm} - \tan\theta_2 = \frac{\tan\theta^{\mathrm{D}}\,(\tan\theta_1 - \tan\theta_2)}{\tan\theta^{\mathrm{D}} \pm \tan\theta_1} < 0.$$

$R^{\mathrm{D},+}$ *generates harmonic beam going radially inward and downward and* $R^{\mathrm{D},-}$ *also emits harmonic beam radially inward but going upward.*

(B) Intersection point: $\eta = (1 + \mathrm{Sr})^{-1}$

Like Case I, the interaction scenario here is analogous to $j = 4$ case in Chapter 4: both incoming beams are propagating horizontally in the same direction but vertically in opposite directions. From Tables 4.6 and 4.7, one would expect high frequency harmonics are produced for $\Psi = +1$ and are forbidden if $\Psi = -1$.

For both $\Psi = \pm 1$, z_I is in between zero and V,

$$\mathrm{B}^{\mathrm{S}} = \Psi\ (\tan\theta_1 \tan\theta_2 + \tan\theta^{\mathrm{S}}), \mathrm{B}^{\mathrm{D}} = \Psi\ (\tan\theta_1 \tan\theta_2 + \tan\theta^{\mathrm{D}})$$

are the same. Δ^{S} and Δ^{D} therefore are always greater than zero because

$$\Delta^{\mathrm{S}} = \tan^2\theta^{\mathrm{S}}\ (\tan\theta_1 + \tan\theta_2)^2 > 0, \Delta^{\mathrm{D}} = \tan^2\theta^{\mathrm{D}}\ (\tan\theta_1 + \tan\theta_2)^2 > 0.$$

After putting everything together, the quadratic formula gives the roots:

$$R^{\mathrm{S},\pm} = \frac{\tan\theta_1 \tan\theta_2 + \tan^2\theta^{\mathrm{S}}}{\tan^2\theta^{\mathrm{S}} - \tan^2\theta_1} \pm \Psi\ \frac{\tan\theta^{\mathrm{S}}(\tan\theta_1 + \tan\theta_2)}{\tan^2\theta^{\mathrm{S}} - \tan^2\theta_1},$$

and

$$R^{\mathrm{D},\pm} = \frac{\tan\theta_1 \tan\theta_2 + \tan^2\theta^{\mathrm{D}}}{\tan^2\theta_1 - \tan^2\theta^{\mathrm{D}}} \pm \Psi\ \frac{\tan\theta^{\mathrm{D}}(\tan\theta_1 + \tan\theta_2)}{\tan^2\theta_1 - \tan^2\theta^{\mathrm{D}}}.$$

(B1) $\Psi = +1$

(i) $\chi > 0, \tan\theta^{\rm S} > \tan\theta_1 > \tan\theta_2$

$$R^{\rm S,+} = \frac{\overbrace{\tan\theta^{\rm S} + \tan\theta_2}^{>0}}{\underbrace{\tan\theta^{\rm S} - \tan\theta_1}_{>0}} > 1, 0 < R^{\rm S,-} = \frac{\overbrace{\tan\theta^{\rm S} - \tan\theta_2}^{>0}}{\underbrace{\tan\theta^{\rm S} + \tan\theta_1}_{>0}} < 1.$$

The corresponding vertical direction group velocity, using the relation that $\mathcal{K}_z^{\rm S} = -R + 1$, has

$$\mathrm{sgn}\{c_z\} = -\mathrm{sgn}\{\mathcal{K}_z^{\rm S}\} \Rightarrow (c_z)^{\rm S,+} > 0, (c_z)^{\rm S,-} < 0.$$

Because the values of $\mathcal{K}_x^{\rm S}$ and $\mathcal{K}_y^{\rm S}$ can actually be determined

$$\begin{aligned} \mathcal{K}_x^{\rm S} &= \cos\phi\,(\tan\theta_1\, R + \tan\theta_2), \\ \mathcal{K}_y^{\rm S} &= \sin\phi\,(\tan\theta_1\, R + \tan\theta_2). \end{aligned}$$

Thus $c_y/c_x = \sin\phi/\cos\phi$ and the group velocity is going radially. It is radially inward or outward can be determined by computing

$$\tan\theta_1\, R^{\rm S,\pm} + \tan\theta_2 = \frac{\tan\theta^{\rm S}\,(\tan\theta_1 + \tan\theta_2)}{\tan\theta_1 \mp \tan\theta^{\rm S}} > 0.$$

$R^{\rm S,+}$ generates harmonic beam going radially outward and upward and $R^{\rm S,-}$ also generates harmonic beam emanating radially outward but downward.

(ii) $\chi < 0, |\chi| < 1/2, \tan\theta_1 > \tan\theta^{\rm D} > \tan\theta_2$

$$R^{\rm D,+} = \frac{\overbrace{\tan\theta_2 + \tan\theta^{\rm D}}^{>0}}{\underbrace{\tan\theta_1 - \tan\theta^{\rm D}}_{>0}} > 0, R^{\rm D,-} = \frac{\overbrace{\tan\theta_2 - \tan\theta^{\rm D}}^{<0}}{\underbrace{\tan\theta_1 + \tan\theta^{\rm D}}_{>0}} < 0.$$

The corresponding vertical group velocity, using the fact that $\mathcal{K}_z^{\rm D} = -R - 1$,

$$\mathrm{sgn}\{c_z\} = -\mathrm{sgn}\{\mathcal{K}_z^{\rm D}\} \Rightarrow (c_z)^{\rm D,+} > 0.$$

Because the values of $\mathcal{K}_x^{\rm D}$ and $\mathcal{K}_y^{\rm D}$ can actually be determined:

$$\begin{aligned} \mathcal{K}_x^{\rm D} &= \cos\phi\,(\tan\theta_1\, R - \tan\theta_2), \\ \mathcal{K}_y^{\rm D} &= \sin\phi\,(\tan\theta_1\, R - \tan\theta_2). \end{aligned}$$

Thus $c_y/c_x = \sin\phi/\cos\phi$ and the group velocity is going radially. It is radially inward or outward can be determined by computing

$$\tan\theta_1\, R^{\mathrm{D},+} - \tan\theta_2 = \frac{\tan\theta^{\mathrm{D}}\,(\tan\theta_1 + \tan\theta_2)}{\tan\theta_1 - \tan\theta^{\mathrm{D}}} > 0.$$

Only one harmonic beam is produced with frequencies $\pm\omega_{\mathrm{diff}}$ and emanating upward and radially outward.

(iii) $\chi < 0, |\chi| = 1/2, \tan\theta_1 > \tan\theta_2 = \tan\theta^{\mathrm{D}}$

$$R^{\mathrm{D},+} = \frac{\overbrace{2\tan\theta_2}^{>0}}{\underbrace{\tan\theta_1 - \tan\theta_2}_{>0}} > 0, R^{\mathrm{D},-} = 0.$$

Similar to (ii), *only one harmonic beam is produced with frequencies $\pm\omega_{\mathrm{diff}}$ and emanating upward and radially outward.*

(iv) $\chi < 0, |\chi| > 1/2, \tan\theta_1 > \tan\theta_2 > \tan\theta^{\mathrm{D}}$

$$R^{\mathrm{D},\pm} = \frac{\overbrace{\tan\theta_2 \pm \tan\theta^{\mathrm{D}}}^{>0}}{\underbrace{\tan\theta_1 \mp \tan\theta^{\mathrm{D}}}_{>0}} > 0.$$

Both harmonic beams are travelling upward but at different azimuthal angles and polar angles if the origin is set to be the intersection point. Since

$$\begin{aligned}
\tan\theta_1\, R^{\mathrm{D},+} - \tan\theta_2 &= \frac{\tan\theta^{\mathrm{D}}\,(\tan\theta_1 + \tan\theta_2)}{\tan\theta_1 - \tan\theta^{\mathrm{D}}} > 0, \\
\tan\theta_1\, R^{\mathrm{D},-} - \tan\theta_2 &= -\frac{\tan\theta^{\mathrm{D}}\,(\tan\theta_1 + \tan\theta_2)}{\tan\theta_1 + \tan\theta^{\mathrm{D}}} < 0,
\end{aligned}$$

$R^{\mathrm{D},+}$ generates harmonic beam going radially outward and $R^{\mathrm{D},-}$ corresponds to harmonic beam emanating radially inward. Both beams are propagating upward but at different polar angles.

(B2) $\Psi = -1$

(i) $\chi > 0, \tan\theta^{\mathrm{S}} < \tan\theta_1 < \tan\theta_2$

$$R^{\mathrm{S},\pm} = -\frac{\overbrace{\tan\theta_2 \mp \tan\theta^{\mathrm{S}}}^{>0}}{\underbrace{\tan\theta_1 \pm \tan\theta^{\mathrm{S}}}_{>0}} < 0.$$

This violates the restriction that $R > 0$ so *no harmonics are permitted.*

(ii) $\chi < 0, |\chi| < 1/2, \tan\theta_1 < \tan\theta^{\mathrm{D}} < \tan\theta_2$

$$R^{\mathrm{D},+} = \frac{\overbrace{\tan\theta_2 - \tan\theta^{\mathrm{D}}}^{>0}}{\underbrace{\tan\theta_1 + \tan\theta^{\mathrm{D}}}_{>0}} > 0, R^{\mathrm{D},-} = \frac{\overbrace{\tan\theta_2 + \tan\theta^{\mathrm{D}}}^{>0}}{\underbrace{\tan\theta_1 - \tan\theta^{\mathrm{D}}}_{<0}} < 0.$$

The corresponding vertical group velocity, using the fact that $\mathcal{K}_z^{\mathrm{D}} = -R - 1$, has

$$\mathrm{sgn}\{c_z\} = -\mathrm{sgn}\{\mathcal{K}_z^{\mathrm{D}}\} \Rightarrow (c_z)^{\mathrm{D},+} > 0.$$

The group velocity is radially inward or outward can be determined by computing

$$\tan\theta_1\, R^{\mathrm{D},+} - \tan\theta_2 = -\frac{\tan\theta^{\mathrm{D}}\,(\tan\theta_1 + \tan\theta_2)}{\tan\theta^{\mathrm{D}} + \tan\theta_1} < 0.$$

$R^{\mathrm{D},+}$ *generates harmonic beam going radially inward and upward.*

(iii) $\chi < 0, |\chi| = 1/2, \tan\theta_1 < \tan\theta_2 = \tan\theta^{\mathrm{D}}$

$$R^{\mathrm{D},+} = 0, R^{\mathrm{D},-} = \frac{\overbrace{2\tan\theta_2}^{>0}}{\underbrace{\tan\theta_1 - \tan\theta_2}_{<0}} < 0.$$

No harmonic beam is permitted.

(iv) $\chi < 0, |\chi| > 1/2, \tan\theta_1 < \tan\theta_2 < \tan\theta^{\mathrm{D}}$

$$R^{\mathrm{D},+} = \frac{\overbrace{\tan\theta_2 - \tan\theta^{\mathrm{D}}}^{<0}}{\underbrace{\tan\theta_1 + \tan\theta^{\mathrm{D}}}_{>0}} < 0, R^{\mathrm{D},-} = \frac{\overbrace{\tan\theta_2 + \tan\theta^{\mathrm{D}}}^{>0}}{\underbrace{\tan\theta_1 - \tan\theta^{\mathrm{D}}}_{<0}} < 0.$$

Similarly, *no harmonic beam is permitted.*

5.4.2 Case V: $V = 0$

Define another non-dimensional vertical coordinate, ζ, in terms of horizontal distance and θ_2,

$$\zeta \equiv \frac{z_I}{2H \tan\theta_2} \tag{5.28}$$

due to the lack of an explicit vertical length scale ($V = 0$).

The locus of the first IGW source in $z = z_I$ plane is $x_I^2 + y_I^2 = z_I^2 \cot^2\theta_1$ and that of the second source is $(x_I - 2H)^2 + y_I^2 = z_I^2 \cot^2\theta_2$. The two double conical IGWs would intersect in the range,

$$\frac{1}{(1+\mathrm{Sr})^2} \le \zeta^2 \le \frac{1}{(1-\mathrm{Sr})^2},$$

and ξ can be expressed in terms of ζ

$$\xi = 1 - (1 - \mathrm{Sr}^2)\zeta^2 = 1 + (\mathrm{Sr}^2 - 1)\zeta^2.$$

Since the interference pattern is reflection-symmetric with respect to $z = 0$ plane, consider $\zeta > 0$ only:

$$\frac{1}{1+\mathrm{Sr}} \le \zeta \le \frac{1}{\Psi\,(1-\mathrm{Sr})}.$$

The intersection points that have $\zeta = \pm 1/(1+\mathrm{Sr})$ are analogous to $j = 2$ case in Chapter 4: both incoming beams are propagating vertically in the same direction but horizontally in opposite directions. But when ζ gradually moves away from $\pm 1/(1+\mathrm{Sr})$, the interaction starts to deviate from the two-dimensional collision scenario. From Tables 4.6 and 4.7, one would expect high frequency harmonics are not produced for $\Psi = +1$ but are produced if $\Psi = -1$ if the intersection points are not too far away from $\pm 1/(1+\mathrm{Sr})$. Similarly, the intersection points that have $\zeta = \pm 1/\Psi(1-\mathrm{Sr})$ are analogous to $j = 1$ case in Chapter 4: both incoming beams are propagating in the same direction vertically and horizontally. But when ζ gradually moves away from $\pm 1/\Psi(1-\mathrm{Sr})$, the interaction starts to deviate from the two-dimensional collision scenario. From Tables 4.6 and 4.7, one would expect high frequency harmonics are not produced for both $\Psi = \pm 1$ if the intersection points are not too far away from $\pm 1/\Psi(1-\mathrm{Sr})$.

[Eq. (B.1)] is used to calculate $\cos\Theta$,

$$\cos\Theta = \frac{\mathrm{Sr}^2 + 1}{2\mathrm{Sr}} - \frac{1}{2\mathrm{Sr}\zeta^2} = \frac{1}{2\mathrm{Sr}}\,(\mathrm{Sr}^2 + 1 - \zeta^{-2}).$$

$\zeta(\xi = 1 - \Psi)$ would be critical to determine the sign of B^{S} or B^{D},

$$\zeta(\xi = 1 - \Psi) = \sqrt{\frac{1}{\Psi\,(1 - \mathrm{Sr}^2)}}.$$

Thus, the intersection range of ζ can be divided into two regions:

$$\frac{1}{1+\mathrm{Sr}} \leq \zeta \leq \zeta(\xi = 1-\Psi) \quad \Rightarrow \quad -1 \leq \cos\Theta \leq (\mathrm{Sr})^{\Psi}, \tag{5.29}$$

$$\zeta(\xi = 1-\Psi) \leq \zeta \leq \frac{1}{\Psi\ (1-\mathrm{Sr})} \quad \Rightarrow \quad (\mathrm{Sr})^{\Psi} \leq \cos\Theta \leq 1. \tag{5.30}$$

Since $\zeta > 0$, from Table 5.1,

$$\mathrm{B^S} = \Psi\,(\tan\theta_1 \tan\theta_2 \cos\Theta - \tan^2\theta^{\mathrm{S}}), \mathrm{B^D} = \Psi\,(\tan\theta_1 \tan\theta_2 \cos\Theta - \tan^2\theta^{\mathrm{D}}), \tag{5.31}$$

and the discriminants are

$$\begin{aligned} \Delta^{\mathrm{S}} &= (\tan\theta_1 \tan\theta_2 \cos\Theta - \tan^2\theta^{\mathrm{S}})^2 \\ &- (\tan^2\theta^{\mathrm{S}} - \tan^2\theta_1)(\tan^2\theta^{\mathrm{S}} - \tan^2\theta_2), \\ \Delta^{\mathrm{D}} &= (\tan\theta_1 \tan\theta_2 \cos\Theta - \tan^2\theta^{\mathrm{D}})^2 \\ &- (\tan^2\theta_1 - \tan^2\theta^{\mathrm{D}})(\tan^2\theta_2 - \tan^2\theta^{\mathrm{D}}). \end{aligned} \tag{5.32}$$

R's for high frequency ($R^{\mathrm{S},\pm}$) and low frequency ($R^{\mathrm{D},\pm}$) harmonics are given by the quadratic formula:

$$\begin{aligned} R^{\mathrm{S},\pm} &= \frac{(\tan\theta_1 \tan\theta_2 \cos\Theta - \tan^2\theta^{\mathrm{S}}) \pm \Psi\sqrt{\Delta^{\mathrm{S}}}}{\tan^2\theta^{\mathrm{S}} - \tan^2\theta_1} \\ R^{\mathrm{D},\pm} &= \frac{(\tan\theta_1 \tan\theta_2 \cos\Theta - \tan^2\theta^{\mathrm{D}}) \pm \Psi\sqrt{\Delta^{\mathrm{D}}}}{\tan^2\theta_1 - \tan^2\theta^{\mathrm{D}}}. \end{aligned} \tag{5.33}$$

(A) $\Psi = +1$

(i) $\chi > 0, \tan\theta^{\mathrm{S}} > \tan\theta_1 > \tan\theta_2$

[Eq. (5.17)] is used to determine the value of Δ^{S}

$$\begin{aligned} \Delta^{\mathrm{S}} &= (\tan\theta_1 \tan\theta_2 \cos\Theta - \tan^2\theta^{\mathrm{S}})^2 \\ &- (\tan\theta_1 \tan\theta_2 \qquad - \tan^2\theta^{\mathrm{S}})^2 + \tan^2\theta^{\mathrm{S}}\ (\tan\theta_1 - \tan\theta_2)^2 \\ &> \tan^2\theta^{\mathrm{S}}\ (\tan\theta_1 - \tan\theta_2)^2 > 0, \end{aligned}$$

and $\mathrm{B^S} = \tan\theta_1 \tan\theta_2 \cos\Theta - \tan^2\theta^{\mathrm{S}} \leq \tan\theta_1 \tan\theta_2 - \tan^2\theta^{\mathrm{S}} < 0$. Therefore, $R^{\mathrm{S},\pm}$ are proved to be less than zero:

$$R^{\mathrm{S},\pm} = \frac{\overbrace{\overbrace{(\tan\theta_1 \tan\theta_2 \cos\Theta - \tan^2\theta^{\mathrm{S}})}^{<0} \pm \overbrace{\sqrt{\Delta^{\mathrm{S}}}}^{<|\mathrm{B^S}|}}^{<0}}{\underbrace{\tan^2\theta^{\mathrm{S}} - \tan^2\theta_1}_{>0}} < 0.$$

The numerator is negative but the denominator is always positive for each root, hence the roots are both negative. This violates the restriction that $R > 0$ so *no harmonics are permitted.*

(ii) $\chi < 0, |\chi| < 1/2, \tan\theta_1 > \tan\theta^{\mathrm{D}} > \tan\theta_2$

The Δ^{D} is always greater than zero since

$$\begin{aligned}\Delta^{\mathrm{D}} &= (\tan\theta_1\tan\theta_2\cos\Theta - \tan^2\theta^{\mathrm{D}})^2 - \overbrace{(\tan\theta_1 - \tan\theta^{\mathrm{D}})}^{>0}\overbrace{(\tan\theta_2 - \tan\theta^{\mathrm{D}})}^{<0} \\ &> (\tan\theta_1\tan\theta_2\cos\Theta - \tan^2\theta^{\mathrm{D}})^2 > 0,\end{aligned}$$

so $R^{\mathrm{D},\pm}$ are both real but the sign of $R^{\mathrm{D},\pm}$ is still needed to determine. The sign of $R^{\mathrm{D},\pm}$ depends on the sign of B^{D}. If $\mathrm{B}^{\mathrm{D}} \geq 0$, $R^{\mathrm{D},+}$ is greater than zero but $R^{\mathrm{D},-}$ is negative. On the other hand, if $\mathrm{B}^{\mathrm{D}} < 0$, both roots are negative and thus violate the requirement that $R > 0$:

$$R^{\mathrm{D},\pm} = \frac{(\tan\theta_1\tan\theta_2\cos\Theta - \tan^2\theta^{\mathrm{D}}) \pm \overbrace{\sqrt{\Delta^{\mathrm{D}}}}^{>|\mathrm{B}^{\mathrm{D}}|}}{\underbrace{\tan^2\theta_1 - \tan^2\theta^{\mathrm{D}}}_{>0}}.$$

$R^{\mathrm{D},-} < 0$ no matter what value B^{D} is. $R^{\mathrm{D},+}$ is greater than unity or not is used to determine the direction of group velocity:

$$R^{\mathrm{D},+} = 1 + \frac{\overbrace{(\tan\theta_1\tan\theta_2\cos\Theta - \tan^2\theta_1)}^{<0} + \sqrt{\Delta^{\mathrm{D}}}}{\tan^2\theta_1 - \tan^2\theta^{\mathrm{D}}}.$$

By using [Eq. (5.18)],

$$\begin{aligned}\Delta^{\mathrm{D}} &= (\tan\theta_1\tan\theta_2\cos\Theta - \tan^2\theta_1)^2 \\ &+ \underbrace{(\tan^2\theta^{\mathrm{D}} - \tan^2\theta_1)}_{<0}\ \underbrace{(\tan^2\theta_1 - 2\tan\theta_1\tan\theta_2 + \tan^2\theta_2)}_{>0} \\ &< (\tan\theta_1\tan\theta_2\cos\Theta - \tan^2\theta_1)^2.\end{aligned}$$

This sets $0 < R^{\mathrm{D},+} < 1$. The corresponding vertical group velocity, using the fact that $\mathcal{K}_z^{\mathrm{D}} = -R + 1$, has

$$\mathrm{sgn}\{c_z\} = -\mathrm{sgn}\{\mathcal{K}_z^{\mathrm{D}}\} \Rightarrow (c_z)^{\mathrm{D},+} < 0.$$

The single low frequency harmonic beam is propagating downward.

(iii) $\chi < 0, |\chi| = 1/2, \tan\theta_1 > \tan\theta_2 = \tan\theta^{\mathrm{D}}$

B^{D} changes sign at $\cos\Theta = \mathrm{Sr}$ where $\zeta = \zeta(\xi = 0)$:

$$\begin{aligned}\mathrm{B}^{\mathrm{D}} &= \tan\theta_1\tan\theta_2\cos\Theta - \tan^2\theta_2 = \begin{cases} \leq 0 & \text{, if } \frac{1}{1+\mathrm{Sr}} \leq \zeta \leq \zeta(\xi=0) \\ > 0 & \text{, if } \zeta(\xi=0) < \zeta \leq \frac{1}{(1-\mathrm{Sr})} \end{cases} \\ \Delta^{\mathrm{D}} &= (\tan\theta_1\tan\theta_2\cos\Theta - \tan^2\theta_2)^2 > 0.\end{aligned}$$

Accordingly, the roots given by the quadratic formula are different, too:

$$R^{\mathrm{D},+}\begin{cases} =0 & , \text{if } \frac{1}{1+\mathrm{Sr}} \le \zeta \le \zeta(\xi=0) \\ = \frac{2\ (\tan\theta_1 \tan\theta_2 \cos\Theta - \tan^2\theta_2)}{\tan^2\theta_1 - \tan^2\theta_2} > 0 & , \text{if } \zeta(\xi=0) < \zeta \le \frac{1}{(1-\mathrm{Sr})} \end{cases},$$

and

$$R^{\mathrm{D},-}\begin{cases} <0 & , \text{if } \frac{1}{1+\mathrm{Sr}} \le \zeta \le \zeta(\xi=0) \\ =0 & , \text{if } \zeta(\xi=0) < \zeta \le \frac{1}{(1-\mathrm{Sr})} \end{cases}.$$

In $\zeta(\xi=0) < \zeta \le (1-\mathrm{Sr})^{-1}$,

$$0 < R^{\mathrm{D},+} = 1 - \frac{(\tan^2\theta_1 - 2\tan\theta_1\tan\theta_2\cos\Theta + \tan^2\theta_2)}{\tan^2\theta_1 - \tan^2\theta_2} < 1.$$

The permitted harmonic beam is going downward if the intersection point is in the region where $\mathrm{Sr} < \cos\Theta \le +1$.

(iv) $\chi < 0, |\chi| > 1/2, \tan\theta_1 > \tan\theta_2 > \tan\theta^{\mathrm{D}}$

$$\Delta^{\mathrm{D}} = (\tan^2\theta_1 \tan^2\theta_2)\ \cos^2\Theta - (2\tan^2\theta^{\mathrm{D}} \tan\theta_1 \tan\theta_2)\ \cos\Theta + \cdots$$

which is a concave up parabola in $\cos\Theta$ and $\Delta^{\mathrm{D}}(\cos\Theta = \pm 1) = \tan^2\theta^{\mathrm{D}}\,(\tan\theta_1 \mp \tan\theta_2)^2 > 0$. Also the minimum of Δ^{D} equals to $-(\tan^2\theta_1 - \tan^2\theta^{\mathrm{D}})\,(\tan^2\theta_2 - \tan^2\theta^{\mathrm{D}}) < 0$ at $0 < \cos\Theta = \mathrm{Sr}\,\tan^2\theta^{\mathrm{D}}\tan^{-2}\theta_2 < \mathrm{Sr}$. Δ^{D} must be negative for some intersection points.

$$\Delta^{\mathrm{D}} = 0 \Rightarrow \cos\Theta^{\mathrm{D},\pm} = \mathrm{Sr}\ \frac{\tan^2\theta^{\mathrm{D}}}{\tan^2\theta_2} \pm \frac{\sqrt{(\tan^2\theta_1 - \tan^2\theta^{\mathrm{D}})(\tan^2\theta_2 - \tan^2\theta^{\mathrm{D}})}}{\tan\theta_1\tan\theta_2},$$

i.e.

$$\Delta^{\mathrm{D}}\begin{cases} \ge 0, & \cos\Theta \in [-1, \cos\Theta^{\mathrm{D},-}] \cup [\cos\Theta^{\mathrm{D},+}, +1] \\ < 0, & \cos\Theta \in (\cos\Theta^{\mathrm{D},-}, \cos\Theta^{\mathrm{D},+}) \end{cases},$$

and $\cos\Theta^{\mathrm{D},-} < \mathrm{Sr} < \cos\Theta^{\mathrm{D},+}$. Correspondingly, B^{D} also changes sign:

$$\mathrm{B}^{\mathrm{D}}\begin{cases} <0 & \cos\Theta \in [-1, \cos\Theta^{\mathrm{D},-}] \\ >0 & \cos\Theta \in [\cos\Theta^{\mathrm{D},+}, +1] \end{cases}.$$

After putting every piece together, R has no real root for $\cos\Theta \in [-1, \cos\Theta^{\mathrm{D},-}]$. For $\cos\Theta \in (\cos\Theta^{\mathrm{D},-}, \cos\Theta^{\mathrm{D},+})$,

$$R^{\mathrm{D},\pm} = \underbrace{\frac{\overbrace{\mathrm{B}^{\mathrm{D}}}^{<0} \pm \overbrace{\sqrt{\Delta^{\mathrm{D}}}}^{<|\mathrm{B}^{\mathrm{D}}|}}{\tan^2\theta_1 - \tan^2\theta^{\mathrm{D}}}}_{>0} < 0,$$

which contradict $R > 0$ definition. Only for $\cos\Theta \in [\cos\Theta^{\mathrm{D},+}, +1]$,

$$R^{\mathrm{D},\pm} = \frac{\overbrace{\mathrm{B}^{\mathrm{D}}}^{>0} \pm \overbrace{\sqrt{\Delta^{\mathrm{D}}}}^{<|\mathrm{B}^{\mathrm{D}}|}}{\underbrace{\tan^2\theta_1 - \tan^2\theta^{\mathrm{D}}}_{>0}} > 0.$$

And after rearrangement,

$$R^{\mathrm{D},\pm} = 1 + \frac{\overbrace{(\tan\theta_1\tan\theta_2\cos\Theta - \tan^2\theta_1)}^{<0} \pm \sqrt{\Delta^{\mathrm{D}}}}{\tan^2\theta_1 - \tan^2\theta^{\mathrm{D}}}.$$

Using the fact that $\Delta^{\mathrm{D}} < (\tan\theta_1\tan\theta_2\cos\Theta - \tan^2\theta_1)^2$, both positive roots are less than unity. The corresponding vertical group velocity are therefore negative since

$$\mathrm{sgn}\{c_z\} = -\mathrm{sgn}\{\mathcal{K}_z^{\mathrm{D}}\} \Rightarrow (c_z)^{\mathrm{D},\pm} < 0.$$

The harmonics are generated in the space where $\cos\Theta \in [\cos\Theta^{\mathrm{D},+}, +1]$ *and are propagating downward.*

(B) $\Psi = -1$

(i) $\chi > 0, \tan\theta^{\mathrm{S}} < \tan\theta_1 < \tan\theta_2$

Similar to the case $\Psi = +1$ and $\chi < 0, |\chi| > 1/2$ just derived,

$$\Delta^{\mathrm{S}} = (\tan^2\theta_1\tan^2\theta_2)\,\cos^2\Theta - (2\tan^2\theta^{\mathrm{S}}\tan\theta_1\tan\theta_2)\,\cos\Theta + \cdots$$

which is also a concave up parabola in $\cos\Theta$. And $\Delta^{\mathrm{S}}(\cos\Theta = \pm 1) = \tan^2\theta^{\mathrm{S}}\,(\tan\theta_1 \mp \tan\theta_2)^2 > 0$. Also the minimum of Δ^{S} equals to $-(\tan^2\theta_1 - \tan^2\theta^{\mathrm{S}})\,(\tan^2\theta_2 - \tan^2\theta^{\mathrm{S}}) < 0$ at $0 < \cos\Theta = \mathrm{Sr}^{-1}\,\tan^2\theta^{\mathrm{S}}\tan^{-2}\theta_1 < \mathrm{Sr}^{-1}$. Δ^{S} must be zero somewhere.

$$\Delta^{\mathrm{S}} = 0 \Rightarrow \cos\Theta^{\mathrm{S},\pm} = \mathrm{Sr}^{-1}\,\frac{\tan^2\theta^{\mathrm{S}}}{\tan^2\theta_1} \pm \frac{\sqrt{(\tan^2\theta_1 - \tan^2\theta^{\mathrm{S}})(\tan^2\theta_2 - \tan^2\theta^{\mathrm{S}})}}{\tan\theta_1\tan\theta_2},$$

i.e.

$$\Delta^{\mathrm{S}} \begin{cases} \geq 0, & \cos\Theta \in [-1, \cos\Theta^{\mathrm{S},-}] \cup [\cos\Theta^{\mathrm{S},+}, +1] \\ < 0, & \cos\Theta \in (\cos\Theta^{\mathrm{S},-}, \cos\Theta^{\mathrm{S},+}) \end{cases},$$

and $\cos\Theta^{\mathrm{S},-} < \mathrm{Sr}^{-1} < \cos\Theta^{\mathrm{S},+}$. B^{S} also changes sign

$$\mathrm{B}^{\mathrm{S}} \begin{cases} > 0 & \cos\Theta \in [-1, \cos\Theta^{\mathrm{S},-}] \\ < 0 & \cos\Theta \in [\cos\Theta^{\mathrm{S},+}, +1] \end{cases}.$$

After putting every piece together, there is no real root for $\cos\Theta \in (\cos\Theta^{\mathrm{S},-}, \cos\Theta^{\mathrm{S},+})$. For $\cos\Theta \in [\cos\Theta^{\mathrm{S},+}, +1]$,

$$R^{\mathrm{S},\pm} = \frac{\overbrace{\mathrm{B}^{\mathrm{S}}}^{<0} \pm \overbrace{\sqrt{\Delta^{\mathrm{S}}}}^{<|\mathrm{B}^{\mathrm{S}}|}}{\underbrace{\tan^2\theta_1 - \tan^2\theta^{\mathrm{S}}}_{>0}} < 0,$$

which contradicts $R > 0$ definition. Only for $\cos\Theta \in [-1, \cos\Theta^{\mathrm{S},-}]$,

$$R^{\mathrm{S},\pm} = \frac{\overbrace{\mathrm{B}^{\mathrm{S}}}^{>0} \pm \overbrace{\sqrt{\Delta^{\mathrm{S}}}}^{<|\mathrm{B}^{\mathrm{S}}|}}{\underbrace{\tan^2\theta_1 - \tan^2\theta^{\mathrm{S}}}_{>0}} > 0.$$

The corresponding vertical group velocity, using $\mathcal{K}_z^{\mathrm{S}} = -R - 1$, has

$$\mathrm{sgn}\{c_z\} = -\mathrm{sgn}\{\mathcal{K}_z^{\mathrm{S}}\} \Rightarrow (c_z)^{\mathrm{S},\pm} > 0.$$

The harmonics are generated in the space where $\cos\Theta \in [-1, \cos\Theta^{\mathrm{S},-}]$ *and are propagating upward.* $\cos\Theta \in [-1, \cos\Theta^{\mathrm{S},-}]$ is analogous to the two-dimensional colliding beams problem with beams having same sign vertical group velocity but opposite sign horizontal group velocity and $\cos\Theta \in [\cos\Theta^{\mathrm{S},+}, +1]$ is similar to that with beams having both same sign horizontal and vertical group velocities. And $\cos\Theta \in (\cos\Theta^{\mathrm{S},-}, \cos\Theta^{\mathrm{S},+})$ does not have any two-dimensional counter-part.

(ii) $\chi < 0, |\chi| < 1/2, \tan\theta_1 < \tan\theta^{\mathrm{D}} < \tan\theta_2$

The discriminant is always greater than zero since

$$\Delta^{\mathrm{D}} > (\tan^2\theta^{\mathrm{D}} - \tan\theta_1 \tan\theta_2 \cos\Theta)^2 > 0.$$

Therefore the quadratic formula gives

$$R^{\mathrm{D},\pm} = \frac{(\tan^2\theta^{\mathrm{D}} - \tan\theta_1 \tan\theta_2 \cos\Theta) \pm \overbrace{\sqrt{\Delta^{\mathrm{D}}}}^{>|\mathrm{B}^{\mathrm{D}}|}}{\underbrace{\tan^2\theta^{\mathrm{D}} - \tan^2\theta_1}_{>0}},$$

where $R^{\mathrm{D},+} > 0$ and $R^{\mathrm{D},-} < 0$. After rearrangement, $R^{\mathrm{D},+}$ is determined to be greater than unity:

$$R^{\mathrm{D},+} = 1 + \frac{(\tan^2\theta_1 - \tan\theta_1 \tan\theta_2 \cos\Theta) + \sqrt{\Delta^{\mathrm{D}}}}{\tan^2\theta^{\mathrm{D}} - \tan^2\theta_1} > 1$$

since $\Delta^{\mathrm{D}} > (\tan^2\theta_1 - \tan\theta_1\tan\theta_2\cos\Theta)^2$. The corresponding vertical group velocity, using $\mathcal{K}_z^{\mathrm{D}} = -R+1$, is greater than zero:

$$\mathrm{sgn}\{c_z\} = -\mathrm{sgn}\{\mathcal{K}_z^{\mathrm{D}}\} \Rightarrow (c_z)^{\mathrm{D},+} > 0.$$

The single low frequency harmonic beam is propagating upward.

(iii) $\chi < 0, |\chi| = 1/2, \tan\theta_1 < \tan\theta_2 = \tan\theta^{\mathrm{D}}$

The discriminant is positive since $\Delta^{\mathrm{D}} = (\tan^2\theta_2 - \tan\theta_1\tan\theta_2\cos\Theta)^2 > 0$. Again, the quadratic formula gives

$$R^{\mathrm{D},+} = 1 + \frac{\overbrace{(\tan^2\theta_2 - 2\tan\theta_1\tan\theta_2\cos\Theta + \tan^2\theta_1)}^{>0}}{\underbrace{\tan^2\theta_2 - \tan^2\theta_1}_{>0}} > 1$$

and

$$R^{\mathrm{D},-} = 0.$$

This also generates a low frequency harmonic beam with $(c_z)^{\mathrm{D},+} > 0$.

(iv) $\chi < 0, |\chi| > 1/2, \tan\theta_1 < \tan\theta_2 < \tan\theta^{\mathrm{D}}$

From $\Delta^{\mathrm{D}} > (\mathrm{B}^{\mathrm{D}})^2 > 0$, the discriminant is greater than zero.

$$R^{\mathrm{D},\pm} = \frac{\overbrace{(\tan^2\theta^{\mathrm{D}} - \tan\theta_1\tan\theta_2\cos\Theta)}^{>0} \pm \overbrace{\sqrt{\Delta^{\mathrm{D}}}}^{<|\mathrm{B}^{\mathrm{D}}|}}{\underbrace{\tan^2\theta^{\mathrm{D}} - \tan^2\theta_1}_{>0}} > 0,$$

and after rearrangement

$$R^{\mathrm{D},\pm} = 1 + \frac{(\tan^2\theta_1 - \tan\theta_1\tan\theta_2\cos\Theta) \pm \sqrt{\Delta^{\mathrm{D}}}}{\tan^2\theta^{\mathrm{D}} - \tan^2\theta_1}.$$

[Eq. (5.19)] tells $\Delta^{\mathrm{D}} > (\tan^2\theta_1 - \tan\theta_1\tan\theta_2\cos\Theta)^2$ so $R^{\mathrm{D},+} > 1$ and $0 < R^{\mathrm{D},-} < 1$. The corresponding vertical group velocity would be $(c_z)^{\mathrm{D},+} > 0$ and $(c_z)^{\mathrm{D},-} < 0$. In other words, *there are two low frequency harmonic beams generated. One harmonic beam is propagating upward and the other one is downward.*

5.4.3 Case VI: $H, V \neq 0$

The ranges of intersection points are dependent on two non-dimensional parameters,

$$\alpha_1 \equiv \frac{V}{2H\tan\theta_1}, \tag{5.34}$$

$$\alpha_2 \equiv \frac{V}{2H\tan\theta_2}. \tag{5.35}$$

The locus of the first IGW source in $z = z_I$ plane is $x_I^2 + y_I^2 = z_I^2 \cot^2\theta_1$ and that of the second source is $(x_I - 2H)^2 + y_I^2 = (V - z_I)^2 \cot^2\theta_2$. The general formula for the coordinates of intersection point is

$$\xi = 1 + \alpha_1^2\eta^2 - \alpha_2^2(\eta - 1)^2. \tag{5.36}$$

The above formula is correct under the following geometric constraint,

$$(\eta - \eta_1)(\eta - \eta_2)(\eta - \eta_3)(\eta - \eta_4) \leq 0, \tag{5.37}$$

which ensures that $(x_I,\ y_I,\ z_I)$ actually belongs to two IGW double cones and where

$$\eta_1 \equiv \frac{\alpha_2 + 1}{\alpha_2 - \alpha_1}, \tag{5.38}$$

$$\eta_2 \equiv \frac{\alpha_2 - 1}{\alpha_2 + \alpha_1}, \tag{5.39}$$

$$\eta_3 \equiv \frac{\alpha_2 + 1}{\alpha_2 + \alpha_1}, \tag{5.40}$$

$$\eta_4 \equiv \frac{\alpha_2 - 1}{\alpha_2 - \alpha_1}. \tag{5.41}$$

It is obviously that the relationship between η_1 to η_4 is dependent on Ψ and α_1, α_2 are greater or less than unity. The intersection regions are concluded as followed,

(A): $\alpha_1, \alpha_2 > 1$.

For $\Psi = +1$, $\alpha_2 > \alpha_1 > 1$ and intersection ranges are region (A1):

$$\eta_1 > \eta > \eta_4 > 1,$$

and region (A2):

$$1 > \eta_3 > \eta > \eta_2 > 0.$$

For $\Psi = -1$, $\alpha_1 > \alpha_2 > 1$ and intersection ranges are region (A1):

$$0 > \eta_4 > \eta > \eta_1,$$

and region (A2):

$$1 > \eta_3 > \eta > \eta_2 > 0.$$

(B): $\max(\alpha_1, \alpha_2) > 1, \min(\alpha_1, \alpha_2) < 1$.

For $\Psi = +1$, $\alpha_2 > 1 > \alpha_1$ and intersection ranges are region (B1):

$$\eta_1 > \eta > \eta_3 > 1,$$

and region (B2):

$$1 > \eta_4 > \eta > \eta_2 > 0.$$

For $\Psi = -1$, $\alpha_1 > 1 > \alpha_2$ and intersection ranges are region (B1):

$$0 > \eta_2 > \eta > \eta_1,$$

and region (B2):

$$1 > \eta_3 > \eta > \eta_4 > 0.$$

(C): $\alpha_1, \alpha_2 < 1$

For $\Psi = +1$, $1 > \alpha_2 > \alpha_1$ and intersection ranges are region (C1):

$$\eta_1 > \eta > \eta_3 > 1,$$

and region (C2):

$$0 > \eta_2 > \eta > \eta_4.$$

For $\Psi = -1$, $1 > \alpha_1 > \alpha_2$ and intersection ranges are region (C1):

$$0 > \eta_2 > \eta > \eta_1,$$

and region (C2):

$$\eta_4 > \eta > \eta_3 > 1.$$

The ranges of $\cos\Theta$ in each region are listed in Appendix B.

(A) $\alpha_1, \alpha_2 > 1$

Region (A1)

Although $z_I > V$ for $\Psi = +1$ and $z_I < 0$ for $\Psi = -1$ in this region, the formal forms of B's, Δ's and roots of R's are exactly the same as in Case V. So [Eqs. (5.31), (5.32) and (5.33)] are still valid. But the ranges of $\cos\Theta$ are different, the selection rules might be different from case to case.

$\Psi = +1$ **in Region (A1)**

(i) $\chi > 0, \tan\theta^{\mathrm{S}} > \tan\theta_1 > \tan\theta_2$

The result is the same as in Case V even though the ranges of $\cos\Theta$ are different. *No harmonic beams are produced.*

(ii) $\chi < 0, |\chi| < 1/2, \tan\theta_1 > \tan\theta^{\mathrm{D}} > \tan\theta_2$

The result is the same as in Case V. *The single permitted low frequency harmonic beam is going downward.*

(iii) $\chi < 0, |\chi| = 1/2, \tan\theta_1 > \tan\theta_2 = \tan\theta^{\mathrm{D}}$

Similar to Case V but this time $\cos\Theta > \mathrm{Sr}$ is valid for every intersection point, therefore

$$0 < R^{\mathrm{D},+} = 1 - \frac{(\tan^2\theta_1 - 2\tan\theta_1\tan\theta_2\cos\Theta + \tan^2\theta_2)}{\tan^2\theta_1 - \tan^2\theta_2} < 1,$$

and $R^{\mathrm{D},-} < 0$. *The single permitted low frequency harmonic beam is going downward.*

(iv) $\chi < 0, |\chi| > 1/2, \tan\theta_1 > \tan\theta_2 > \tan\theta^{\rm D}$

The minimum of $\cos\Theta$ equals to $\cos\Theta(\eta = \eta_{\rm c}^{+}) > {\rm Sr} > 0$. The selection rules are identical to the one in Case V except the regions where the harmonics are allowed to generate may be different. From [Eq. (C.1a)] and [Eq. (C.1b)],

$$\begin{aligned} \text{if } \frac{1}{\alpha_1^2} > \frac{\tan^2\theta^{\rm D}}{\tan^2\theta_2} \quad &\Rightarrow \quad \cos\Theta \in [\cos\Theta^{\rm D,+}, +1], \\ \text{if } \frac{1}{\alpha_1^2} < \frac{\tan^2\theta^{\rm D}}{\tan^2\theta_2} \quad &\Rightarrow \quad \cos\Theta \in [\cos\Theta(\eta = \eta_{\rm c}^{+}), +1], \end{aligned}$$

are the regions where the harmonics are allowed to produce. *Both low frequency harmonic beams, if existed, are propagating downward.*

$\Psi = -1$ in Region (A1)

The selection rules are similar to Case V after applying the reflection-symmetry about z-axis.

(i) $\chi > 0, \tan\theta^{\rm S} < \tan\theta_1 < \tan\theta_2$

The results from Case V show that the harmonics are generated if $\cos\Theta$ is in the interval $[-1, \cos\Theta^{\rm S,-}]$ where $\cos\Theta^{\rm S,-} < {\rm Sr}^{-1}$. But [Eq. (B.13)] shows $\cos\Theta > {\rm Sr}^{-1}$ in region (A1). Consequently, *there is no harmonic wave generated.*

(ii) $\chi < 0, |\chi| < 1/2, \tan\theta_1 < \tan\theta^{\rm D} < \tan\theta_2$

The single low frequency harmonic beam is propagating downward.

(iii) $\chi < 0, |\chi| = 1/2, \tan\theta_1 < \tan\theta_2 = \tan\theta^{\rm D}$

The single low frequency harmonic beam is also propagating downward.

(iv) $\chi < 0, |\chi| > 1/2, \tan\theta_1 < \tan\theta_2 < \tan\theta^{\rm D}$

Two low frequency harmonic beams are generated. One harmonic beam is propagating downward and the other one is upward.

Region (A2)

In this case, the geometric constraint requires that $\cos\Theta \geq \cos\Theta(\eta = \eta_{\rm c}^{-}) > -{\rm Sr}^{\Psi}$.

Since $0 < \eta < 1$, from Table 5.1, the formulas of B's and the discriminants are

$$\begin{aligned} {\rm B}^{\rm S} &= \Psi\,(\tan\theta_1 \tan\theta_2 \cos\Theta + \tan^2\theta^{\rm S}), \\ {\rm B}^{\rm D} &= \Psi\,(\tan\theta_1 \tan\theta_2 \cos\Theta + \tan^2\theta^{\rm D}), \end{aligned} \tag{5.42}$$

and

$$\begin{aligned}\Delta^{\mathrm{S}} &= (\tan\theta_1\tan\theta_2\cos\Theta+\tan^2\theta^{\mathrm{S}})^2 \\ &- (\tan^2\theta^{\mathrm{S}}-\tan^2\theta_1)(\tan^2\theta^{\mathrm{S}}-\tan^2\theta_2), \\ \Delta^{\mathrm{D}} &= (\tan\theta_1\tan\theta_2\cos\Theta+\tan^2\theta^{\mathrm{D}})^2 \\ &- (\tan^2\theta_1-\tan^2\theta^{\mathrm{D}})(\tan^2\theta_2-\tan^2\theta^{\mathrm{D}}). \end{aligned} \tag{5.43}$$

Therefore, the roots given by quadratic formula are

$$\begin{aligned} R^{\mathrm{S},\pm} &= \frac{(\tan\theta_1\tan\theta_2\cos\Theta+\tan^2\theta^{\mathrm{S}})\pm\Psi\sqrt{\Delta^{\mathrm{S}}}}{\tan^2\theta^{\mathrm{S}}-\tan^2\theta_1}, \\ R^{\mathrm{D},\pm} &= \frac{(\tan\theta_1\tan\theta_2\cos\Theta+\tan^2\theta^{\mathrm{D}})\pm\Psi\sqrt{\Delta^{\mathrm{D}}}}{\tan^2\theta_1-\tan^2\theta^{\mathrm{D}}}. \end{aligned} \tag{5.44}$$

$\Psi=+1$ in Region (A2)

(i) $\chi>0, \tan\theta^{\mathrm{S}}>\tan\theta_1>\tan\theta_2$
[Eq. (5.17)] is used to determine the value of Δ^{S} where

$$\begin{aligned}\Delta^{\mathrm{S}} &= (\tan\theta_1\tan\theta_2\cos\Theta+\tan^2\theta^{\mathrm{S}})^2 \\ &- (\tan\theta_1\tan\theta_2 \quad -\tan^2\theta^{\mathrm{S}})^2+\tan^2\theta^{\mathrm{S}}\,(\tan\theta_1-\tan\theta_2)^2 \\ &> \tan^2\theta^{\mathrm{S}}\,(\tan\theta_1-\tan\theta_2)^2>0,\end{aligned}$$

and $\mathrm{B}^{\mathrm{S}}=\tan\theta_1\tan\theta_2\cos\Theta+\tan^2\theta^{\mathrm{S}}\geq\tan^2\theta^{\mathrm{S}}-\tan\theta_1\tan\theta_2>0$. Therefore, the values of $R^{\mathrm{S},\pm}$ can be determined to be greater than zero:

$$R^{\mathrm{S},\pm}=\frac{\overbrace{(\tan\theta_1\tan\theta_2\cos\Theta+\tan^2\theta^{\mathrm{S}})}^{>0}\pm\overbrace{\sqrt{\Delta^{\mathrm{S}}}}^{<|\mathrm{B}^{\mathrm{S}}|}}{\underbrace{\tan^2\theta^{\mathrm{S}}-\tan^2\theta_1}_{>0}}>0,$$

and

$$R^{\mathrm{S},\pm}=1+\frac{(\tan\theta_1\tan\theta_2\cos\Theta+\tan^2\theta_1)\pm\sqrt{\Delta^{\mathrm{S}}}}{\tan^2\theta^{\mathrm{S}}-\tan^2\theta_1}.$$

With the use of [Eq. (5.19)], $\Delta^{\mathrm{S}}>(\tan\theta_1\tan\theta_2\cos\Theta+\tan^2\theta_1)^2$. This shows that $R^{\mathrm{S},+}>1$ and $0<R^{\mathrm{S},-}<1$. The corresponding vertical direction group velocity, using the relation $\mathcal{K}_z^{\mathrm{S}}=-R+1$, has

$$\mathrm{sgn}\{c_z\}=-\mathrm{sgn}\{\mathcal{K}_z^{\mathrm{S}}\}\Rightarrow(c_z)^{\mathrm{S},+}>0,(c_z)^{\mathrm{S},-}<0.$$

There are two high frequency harmonic beams generated. One beam is emanating upward and the other one is downward.

(ii) $\chi<0, |\chi|<1/2, \tan\theta_1>\tan\theta^{\mathrm{D}}>\tan\theta_2$

The discriminant can be determined to be greater than zero by carefully identifying the sign of each term:

$$\begin{aligned}\Delta^{\mathrm{D}} &= (\tan\theta_1\tan\theta_2\cos\Theta+\tan^2\theta^{\mathrm{D}})^2-\overbrace{(\tan\theta_1-\tan\theta^{\mathrm{D}})}^{>0}\overbrace{(\tan\theta_2-\tan\theta^{\mathrm{D}})}^{<0}\\ &> (\tan\theta_1\tan\theta_2\cos\Theta+\tan^2\theta^{\mathrm{D}})^2=\left(\mathrm{B}^{\mathrm{D}}\right)^2>0.\end{aligned}$$

Since $\Delta^{\mathrm{D}}>\left(\mathrm{B}^{\mathrm{D}}\right)^2$, $R^{\mathrm{D},\pm}$ are defined as follows,

$$R^{\mathrm{D},\pm}=\frac{(\tan\theta_1\tan\theta_2\cos\Theta+\tan^2\theta^{\mathrm{D}})\pm\overbrace{\sqrt{\Delta^{\mathrm{D}}}}^{>\left|\mathrm{B}^{\mathrm{D}}\right|}}{\underbrace{\tan^2\theta_1-\tan^2\theta^{\mathrm{D}}}_{>0}}.$$

Obviously, $R^{\mathrm{D},-}<0$ and $R^{\mathrm{D},+}>0$ no matter what value B^{D} is. The corresponding vertical group velocity, knowing that $\mathcal{K}_z^{\mathrm{D}}=-R-1$, has

$$\mathrm{sgn}\{c_z\}=-\mathrm{sgn}\{\mathcal{K}_z^{\mathrm{D}}\}\Rightarrow(c_z)^{\mathrm{D},+}>0.$$

The single low frequency harmonic beam generated is going upward.

(iii) $\chi<0, |\chi|=1/2, \tan\theta_1>\tan\theta_2=\tan\theta^{\mathrm{D}}$

The geometric constraint $\cos\Theta>-\mathrm{Sr}$ shows

$$\begin{aligned}\mathrm{B}^{\mathrm{D}} &= \tan\theta_1\tan\theta_2\cos\Theta+\tan^2\theta_2>0,\\ \Delta^{\mathrm{D}} &= (\tan\theta_1\tan\theta_2\cos\Theta+\tan^2\theta_2)^2=\left(\mathrm{B}^{\mathrm{D}}\right)^2>0.\end{aligned}$$

Therefore the sign of $R^{\mathrm{D},\pm}$ can be determined too:

$$R^{\mathrm{D},+}=\frac{2\,(\tan\theta_1\tan\theta_2\cos\Theta+\tan^2\theta_2)}{\tan^2\theta_1-\tan^2\theta_2}>0$$

and $R^{\mathrm{D},-}=0$. *The permitted low frequency harmonic beam is going upward.*

(iv) $\chi<0, |\chi|>1/2, \tan\theta_1>\tan\theta_2>\tan\theta^{\mathrm{D}}$

The discriminant has the form:

$$\Delta^{\mathrm{D}}=(\tan^2\theta_1\tan^2\theta_2)\,\cos^2\Theta+(2\tan^2\theta^{\mathrm{D}}\tan\theta_1\tan\theta_2)\,\cos\Theta+\cdots$$

which is a concave up parabola in $\cos\Theta$. And $\Delta^{\mathrm{D}}(\cos\Theta=\pm1)=\tan^2\theta^{\mathrm{D}}\,(\tan\theta_1\pm\tan\theta_2)^2>0$. Also minimum of Δ^{D} equals to $-(\tan^2\theta_1-\tan^2\theta^{\mathrm{D}})\,(\tan^2\theta_2-\tan^2\theta^{\mathrm{D}})<0$ at $0>\cos\Theta=-\mathrm{Sr}\,\tan^2\theta^{\mathrm{D}}\tan^{-2}\theta_2>-\mathrm{Sr}$. Δ^{D} may be negative.

$$\Delta^{\mathrm{D}}=0\Rightarrow\cos\Theta^{\mathrm{D},\pm}=-\mathrm{Sr}\,\frac{\tan^2\theta^{\mathrm{D}}}{\tan^2\theta_2}\pm\frac{\sqrt{(\tan^2\theta_1-\tan^2\theta^{\mathrm{D}})(\tan^2\theta_2-\tan^2\theta^{\mathrm{D}})}}{\tan\theta_1\tan\theta_2}$$

i.e.

$$\Delta^{\mathrm{D}} \begin{cases} \geq 0, & \cos\Theta \in [-1, \cos\Theta^{\mathrm{D},-}] \cup [\cos\Theta^{\mathrm{D},+}, +1] \\ < 0, & \cos\Theta \in (\cos\Theta^{\mathrm{D},-}, \cos\Theta^{\mathrm{D},+}) \end{cases},$$

where $\cos\Theta^{\mathrm{D},-} < -\mathrm{Sr} < \cos\Theta^{\mathrm{D},+}$. Accordingly,

$$\mathrm{B}^{\mathrm{D}} > 0 \text{ for } \cos\Theta \in [\cos\Theta^{\mathrm{D},+}, +1].$$

From [Eq. (C.2a)] and [Eq. (C.2b)],

$$\text{if } \alpha_1^{-2} > \frac{\tan^2\theta^{\mathrm{D}}}{\tan^2\theta_2} \;\Rightarrow\; \cos\Theta^{\mathrm{D},-} < -\mathrm{Sr} < \cos\Theta(\eta_{\mathrm{c}}^-) < \cos\Theta^{\mathrm{D},+},$$
$$\text{if } \alpha_1^{-2} < \frac{\tan^2\theta^{\mathrm{D}}}{\tan^2\theta_2} \;\Rightarrow\; \cos\Theta^{\mathrm{D},-} < -\mathrm{Sr} < \cos\Theta^{\mathrm{D},+} < \cos\Theta(\eta_{\mathrm{c}}^-),$$

Hence, if $\alpha_1^{-2} > \tan^2\theta^{\mathrm{D}} \tan^{-2}\theta_2$, for $\cos\Theta \in (\cos\Theta(\eta_{\mathrm{c}}^-), \cos\Theta^{\mathrm{D},+})$ there is no real root. But for $\cos\Theta \in [\cos\Theta^{\mathrm{D},+}, +1]$ if $\alpha_1^{-2} > \tan^2\theta^{\mathrm{D}} \tan^{-2}\theta_2$ and for every intersection point if $\alpha_1^{-2} < \tan^2\theta^{\mathrm{D}} \tan^{-2}\theta_2$,

$$R^{\mathrm{D},\pm} = \frac{\overbrace{\mathrm{B}^{\mathrm{D}}}^{>0} \pm \overbrace{\sqrt{\Delta^{\mathrm{D}}}}^{<|\mathrm{B}^{\mathrm{D}}|}}{\underbrace{\tan^2\theta_1 - \tan^2\theta^{\mathrm{D}}}_{>0}} > 0.$$

The corresponding vertical group velocity has

$$\mathrm{sgn}\{c_z\} = -\mathrm{sgn}\{\mathcal{K}_z^{\mathrm{D}}\} \Rightarrow (c_z)^{\mathrm{D},\pm} > 0.$$

There are two low frequency harmonic beams generated from each intersection point satisfying $\cos\Theta \in [\max(\cos\Theta^{\mathrm{D},+}, \cos\Theta(\eta_{\mathrm{c}}^-)), +1]$. *Both beams are propagating upward. The selection rules are verified by numerical simulation, see (Fig. 5.4).*

$\Psi = -1$ in Region (A2)

(i) $\chi > 0, \tan\theta^{\mathrm{S}} < \tan\theta_1 < \tan\theta_2$

The discriminant has the form:

$$\Delta^{\mathrm{S}} = (\tan^2\theta_1 \tan^2\theta_2)\cos^2\Theta + (2\tan^2\theta^{\mathrm{S}} \tan\theta_1 \tan\theta_2)\cos\Theta + \cdots$$

which is also a concave up parabola in $\cos\Theta$. And $\Delta^{\mathrm{S}}(\cos\Theta = \pm 1) = \tan^2\theta^{\mathrm{S}}(\tan\theta_1 \pm \tan\theta_2)^2 > 0$. The minimum of Δ^{S} equals to $-(\tan^2\theta_1 - \tan^2\theta^{\mathrm{S}})(\tan^2\theta_2 - \tan^2\theta^{\mathrm{S}}) < 0$ at $0 > \cos\Theta = -\mathrm{Sr}^{-1} \tan^2\theta^{\mathrm{S}} \tan^{-2}\theta_1 > -\mathrm{Sr}^{-1}$. Δ^{S} may be less than zero for some $\cos\Theta$.

$$\Delta^{\mathrm{S}} = 0 \Rightarrow \cos\Theta^{\mathrm{S},\pm} = -\mathrm{Sr}^{-1} \frac{\tan^2\theta^{\mathrm{S}}}{\tan^2\theta_1} \pm \frac{\sqrt{(\tan^2\theta_1 - \tan^2\theta^{\mathrm{S}})(\tan^2\theta_2 - \tan^2\theta^{\mathrm{S}})}}{\tan\theta_1 \tan\theta_2},$$

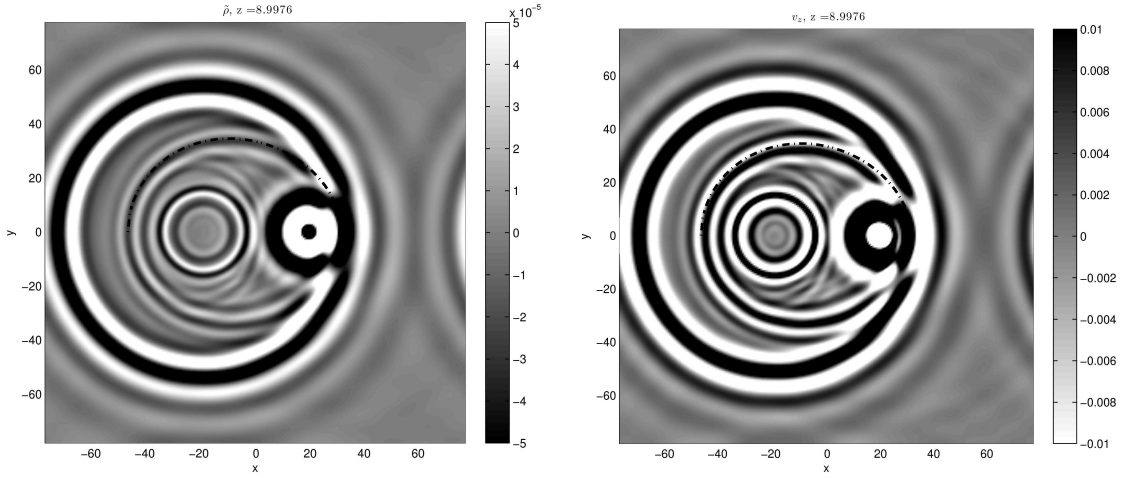

(a) (b)

Figure 5.4 In this numerical simulation, Brunt-Väisälä frequency, N, equals to 1.5394 rad s^{-1}, $f = N/4$ and forcing frequencies are 0.6583 rad s^{-1} located at $(-H, 0, -V/2)$ and 0.5629 rad s^{-1} emanated from $(H, 0, V/2)$. The figures are horizontal slices of the density and vertical velocity fields at $z = 0.4V$. The colormap is chosen to emphasize the second harmonics. $\alpha_2 = 2.0080 > \alpha_1 = 1.5 > 1$ corresponds to Case VIA2. The long dotted curve is the theoretical locus of second harmonics propagating upward calculated by applying the selection rules. (a) (left) Density field. (b) (right) Vertical velocity field.

i.e.

$$\Delta^{\mathrm{S}} \begin{cases} \geq 0, & \cos\Theta \in [-1, \cos\Theta^{\mathrm{S},-}] \cup [\cos\Theta^{\mathrm{S},+}, +1] \\ < 0, & \cos\Theta \in (\cos\Theta^{\mathrm{S},-}, \cos\Theta^{\mathrm{S},+}) \end{cases},$$

where $\cos\Theta^{\mathrm{S},-} < -\mathrm{Sr}^{-1} < \cos\Theta^{\mathrm{S},+}$. Also from [Eq. (B.14)], $\cos\Theta > -\mathrm{Sr}^{-1}$. Correspondingly,

$$\mathrm{B}^{\mathrm{S}} < 0 \text{ for } \cos\Theta \in [\cos\Theta^{\mathrm{S},+}, +1].$$

From [Eq. (C.2c)] and [Eq. (C.2d)],

$$\text{if } \alpha_2^{-2} > \frac{\tan^2\theta^{\mathrm{S}}}{\tan^2\theta_1} \quad \Rightarrow \quad \cos\Theta^{\mathrm{S},-} < -\mathrm{Sr}^{-1} < \cos\Theta(\eta_{\mathrm{c}}^-) < \cos\Theta^{\mathrm{S},+},$$
$$\text{if } \alpha_2^{-2} < \frac{\tan^2\theta^{\mathrm{S}}}{\tan^2\theta_1} \quad \Rightarrow \quad \cos\Theta^{\mathrm{S},-} < -\mathrm{Sr}^{-1} < \cos\Theta^{\mathrm{S},+} < \cos\Theta(\eta_{\mathrm{c}}^-).$$

Therefore, if $\alpha_2^{-2} > \tan^2\theta^{\mathrm{S}} \tan^{-2}\theta_1$, for $\cos\Theta \in (\cos\Theta^{\mathrm{S},-}, \cos\Theta^{\mathrm{S},+})$ there is no real root. For $\cos\Theta \in [\cos\Theta^{\mathrm{S},+}, +1]$ if $\alpha_2^{-2} > \tan^2\theta^{\mathrm{S}} \tan^{-2}\theta_1$ and for every intersection point if

$\alpha_2^{-2} < \tan^2\theta^{\mathrm{S}} \tan^{-2}\theta_1$,

$$R^{\mathrm{S},\pm} = \frac{\overbrace{\mathrm{B}^{\mathrm{S}}}^{<0} \pm \overbrace{\sqrt{\Delta^{\mathrm{S}}}}^{<\left|\mathrm{B}^{\mathrm{S}}\right|}}{\underbrace{\tan^2\theta_1 - \tan^2\theta^{\mathrm{S}}}_{>0}} < 0$$

which contradicts $R > 0$ definition. *No high frequency harmonics are allowed to generate.*

(ii) $\chi < 0, |\chi| < 1/2, \tan\theta_1 < \tan\theta^{\mathrm{D}} < \tan\theta_2$
The discriminant has

$$\Delta^{\mathrm{D}} > (\tan^2\theta^{\mathrm{D}} + \tan\theta_1 \tan\theta_2 \cos\Theta)^2 = \left(\mathrm{B}^{\mathrm{D}}\right)^2 > 0.$$

Since $\Delta^{\mathrm{D}} > \left(\mathrm{B}^{\mathrm{D}}\right)^2$, $R^{\mathrm{D},\pm}$ are defined as follows

$$R^{\mathrm{D},\pm} = \frac{(\tan^2\theta^{\mathrm{D}} + \tan\theta_1 \tan\theta_2 \cos\Theta) \pm \overbrace{\sqrt{\Delta^{\mathrm{D}}}}^{>\left|\mathrm{B}^{\mathrm{D}}\right|}}{\underbrace{\tan^2\theta^{\mathrm{D}} - \tan^2\theta_1}_{>0}}.$$

So $R^{\mathrm{D},-} < 0$ and $R^{\mathrm{D},+} > 0$. The corresponding vertical group velocity, using $\mathcal{K}_z^{\mathrm{D}} = -R - 1$, has

$$\mathrm{sgn}\{c_z\} = -\mathrm{sgn}\{\mathcal{K}_z^{\mathrm{D}}\} \Rightarrow (c_z)^{\mathrm{D},+} > 0.$$

There is only one low frequency harmonic beam generated from every intersection point and is propagating upward.

(iii) $\chi < 0, |\chi| = 1/2, \tan\theta_1 < \tan\theta_2 = \tan\theta^{\mathrm{D}}$
The geometric constraint, $\cos\Theta > -\mathrm{Sr}$, shows

$$\Delta^{\mathrm{D}} = \left(\tan^2\theta_2 + \tan\theta_1 \tan\theta_2 \cos\Theta\right)^2 > 0,$$

and therefore

$$R^{\mathrm{D},\pm} = \frac{\overbrace{-(\tan^2\theta_2 + \tan\theta_1 \tan\theta_2 \cos\Theta)}^{<0} \pm \sqrt{\Delta^{\mathrm{D}}}}{\underbrace{\tan^2\theta_2 - \tan^2\theta_1}_{>0}},$$

i.e. $R^{\mathrm{D},+} = 0$ and $R^{\mathrm{D},-} < 0$. *There is no low frequency harmonic beam permitted to generate.*

(iv) $\chi < 0, |\chi| > 1/2, \tan\theta_1 < \tan\theta_2 < \tan\theta^{\rm D}$
From [Eq. (5.17)], $\Delta^{\rm D} > ({\rm B}^{\rm D})^2 > 0$ and therefore

$$R^{{\rm D},\pm} = \frac{\overbrace{-(\tan^2\theta^{\rm D} + \tan\theta_1\tan\theta_2\cos\Theta)}^{<0} \pm \overbrace{\sqrt{\Delta^{\rm D}}}^{<|{\rm B}^{\rm D}|}}{\underbrace{\tan^2\theta^{\rm D} - \tan^2\theta_1}_{>0}} < 0.$$

There is no low frequency harmonic beam permitted to generate.

(B) $\max(\alpha_1, \alpha_2) > 1, \min(\alpha_1, \alpha_2) < 1$

Region (B1)

The selection rules are identical to Case V although application of reflection-symmetries is needed for $\Psi = -1$.

Region (B2)

In this case, ${\rm B}^{\rm S}$, ${\rm B}^{\rm D}$ and therefore $\Delta^{\rm S}$ and $\Delta^{\rm D}$ are formally the same as in region (A2) of Case VI (A). But $\cos\Theta \in [-1, 1]$ is different from that in region (A2) of Case VI (A) and changes the selection rules in a case by case sense.

$\Psi = +1$ **in Region (B2)**

(i) $\chi > 0, \tan\theta^{\rm S} > \tan\theta_1 > \tan\theta_2$
The result is the same as that in region (A2) of Case VI (A).

(ii) $\chi < 0, |\chi| < 1/2, \tan\theta_1 > \tan\theta^{\rm D} > \tan\theta_2$
Nothing is different from region (A2) of Case VI (A).

(iii) $\chi < 0, |\chi| = 1/2, \tan\theta_1 > \tan\theta_2 = \tan\theta^{\rm D}$
${\rm B}^{\rm D}$ changes sign when $\cos\Theta = -{\rm Sr}$:

$$\begin{aligned} {\rm B}^{\rm D} &= \tan\theta_1\tan\theta_2\cos\Theta + \tan^2\theta_2 > 0 \text{ if } \cos\Theta > -{\rm Sr}, \\ {\rm B}^{\rm D} &= \tan\theta_1\tan\theta_2\cos\Theta + \tan^2\theta_2 \le 0 \text{ if } \cos\Theta \le -{\rm Sr}. \end{aligned}$$

and $\Delta^{\rm D} = (\tan\theta_1\tan\theta_2\cos\Theta + \tan^2\theta_2)^2 > 0$. *Therefore,*

$$R^{{\rm D},+} = \frac{2\left(\tan\theta_1\tan\theta_2\cos\Theta + \tan^2\theta_2\right)}{\tan^2\theta_1 - \tan^2\theta_2} > 0$$

and $R^{{\rm D},-} = 0$ *if* $\cos\Theta \in (-{\rm Sr}, +1]$. *The permitted low frequency harmonic beam is going upward. Also if* $\cos\Theta \in [-1, -{\rm Sr}]$, $R^{{\rm D},+} = 0$ *and* $R^{{\rm D},-} < 0$. *Low frequency harmonic beams are forbidden.*

(iv) $\chi<0, |\chi|>1/2, \tan\theta_1>\tan\theta_2>\tan\theta^{\mathrm{D}}$
Recall, in region (A2) of Case VI (A),

$$\Delta^{\mathrm{D}}\begin{cases}\geq 0, & \cos\Theta\in[-1,\cos\Theta^{\mathrm{D},-}]\cup[\cos\Theta^{\mathrm{D},+},+1]\\ <0, & \cos\Theta\in(\cos\Theta^{\mathrm{D},-},\cos\Theta^{\mathrm{D},+})\end{cases},$$

and

$$\cos\Theta^{\mathrm{D},-}<-\mathrm{Sr}<\cos\Theta^{\mathrm{D},+}.$$

Consequently,

$$\mathrm{B}^{\mathrm{D}}\begin{cases}<0 & \cos\Theta\in[-1,\cos\Theta^{\mathrm{D},-}]\\ >0 & \cos\Theta\in[\cos\Theta^{\mathrm{D},+},+1]\end{cases}.$$

Therefore, for $\cos\Theta\in(\cos\Theta^{\mathrm{D},-},\cos\Theta^{\mathrm{D},+})$ there is no real root.
For $\cos\Theta\in[-1,\cos\Theta^{\mathrm{D},-}]$,

$$R^{\mathrm{D},\pm}=\frac{\overbrace{\mathrm{B}^{\mathrm{D}}}^{<0}\pm\overbrace{\sqrt{\Delta^{\mathrm{D}}}}^{<|\mathrm{B}^{\mathrm{D}}|}}{\underbrace{\tan^2\theta_1-\tan^2\theta^{\mathrm{D}}}_{>0}}<0,$$

which contradicts $R>0$ definition. Only for $\cos\Theta\in[\cos\Theta^{\mathrm{D},+},+1]$,

$$R^{\mathrm{D},\pm}=\frac{\overbrace{\mathrm{B}^{\mathrm{D}}}^{>0}\pm\overbrace{\sqrt{\Delta^{\mathrm{D}}}}^{<|\mathrm{B}^{\mathrm{D}}|}}{\underbrace{\tan^2\theta_1-\tan^2\theta^{\mathrm{D}}}_{>0}}>0.$$

The corresponding vertical group velocity has $\mathrm{sgn}\{c_z\}=-\mathrm{sgn}\{\mathcal{K}_z^{\mathrm{D}}\}\Rightarrow(c_z)^{\mathrm{D},\pm}>0$. *There are two low frequency harmonic beams generated from every intersection point satisfying* $\cos\Theta\in[\cos\Theta^{\mathrm{D},+},+1]$. *Both beams, if existed, are propagating upward. The selection rules are verified using numerical simulation, see (Fig. 5.5).*

$\Psi=-1$ in Region (B2)

(i) $\chi>0, \tan\theta^{\mathrm{S}}<\tan\theta_1<\tan\theta_2$
Recall, in region (A2) of Case VI (A),

$$\Delta^{\mathrm{S}}\begin{cases}\geq 0, & \cos\Theta\in[-1,\cos\Theta^{\mathrm{S},-}]\cup[\cos\Theta^{\mathrm{S},+},+1]\\ <0, & \cos\Theta\in(\cos\Theta^{\mathrm{S},-},\cos\Theta^{\mathrm{S},+})\end{cases},$$

and

$$\cos\Theta^{\mathrm{S},-}<\mathrm{Sr}^{-1}<\cos\Theta^{\mathrm{S},+}.$$

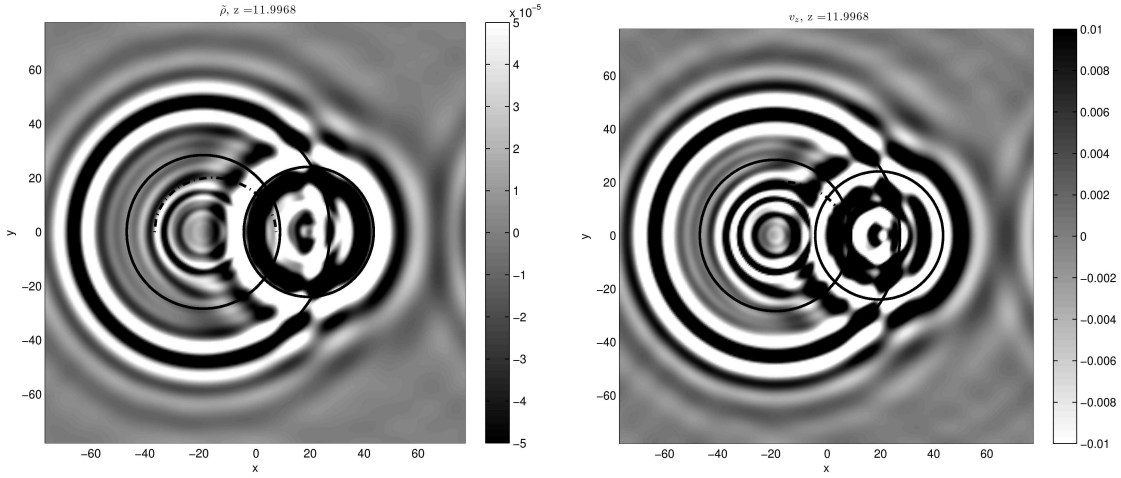

(a) (b)

Figure 5.5 In this numerical simulation, Brunt-Väisälä frequency, N, equals to 1.5394 rad s^{-1}, $f = N/4$ and forcing frequencies are 0.6583 rad s^{-1} located at $(-H, 0, -V/2)$ and 0.5274 rad s^{-1} emanated from $(H, 0, V/2)$. The figures are horizontal slices of the density and vertical velocity fields at $z = V$. The colormap is chosen to emphasize the second harmonics. $\alpha_2 = 1.2317 > 1 > \alpha_1 = 0.8$ corresponds to region (B2) of Case VI. The long dotted curve is the theoretical locus of second harmonics propagating upward calculated by applying the selection rules. The thin solid circles represent the primary conical waves emanated from the sources at frequencies $\pm\omega_1$, $\pm 2\,\omega_1$ and $\pm\omega_2$. (a) (left) Density field. (b) (right) Vertical velocity field.

Correspondingly,

$$\mathrm{B}^{\mathrm{S}} \begin{cases} > 0 & \cos\Theta \in [-1, \cos\Theta^{\mathrm{S},-}] \\ < 0 & \cos\Theta \in [\cos\Theta^{\mathrm{S},+}, +1] \end{cases} .$$

After putting everything together, for $\cos\Theta \in (\cos\Theta^{\mathrm{S},-}, \cos\Theta^{\mathrm{S},+})$ there is no real root.

For $\cos\Theta \in [\cos\Theta^{\mathrm{S},+}, +1]$,

$$R^{\mathrm{S},\pm} = \underbrace{\frac{\overbrace{\mathrm{B}^{\mathrm{S}}}^{<0} \pm \overbrace{\sqrt{\Delta^{\mathrm{S}}}}^{<|\mathrm{B}^{\mathrm{S}}|}}{\tan^2\theta_1 - \tan^2\theta^{\mathrm{S}}}}_{>0} < 0,$$

which contradicts $R > 0$ definition. Only for $\cos\Theta \in [-1, \cos\Theta^{\mathrm{S},-}]$,

$$R^{\mathrm{S},\pm} = \frac{\overbrace{\mathrm{B}^{\mathrm{S}}}^{>0} \pm \overbrace{\sqrt{\Delta^{\mathrm{S}}}}^{<|\mathrm{B}^{\mathrm{S}}|}}{\underbrace{\tan^2\theta_1 - \tan^2\theta^{\mathrm{S}}}_{>0}} > 0.$$

And rearrange the above equation, recall $\Delta^{\mathrm{S}} < (\tan\theta_1 \tan\theta_2 \cos\Theta + \tan^2\theta_1)^2$,

$$R^{\mathrm{S},\pm} = 1 + \frac{\overbrace{-(\tan\theta_1 \tan\theta_2 \cos\Theta + \tan^2\theta_1)}^{>0} \pm \sqrt{\Delta^{\mathrm{S}}}}{\tan^2\theta_1 - \tan^2\theta^{\mathrm{S}}} > 1.$$

The corresponding vertical group velocity, using $\mathcal{K}_z^{\mathrm{S}} = -R + 1$,

$$\mathrm{sgn}\{c_z\} = -\mathrm{sgn}\{\mathcal{K}_z^{\mathrm{S}}\} \Rightarrow (c_z)^{\mathrm{S},\pm} > 0.$$

There are two high frequency harmonic beams generated from every intersection point satisfying $\cos\Theta \in [-1, \cos\Theta^{\mathrm{S},-}]$. *Both beams, if existed, are propagating upward.*

(ii) $\chi < 0$

The results from region (A2) of Case VI (A) are also valid here.

(C) $\alpha_1, \alpha_2 < 1$

Region (C1)

The selection rules are identical to Case V although application of reflection-symmetries is needed for $\Psi = -1$.

Region (C2)

The selection rules are identical to Case V although application of reflection-symmetries is needed for $\Psi = +1$.

5.5 Short Summary

In general, the selection rules are analogous to two-dimensional collision counterparts if $\cos\Theta \to \pm 1$. In the traditional branch, $N^2 > f^2$, the high frequency harmonics are only allowed to generate if and only if one of the two interacting conical waves is travelling downward and the other upward. *This constraint is satisfied when there is no horizontal distance* ($H = 0$) *between two IGW sources or at least one of two nondimensional parameters is greater than unity, i.e.* $\max(\alpha_1, \alpha_2) > 1$. *The phase difference between two internal gravity waves is NOT AT ALL important in determining interference pattern.*

On the other hand, *the high frequency harmonic beams are permitted when two IGWs satisfy the geometric constraint,* $\cos\Theta \in [-1, \cos\Theta^{S,-}]$ *in the non-traditional branch,* $f^2 > N^2$*. This constraint is satisfied when there is no vertical distance (*$V = 0$*) between two IGW sources or at least one of two nondimensional parameters is less than unity, i.e.* $\min(\alpha_1, \alpha_2) < 1$. This requires the intersection point is not too far away from the sources. Consequently, the harmonic waves can only be detected in a confined space in the vicinity of the sources.

Unfortunately, due to the limited time and resource, only a few selection rules are well testified. The cases confirmed by numerical simulations are Case I to Case V and region (A2), (B2) of Case VI for traditional branch, $\Psi = +1$, only. The verification of all selection rules by numeric experiments will be addressed as part of future work.

Chapter 6

Nonlinear Interaction of the Quasi-Two-Dimensional Inertia-Gravity Waves with More Realistic Coriolis Force

6.1 Introduction

The selection rules can be extended to deal with more general rotational effect. Instead of $\mathbf{f} = f\mathbf{z}$, consider $\mathbf{f} = f_x\mathbf{x} + f_y\mathbf{y} + f_z\mathbf{z}$ where f_x, f_y, f_z are constant. The general dispersion relation has the following form, with constant Brunt-Väisälä frequency,

$$\omega^2 = \frac{k_\perp^2}{k^2}\, N^2 + \frac{(\mathbf{k}\cdot\mathbf{f})^2}{k^2} = \frac{k_\perp}{k^2}\, N^2 + \frac{(\mathbf{k}\cdot\mathbf{f})^2}{k^2\, f^2}\, f^2, \tag{6.1}$$

and $f = |\mathbf{f}|$. The last term reduces to $(k_z^2/k^2)\, f^2$ if $\mathbf{f} = f\mathbf{z}$.

The group velocity and phase velocity with respect to the general dispersion relation would be,

$$\begin{aligned} (\omega^2\, k^2)\, \mathbf{c} &= \left[(N^2 - \omega^2)\, \omega\, k_x + (\mathbf{k}\cdot\mathbf{f})\, \omega\, f_x\right]\, \mathbf{x} \\ &+ \left[(N^2 - \omega^2)\, \omega\, k_y + (\mathbf{k}\cdot\mathbf{f})\, \omega\, f_y\right]\, \mathbf{y} \\ &+ \left[\quad -\omega^2\ \ \omega\, k_z + (\mathbf{k}\cdot\mathbf{f})\, \omega\, f_z\right]\, \mathbf{z}, \end{aligned} \tag{6.2}$$

and

$$(\omega^2\, k^2)\, \mathbf{c}_\mathrm{p} = \left(\frac{k_\perp^2}{k^2}\, N^2 + \frac{(\mathbf{k}\cdot\mathbf{f})^2}{k^2}\right)(\omega\mathbf{k})\,. \tag{6.3}$$

The orthogonality of phase and group velocities is still valid, i.e. $\mathbf{c}\cdot\mathbf{c}_\mathrm{p} = 0$.

Consider a simpler quasi-two-dimensional special case by rotating the coordinate system such that x-axis is parallel to the horizontal group velocity vector and without loss of

generality also setting $f_y\, f_z > 0$. This is suitable for IGWs propagating in the northern hemisphere where positive y-axis is pointing to higher latitude in general and to north pole if x-axis is parallel to longitudinal direction. In most part of the IGW beam (not too close to the source and the propagating front of the beam), k_x can be approximated by zero. The approximation is confirmed by GCM numerical simulations (Chavanne et al., 2010) where the IGW is generated through tides flowing over topography. The dispersion relation then is function of

$$k_{\text{ratio}} \equiv \frac{k_y}{k_z} = \frac{\omega\, k_y}{\omega\, k_z} \tag{6.4}$$

only and the group velocity is dependent on k_{ratio} and $\omega\, k_z$. The dispersion relation is a constant coefficient quadratic equation in k_{ratio}. Therefore, if the solvability condition is satisfied, there are only two fixed value k_{ratio}'s satisfying dispersion relation. Notice that, if k_{ratio} is fixed, the group velocity is also fixed up to a constant, i.e. the magnitude of the group velocity. That says, all IGW plane waves with same sign but different vertical modal numbers ($\omega\, k_z$'s) would propagate in the same direction, in other words a beam, if they have the same k_{ratio}. The group velocity in terms of k_{ratio} is

$$\begin{aligned}
(\omega^2\, k^2)\, \mathbf{c} &= [(f_x\, f_y)\, k_{\text{ratio}} + (f_x\, f_z)]\ (\omega\, k_z)\, \mathbf{x} \\
&+ \left[(N^2 - \omega^2 + f_y^2)\, k_{\text{ratio}} + (f_y\, f_z)\right]\ (\omega\, k_z)\, \mathbf{y} \\
&+ \left[(\quad - \omega^2 + f_z^2) + (f_y\, f_z)\, k_{\text{ratio}}\right]\ (\omega\, k_z)\, \mathbf{z},
\end{aligned}$$

and the dispersion relation leads to a quadratic equation in k_{ratio}:

$$(N^2 - \omega^2 + f_y^2)\, k_{\text{ratio}}^2 + 2\, f_y\, f_z\, k_{\text{ratio}} + (f_z^2 - \omega^2) = 0. \tag{6.5}$$

k_{ratio}'s must be real by definition, from the well-known quadratic formula, the discriminant therefore must be greater than or equal to zero:

$$\Delta \equiv f_y^2\, f_z^2 + (N^2 - \omega^2 + f_y^2)\, (\omega^2 - f_z^2) = (N^2 - \omega^2)\, (\omega^2 - f_z^2) + f_y^2\, \omega^2 \geq 0.$$

This is equivalent to:

$$\omega_{\text{min}}^2 \leq \omega^2 \leq \omega_{\text{max}}^2,$$

where

$$\begin{aligned}
\omega_{\text{min}}^2 &\equiv \frac{(N^2 + f_y^2 + f_z^2) - \sqrt{(N^2 + f_y^2 + f_z^2)^2 - 4\, f_z^2\, N^2}}{2}, \\
\omega_{\text{max}}^2 &\equiv \frac{(N^2 + f_y^2 + f_z^2) + \sqrt{(N^2 + f_y^2 + f_z^2)^2 - 4\, f_z^2\, N^2}}{2},
\end{aligned}$$

and $f_z^2, (N^2 + f_y^2) \in (\omega_{\text{min}}^2, \omega_{\text{max}}^2)$. Similarly, redefine the variable $\Psi = \text{sgn}\{(N^2 + f_y^2) - f_z^2\}$, there are still two branches of IGW permitted: one would be $\omega_{\text{min}}^2 < f_z^2 < N^2 + f_y^2 < \omega_{\text{max}}^2$ corresponding to $\Psi = +1$ and the other one is $\omega_{\text{min}}^2 < N^2 + f_y^2 < f_z^2 < \omega_{\text{max}}^2$ where $\Psi = -1$.

The solvability condition does not rule out the possibility that $(N^2 + f_y^2) = f_z^2$. But for simplicity, $(N^2 + f_y^2) = f_z^2$ or $\Psi = -1$ cases are not considered here.

When the solvability condition is met, there are two real roots of k_{ratio}:

$$k_{\text{ratio}}^{\pm} = \frac{-f_y\, f_z \pm \sqrt{\Delta}}{N^2 + f_y^2 - \omega^2}, \tag{6.6}$$

and recall $\Delta \equiv f_y^2\, f_z^2 + (N^2 + f_y^2 - \omega^2)\,(\omega^2 - f_z^2)$. Accordingly, for $\Psi = +1$,

$$\Delta \begin{cases} > f_y^2\, f_z^2 & , f_z^2 < \omega^2 < N^2 + f_y^2 \\ = f_y^2\, f_z^2 & , \omega^2 = f_z^2 \\ < f_y^2\, f_z^2 & , \omega_{\text{min}}^2 < \omega^2 < f_z^2 \cup \omega_{\text{max}}^2 > \omega^2 > N^2 + f_y^2 \end{cases},$$

and correspondingly,

$$(k_{\text{ratio}}^{+})\,(k_{\text{ratio}}^{-}) \begin{cases} < 0 & , f_z^2 < \omega^2 < N^2 + f_y^2 \\ = 0 & , \omega^2 = f_z^2 \\ > 0 & , \omega_{\text{min}}^2 < \omega^2 < f_z^2 \cup \omega_{\text{max}}^2 > \omega^2 > N^2 + f_y^2. \end{cases}.$$

The range of allowable frequency band is therefore divided into four intervals, $\omega_{\text{min}}^2 < \omega^2 < f_z^2$, $\omega^2 = f_z^2$, $f_z^2 < \omega^2 < N^2 + f_y^2$ and $\omega_{\text{max}}^2 > \omega^2 > N^2 + f_y^2$.

$k_{\text{ratio}}^{\pm}$ correspond to beams propagating at different angles $\psi^{\pm}$ measured relative to the positive x-axis,

$$\cot\psi^{\pm} \equiv \frac{c_y}{c_z} = -(k_{\text{ratio}}^{\pm})^{-1} = -\frac{k_z}{k_y} \Rightarrow \tan\psi^{\pm} = -k_{\text{ratio}}^{\pm}, \tag{6.7}$$

and

$$c_y = (\omega\, k_y)\,(\omega^2\, k^2)^{-1}\,(\pm\sqrt{\Delta})\,(k_{\text{ratio}}^{\pm})^{-1}, \tag{6.8}$$

$$c_z = -(\omega\, k_z)\,(\omega^2\, k^2)^{-1}\,(\pm\sqrt{\Delta})\,(k_{\text{ratio}}^{\pm}). \tag{6.9}$$

It can be proved (the derivation is straightforward but tedious) that

$$\frac{d\, k_{\text{ratio}}^{+}}{d\,\omega^2} > 0, \tag{6.10}$$

$$\frac{d\, k_{\text{ratio}}^{-}}{d\,\omega^2} < 0. \tag{6.11}$$

These two relations are used to compare values of k_{ratio}'s at different frequencies.

Applying [Eq. (6.6)], [Eq. (6.8)] and [Eq. (6.9)], the signs of $k_{\text{ratio}}^{\pm}$ and the relation between phase and group velocities are listed in Table 6.1. Beware that the relation between phase and group velocities is different for each frequency interval that solvability condition is met.

The general theory is not ready yet at this point, but several special cases would be presented here.

Table 6.1 The signs of $k^{\pm}_{\rm ratio}$ and the relation between phase and group velocities in different frequency intervals are listed here.

	$\omega^2_{\rm min} < \omega^2 < f_z^2$	$\omega^2 = f_z^2$	$f_z^2 < \omega^2 < N^2 + f_y^2$	$\omega^2_{\rm max} > \omega^2 > N^2 + f_y^2$
$k^+_{\rm ratio}$	< 0	$= 0$	> 0	> 0
$k^-_{\rm ratio}$	< 0	< 0	< 0	> 0
$\mathrm{sgn}\{c_y^+\}$	$-\mathrm{sgn}\{\omega\, k_y^+\}$	$+\mathrm{sgn}\{\omega\, k_y^+\}$	$+\mathrm{sgn}\{\omega\, k_y^+\}$	$+\mathrm{sgn}\{\omega\, k_y^+\}$
$\mathrm{sgn}\{c_z^+\}$	$+\mathrm{sgn}\{\omega\, k_z^+\}$	$-\mathrm{sgn}\{\omega\, k_z^+\}$	$-\mathrm{sgn}\{\omega\, k_z^+\}$	$-\mathrm{sgn}\{\omega\, k_z^+\}$
$\mathrm{sgn}\{c_y^-\}$	$+\mathrm{sgn}\{\omega\, k_y^-\}$	$+\mathrm{sgn}\{\omega\, k_y^-\}$	$+\mathrm{sgn}\{\omega\, k_y^-\}$	$-\mathrm{sgn}\{\omega\, k_y^-\}$
$\mathrm{sgn}\{c_z^-\}$	$-\mathrm{sgn}\{\omega\, k_z^-\}$	$-\mathrm{sgn}\{\omega\, k_z^-\}$	$-\mathrm{sgn}\{\omega\, k_z^-\}$	$+\mathrm{sgn}\{\omega\, k_z^-\}$

6.2 IGW Sources Forced at Frequency, $f_z^2 < \omega^2 < N^2 + f_y^2$

First, consider the simplest case that two sources are forcing at the same frequency ω where $f_z^2 < \omega^2 < N^2 + f_y^2$. There are two collision configurations: the first one is that both primary beams have the same sign horizontal group velocity, like in (Fig. 6.1(a)) and (Fig. 6.2(a)), and the other one is with same sigh vertical group velocity, see (Fig. 6.1(b)) and (Fig. 6.2(b)). The outgoing second harmonics therefore may fall into two different frequency intervals, $f_z^2 < (2\omega)^2 < N^2 + f_y^2$, see (Fig. 6.1), or $\omega^2_{\rm max} > (2\omega)^2 > N^2 + f_y^2$, see (Fig. 6.2).

In the first configuration, label the beam from the quadrant II as the first beam and that from quadrant III as the second beam. Since $f_z^2 < \omega^2 < N^2 + f_y^2$ and the group velocities are known, from Table 6.1:

$$\omega\, k_{y,1} > 0,\ \omega\, k_{z,1} > 0,$$
$$\omega\, k_{y,2} > 0,\ \omega\, k_{z,2} < 0,$$

and

$$k_{y,1} = k^+_{\rm ratio}\, k_{z,1}, k_{y,2} = k^-_{\rm ratio}\, k_{z,2}.$$

Applying the constraint that the harmonics are generated from nonlinear interaction of the two primary beams, the wave vectors of harmonic beams in component form are

$$\begin{aligned} (2\omega)\, k_y^{\rm H} &= 2\,(\omega\, k_{y,1} + \omega\, k_{y,2}) > 0, \\ (2\omega)\, k_z^{\rm H} &= 2\,(\omega\, k_{z,1} + \omega\, k_{z,2}), \end{aligned} \tag{6.12}$$

and must satisfy [Eq. (6.7)]

$$\frac{k_y^{\rm H}}{k_z^{\rm H}} = k^{{\rm H},\pm}_{\rm ratio} = \frac{k^+_{\rm ratio}\, k_{z,1} + k^-_{\rm ratio}\, k_{z,2}}{k_{z,1} + k_{z,2}}.$$

The above equation can be rewritten in the form:

$$\underbrace{\frac{k_{z,1}}{k_{z,2}}}_{<0} = -\frac{k_{\text{ratio}}^{\text{H},\pm} - k_{\text{ratio}}^{-}}{k_{\text{ratio}}^{\text{H},\pm} - k_{\text{ratio}}^{+}}.$$

The right-hand side of the above equation must be less than zero otherwise there is a contradiction. If there is no contradiction, the harmonics are permitted to generate. Otherwise, the harmonics are forbidden since the dispersion relation is not satisfied. And this is how the "selection rule" works.

If the harmonic frequency falls in $f_z^2 < (2\omega)^2 < N^2 + f_y^2$, by using [Eq. (6.10)] and [Eq. (6.11)]:

$$k_{\text{ratio}}^{\text{H},+} > k_{\text{ratio}}^{+} > 0 > k_{\text{ratio}}^{-} > k_{\text{ratio}}^{\text{H},-}.$$

Use the above relation to testify the selection rule

$$\begin{aligned}
\underbrace{\frac{k_{z,1}}{k_{z,2}}}_{<0} &= -\frac{\overbrace{k_{\text{ratio}}^{\text{H},+} - k_{\text{ratio}}^{-}}^{>0}}{\underbrace{k_{\text{ratio}}^{\text{H},+} - k_{\text{ratio}}^{+}}_{>0}} < 0, \\
\underbrace{\frac{k_{z,1}}{k_{z,2}}}_{<0} &= -\frac{\overbrace{k_{\text{ratio}}^{\text{H},-} - k_{\text{ratio}}^{-}}^{<0}}{\underbrace{k_{\text{ratio}}^{\text{H},-} - k_{\text{ratio}}^{+}}_{<0}} < 0.
\end{aligned}$$

There are two fixed valued $(k_{z,1}/k_{z,2})$ satisfying the selection rule, i.e. two beams emanating at individual fixed angles which correspond to $k_{\text{ratio}}^{\text{H},\pm}$. The $k_{\text{ratio}}^{\text{H},+}$ beam has group velocity $c_y^{\text{H},+} > 0$ (known from [Eq. (6.12)]) and therefore $c_z^{\text{H},+} < 0$, i.e. propagating into quadrant IV. Similarly, $k_{\text{ratio}}^{\text{H},-}$ beam has group velocity $c_y^{\text{H},-} > 0$ and $c_z^{\text{H},-} > 0$ corresponds to the beam emanating into quadrant I.

If the harmonics have frequency in $\omega_{\max}^2 > (2\omega)^2 > N^2 + f_y^2$ interval,

$$k_{\text{ratio}}^{\text{H},-} > k_{\text{ratio}}^{\text{H},+} > k_{\text{ratio}}^{+} > 0 > k_{\text{ratio}}^{-}.$$

Similar to above procedures, this time

$$\begin{aligned}
\underbrace{\frac{k_{z,1}}{k_{z,2}}}_{<0} &= -\frac{\overbrace{k_{\text{ratio}}^{\text{H},+} - k_{\text{ratio}}^{-}}^{>0}}{\underbrace{k_{\text{ratio}}^{\text{H},+} - k_{\text{ratio}}^{+}}_{>0}} < 0, \\
\underbrace{\frac{k_{z,1}}{k_{z,2}}}_{<0} &= -\frac{\overbrace{k_{\text{ratio}}^{\text{H},-} - k_{\text{ratio}}^{-}}^{>0}}{\underbrace{k_{\text{ratio}}^{\text{H},-} - k_{\text{ratio}}^{+}}_{>0}} < 0.
\end{aligned}$$

There are also two fixed valued $(k_{z,1}/k_{z,2})$ satisfying the selection rule. The $k_{\rm ratio}^{\rm H,+}$ beam has group velocity $c_y^{\rm H,+} > 0$ and $c_z^{\rm H,+} < 0$, i.e. propagating into quadrant IV. But $k_{\rm ratio}^{\rm H,-}$ beam has group velocity $c_y^{\rm H,-} < 0$ (using last column of Table 6.1 and be aware that the relation between phase velocity and group velocity is different from the "traditional" one) and $c_z^{\rm H,-} > 0$ corresponds to the beam emanating into quadrant II (introducing f_y where $f_y\, f_z > 0$ is like counterclockwisely rotating the "St. Andrew's cross").

The result is confirmed by numerical simulations, see (Fig. 6.1(a)) and (Fig. 6.2(a)).

In the other configuration, label the beam from the quadrant II as the first beam and that from quadrant I as the second beam. Similarly, judging from the group velocities and Table 6.1:

$$\omega\, k_{y,1} > 0,\ \omega\, k_{z,1} > 0,$$
$$\omega\, k_{y,2} < 0,\ \omega\, k_{z,2} > 0,$$

and

$$\begin{aligned} k_{y,1} &= k_{\rm ratio}^{+}\, k_{z,1}, \\ k_{y,2} &= k_{\rm ratio}^{-}\, k_{z,2}. \end{aligned}$$

Applying the constraint that the harmonics are generated from nonlinear interaction of the two primary beams, the wave vectors of harmonic beams in component form are

$$\begin{aligned} (2\omega)\, k_y^{\rm H} &= 2\,(\omega\, k_{y,1} + \omega\, k_{y,2}), \\ (2\omega)\, k_z^{\rm H} &= 2\,(\omega\, k_{z,1} + \omega\, k_{z,2}) > 0 \end{aligned} \tag{6.13}$$

and must satisfy [Eq. (6.7)]:

$$\underbrace{\frac{k_{z,1}}{k_{z,2}}}_{>0} = -\frac{k_{\rm ratio}^{\rm H,\pm} - k_{\rm ratio}^{-}}{k_{\rm ratio}^{\rm H,\pm} - k_{\rm ratio}^{+}}.$$

The right-hand side of the above equation must be greater than zero otherwise there is a contradiction.

If the harmonic frequency falls in $f_z^2 < (2\omega)^2 < N^2 + f_y^2$, recall

$$k_{\rm ratio}^{\rm H,+} > k_{\rm ratio}^{+} > 0 > k_{\rm ratio}^{-} > k_{\rm ratio}^{\rm H,-}.$$

Use the above relation to testify the selection rule,

$$\underbrace{\frac{k_{z,1}}{k_{z,2}}}_{>0} = -\frac{\overbrace{k_{\rm ratio}^{\rm H,+} - k_{\rm ratio}^{-}}^{>0}}{\underbrace{k_{\rm ratio}^{\rm H,+} - k_{\rm ratio}^{+}}_{>0}} < 0,$$

$$\underbrace{\frac{k_{z,1}}{k_{z,2}}}_{>0} = -\frac{\overbrace{k_{\rm ratio}^{\rm H,-} - k_{\rm ratio}^{-}}^{<0}}{\underbrace{k_{\rm ratio}^{\rm H,-} - k_{\rm ratio}^{+}}_{<0}} < 0,$$

yield a contradiction, i.e. LHS is greater than zero but RHS is less than zero. The harmonics are therefore forbidden.

If the harmonics have frequency in $\omega_{\rm max}^2 > (2\omega)^2 > N^2 + f_y^2$ interval,

$$k_{\rm ratio}^{\rm H,-} > k_{\rm ratio}^{\rm H,+} > k_{\rm ratio}^{+} > 0 > k_{\rm ratio}^{-}.$$

Similar to above procedures, this time

$$\begin{aligned}
\underbrace{\frac{k_{z,1}}{k_{z,2}}}_{>0} &= -\frac{\overbrace{k_{\rm ratio}^{\rm H,+} - k_{\rm ratio}^{-}}^{>0}}{\underbrace{k_{\rm ratio}^{\rm H,+} - k_{\rm ratio}^{+}}_{>0}} < 0, \\
\underbrace{\frac{k_{z,1}}{k_{z,2}}}_{>0} &= -\frac{\overbrace{k_{\rm ratio}^{\rm H,-} - k_{\rm ratio}^{-}}^{>0}}{\underbrace{k_{\rm ratio}^{\rm H,-} - k_{\rm ratio}^{+}}_{>0}} < 0.
\end{aligned}$$

No harmonics are permitted, either.

The results are demonstrated in (Fig. 6.1(b)) and (Fig. 6.2(b)).

6.3 IGW Sources Forced at Frequency, $\omega_{\rm min}^2 < \omega^2 < f_z^2$

This time, consider if two sources are forcing at the same frequency ω where $\omega_{\rm min}^2 < \omega^2 < f_z^2$. There are also two collision configurations: the first one is that both primary beams have the same sign horizontal group velocity, like in (Fig. 6.3(a)), and the other one is both beams are heading toward each other, see (Fig. 6.3(b)). The outgoing second harmonics therefore may fall into three different frequency intervals, $f_z^2 < (2\omega)^2 < N^2 + f_y^2$, see (Fig. 6.3), or $\omega_{\rm min}^2 < (2\omega)^2 < f_z^2$ and $\omega_{\rm max}^2 > (2\omega)^2 > N^2 + f_y^2$ which numerical simulations currently are not available.

In the first configuration, label the bottom source as the first beam and top one as the second beam. Since $\omega_{\rm min}^2 < \omega^2 < f_z^2$ and the group velocities are known, from Table 6.1:

$$\begin{aligned}
\omega\, k_{y,1} > 0,\ \omega\, k_{z,1} < 0, \\
\omega\, k_{y,2} < 0,\ \omega\, k_{z,2} > 0,
\end{aligned}$$

and

$$\begin{aligned}
k_{y,1} &= k_{\rm ratio}^{+}\, k_{z,1}, \\
k_{y,2} &= k_{\rm ratio}^{-}\, k_{z,2}.
\end{aligned}$$

Applying the constraint that the harmonics are generated from nonlinear interaction of the two primary beams, the wave vectors of harmonic beams in component form are

$$\begin{aligned}
(2\omega)\, k_y^{\rm H} &= 2\,(\omega\, k_{y,1} + \omega\, k_{y,2}), \\
(2\omega)\, k_z^{\rm H} &= 2\,(\omega\, k_{z,1} + \omega\, k_{z,2}),
\end{aligned}$$

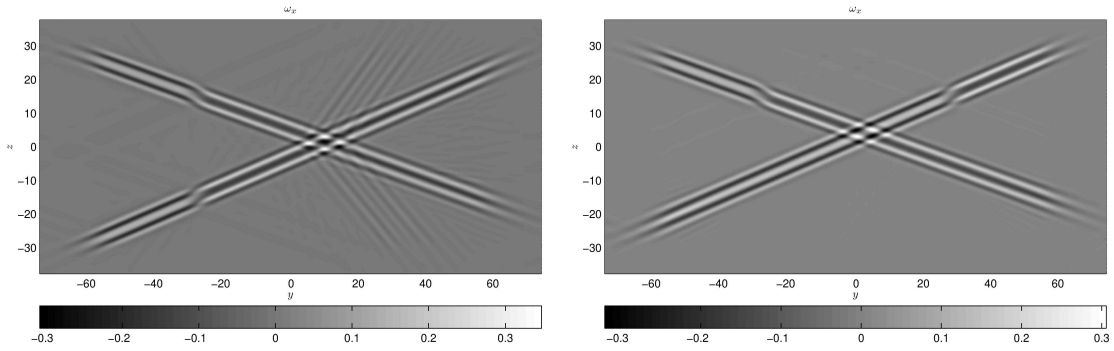

(a) (b)

Figure 6.1 Numerical simulations of physical beams, shown by the magnitude of their x-dir vorticity. Each primary beam has frequency of ω with $f_z^2 < \omega^2 < N^2 + f_y^2$ and second harmonics have frequency in $f_z^2 < (2\omega)^2 < N^2 + f_y^2$ interval, too. In these simulations, $f/N = 1/4$, $f_y = f\cos 40°, f_z = f\sin 40°$ and $|\omega|/f_z = 2.51$. The angles ψ for primary beams are 161.1° (from quadrant II), 203.4° (from quadrant III) and 23.4° (from quadrant I) respectively and that for second harmonics are 310° (into quadrant IV) and 53.5° (into quadrant I). (a) (left) The primary beam sources lie in the corners on the left side of the panel. Both primary beams propagate to the right, interact, and create two harmonic beams or "legs" with frequencies $\pm 2\omega$. (b) (right) As in panel (a), but with sources at the top. No harmonic beams are produced.

and must satisfy [Eq. (6.7)]

$$\underbrace{\frac{k_{z,1}}{k_{z,2}}}_{<0} = -\frac{k_{\text{ratio}}^{\text{H},\pm} - k_{\text{ratio}}^{-}}{k_{\text{ratio}}^{\text{H},\pm} - k_{\text{ratio}}^{+}}.$$

If the harmonic frequency falls in $f_z^2 < (2\omega)^2 < N^2 + f_y^2$, by using [Eq. (6.10)] and [Eq. (6.11)]:

$$k_{\text{ratio}}^{\text{H},+} > 0 > k_{\text{ratio}}^{+} > k_{\text{ratio}}^{-} > k_{\text{ratio}}^{\text{H},-}.$$

Use the above relation to testify the selection rule

$$\underbrace{\frac{k_{z,1}}{k_{z,2}}}_{<0} = -\frac{\overbrace{k_{\text{ratio}}^{\text{H},+} - k_{\text{ratio}}^{-}}^{>0}}{\underbrace{k_{\text{ratio}}^{\text{H},+} - k_{\text{ratio}}^{+}}_{>0}} < -1,$$

$$\underbrace{\frac{k_{z,1}}{k_{z,2}}}_{<0} = -\frac{\overbrace{k_{\text{ratio}}^{\text{H},-} - k_{\text{ratio}}^{-}}^{<0}}{\underbrace{k_{\text{ratio}}^{\text{H},-} - k_{\text{ratio}}^{+}}_{<0}} < 0, > -1.$$

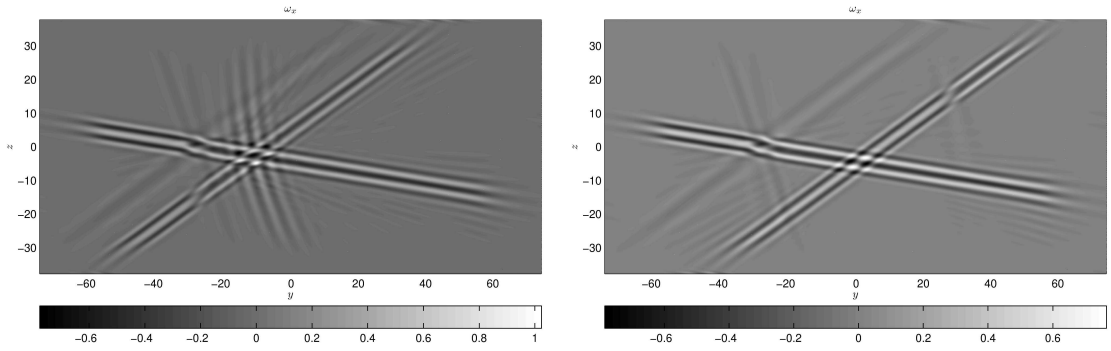

(a) (b)

Figure 6.2 Numerical simulations of physical beams, shown by the magnitude of their x-dir vorticity. Each primary beam has frequency of ω with $f_z^2 < \omega^2 < N^2 + f_y^2$ but second harmonics have frequency $\omega_{\max}^2 > (2\omega)^2 > N^2 + f_y^2$. In these simulations, $f/N = 3/4$, $f_y = f\,\cos 40°$, $f_z = f\,\sin 40°$ and $|\omega|/f_z = 1.22$. The angles ψ for primary beams are 170.7° (from quadrant II), 216.0° (from quadrant III) and 36.0° (from quadrant I) respectively and that for second harmonics are 286.1° (into quadrant IV) and 100.7° (into quadrant II). The ratio of Coriolis parameter to Brunt-Väisälä frequency is chosen to emphasize the possibility that the second harmonic beam is able to propagating into quadrant II (which is impossible if $f_z^2 < (2\omega)^2 < N^2 + f_y^2$, as in (Fig. 6.1(a))). (a) (left) The primary beam sources lie in the corners on the left side of the panel. Both primary beams propagate to the right, interact, and create two harmonic beams with frequencies $\pm 2\omega$. (b) (right) As in panel (a), but with sources at the top. No harmonic beams are produced.

There are two fixed valued $(k_{z,1}/k_{z,2})$ satisfying the selection rule, i.e. two beams emanating at individual fixed angles which correspond to $k_{\rm ratio}^{\rm H,\pm}$. The $k_{\rm ratio}^{\rm H,+}$ beam has group velocity $c_z^{\rm H,+} > 0$ (since $\omega\,k_{z,2} < -\omega\,k_{z,1} \Rightarrow (\omega\,k_{z,1} + \omega\,k_{z,2}) < 0 \Rightarrow (2\omega)\,k_z^{\rm H,+} < 0$) and therefore $c_y^{\rm H,+} < 0$, i.e. propagating into quadrant II. Similarly, $k_{\rm ratio}^{\rm H,-}$ beam has group velocity $c_z^{\rm H,-} < 0$ (since $\omega\,k_{z,2} > -\omega\,k_{z,1} \Rightarrow (\omega\,k_{z,1} + \omega\,k_{z,2}) > 0 \Rightarrow (2\omega)\,k_z^{\rm H,+} > 0$) and $c_y^{\rm H,-} < 0$ corresponds to the beam emanating into quadrant III.

In the second configuration, label the beam from quadrant III as the first beam and that from quadrant I as the second beam. From Table 6.1 and the known group velocities:

$$\omega\,k_{y,1} < 0,\ \omega\,k_{z,1} > 0,$$
$$\omega\,k_{y,2} < 0,\ \omega\,k_{z,2} > 0,$$

and

$$\begin{aligned} k_{y,1} &= k_{\rm ratio}^{+}\,k_{z,1}, \\ k_{y,2} &= k_{\rm ratio}^{-}\,k_{z,2}. \end{aligned}$$

Applying the constraint that the harmonics are generated from nonlinear interaction of the two primary beams, the wave vectors of harmonic beams in component form are

$$\begin{aligned}(2\omega)\, k_y^{\mathrm{H}} &= 2\,(\omega\, k_{y,1} + \omega\, k_{y,2}) < 0,\\ (2\omega)\, k_z^{\mathrm{H}} &= 2\,(\omega\, k_{z,1} + \omega\, k_{z,2}) > 0,\end{aligned}$$

and must satisfy [Eq. (6.7)]

$$\underbrace{\frac{k_{z,1}}{k_{z,2}}}_{>0} = -\frac{k_{\mathrm{ratio}}^{\mathrm{H},\pm} - k_{\mathrm{ratio}}^{-}}{k_{\mathrm{ratio}}^{\mathrm{H},\pm} - k_{\mathrm{ratio}}^{+}}.$$

If the harmonic frequency falls in $f_z^2 < (2\omega)^2 < N^2 + f_y^2$, by using [Eq. (6.10)] and [Eq. (6.11)]:

$$k_{\mathrm{ratio}}^{\mathrm{H},+} > 0 > k_{\mathrm{ratio}}^{+} > k_{\mathrm{ratio}}^{-} > k_{\mathrm{ratio}}^{\mathrm{H},-}.$$

Use the above relation and testify the selection rule

$$\begin{aligned}\underbrace{\frac{k_{z,1}}{k_{z,2}}}_{>0} &= -\frac{\overbrace{k_{\mathrm{ratio}}^{\mathrm{H},+} - k_{\mathrm{ratio}}^{-}}^{>0}}{\underbrace{k_{\mathrm{ratio}}^{\mathrm{H},+} - k_{\mathrm{ratio}}^{+}}_{>0}} < -1,\\ \underbrace{\frac{k_{z,1}}{k_{z,2}}}_{>0} &= -\frac{\overbrace{k_{\mathrm{ratio}}^{\mathrm{H},-} - k_{\mathrm{ratio}}^{-}}^{<0}}{\underbrace{k_{\mathrm{ratio}}^{\mathrm{H},-} - k_{\mathrm{ratio}}^{+}}_{<0}} < 0, > -1.\end{aligned}$$

The contradiction here means there is no harmonic beam permitted.

The second configuration can be extended to explain the reflection from the flat bottom, see (Fig. 6.4). Unlike the beam in the frequency band $f_z^2 < \omega^2 < N^2 + f_y^2$ or the more familiar case $f_z^2 < \omega^2 < N^2$, the reflected beam is back into quadrant I instead of propagating into quadrant II. Also there is no second harmonics generated. This example offers a possible explanation for the trapping of near-inertial band energy in $28-30^\circ$ north where the Coriolis parameter f coincides with diurnal tidal frequency (van Haren, 2005). The reflected beam has the same sign slope as that of the incoming beam would confine the near-inertial band energy transfer in the vicinity of the generation site and there is no second harmonics generated might be the cause of the drop of the semidiurnal energy flux in lower latitudes.

6.4 Conclusion

The selection rules are still similar to the quasi-two-dimensional inertia-gravity waves with simple Coriolis effect. With the introduction of more realistic Coriolis parameter, the solvability condition for inertia-gravity waves has a broader frequency band $\omega_{\mathrm{min}}^2 < f_z^2 <$

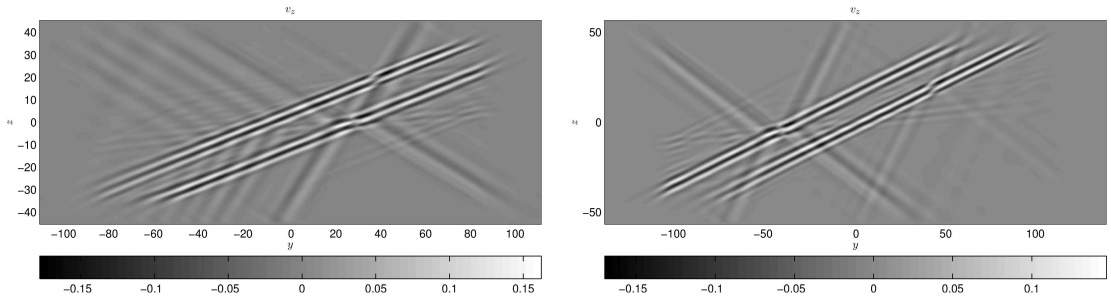

(a) (b)

Figure 6.3 Numerical simulations of physical beams, shown by the magnitude of their z-dir velocity. Each primary beam has frequency of ω with $\omega_{\min}^2 < \omega^2 < f_z^2$ but second harmonics have frequency $f_z^2 < (2\omega)^2 < N^2 + f_y^2$. In these simulations, $f/N = 3/4$, $f_y = f\,\cos 40°$, $f_z = f\,\sin 40°$ and $|\omega|/f_z = 0.91$. The angles ψ for primary beams are 5.2° (from quadrant I), 21.6° (also from quadrant I) and 185.2° (from quadrant III) respectively and that for second harmonics are 149.1° (into quadrant II) and 237.6° (into quadrant III). (a) (left) The primary beam sources lie in the corners on the right side of the panel. Both primary beams propagate to the left, interact, and create two harmonic beams with frequencies $\pm 2\omega$. (b) (right) As in panel (a), but with one source at the top and the other one at the bottom. No harmonic beams are produced.

$N^2 + f_y^2 < \omega_{\max}^2$ and thus changes the relation between group velocity and phase velocity in the frequency intervals $\omega_{\min}^2 < \omega^2 < f_z^2$ and $\omega_{\max}^2 > (2\omega)^2 > N^2 + f_y^2$. The reflection from flat bottom in the frequency interval $\omega_{\min}^2 < \omega^2 < f_z^2$ example offers a possible solution to explain the trapping of energy transfer in near-inertial frequency band and drop of semidiurnal energy flux in lower latitudes near the $28 - 30°$ north where the Coriolis parameter f coincides with diurnal tidal frequency (van Haren, 2005).

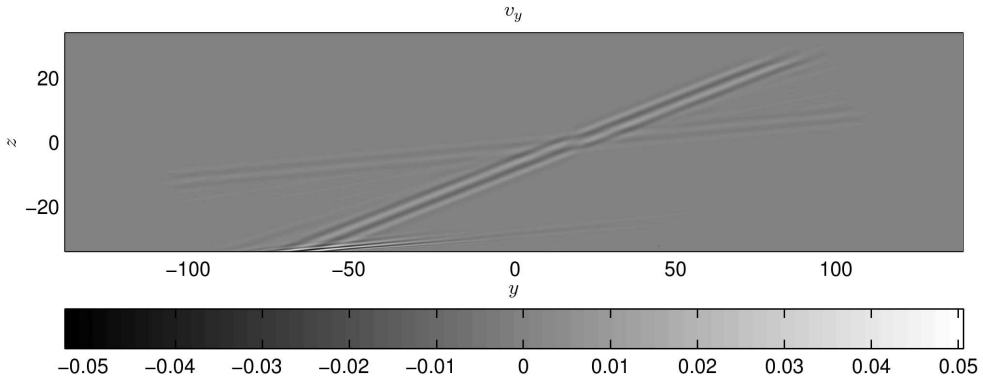

Figure 6.4 Numerical simulations of physical beams, shown by the magnitude of their y-dir velocity. The primary beam has frequency of ω with $\omega_{\min}^2 < \omega^2 < f_z^2$ but the harmonics, if exist, lie in $f_z^2 < (2\omega)^2 < N^2 + f_y^2$ interval. In this simulation, $f/N = 3/4$, $f_y = f\cos 40°, f_z = f\sin 40°$, $|\omega|/f_z = 0.91$ and $|\omega|/\omega_{\min} = 1.07$. The angles ψ for primary beams are 21.6° and 5.2° respectively and that for second harmonics, if exist, are 57.6° and 30.9°. This example is used to explain the trapping of near-inertial internal gravity wave energy flux near the $28 - 30°$ north where the Coriolis parameter f coincides with diurnal tidal frequency (van Haren, 2005). The reflected beam has the same sign slope as that of the incoming beam would confine the near-inertial band energy transfer in the vicinity of the generation site and there is no second harmonics generated might be the cause of the drop of the semidiurnal energy flux in lower latitudes

Chapter 7

Summary and Future Work

After all, a question naturally arises: Are the selection rules specific to internal gravity waves or inertia-gravity waves? If the answer is "no" to this question, can selection rules be extended to waves with any form of dispersion relation? Or, what are the properties of dispersion relation that are necessary/sufficient for the existence of selection rules?

Let's consider a generic setup: Suppose two two-dimensional plane waves with known frequencies, ω_1, ω_2, and known wave vectors, $\mathbf{k}_1, \mathbf{k}_2$ interact nonlinearly and thus generate an interacted plane wave with unknown frequency, ω^{H}, and unknown wave vector, $\mathbf{k}^{\mathrm{H}}$. Each interacting plane wave must satisfy a generic dispersion relation, $\mathcal{D}$, such that

$$\begin{aligned} \mathcal{D}\left(\omega_1, k_{x,1}, k_{z,1}\right) &= 0, \\ \mathcal{D}\left(\omega_2, k_{x,2}, k_{z,2}\right) &= 0, \end{aligned}$$

and the unknown frequency and wave vector of interacted harmonic then are obtained by applying quadratic nonlinearities:

$$\begin{aligned} \omega^{\mathrm{H}} &= \omega_1 + \omega_2, \\ k_x^{\mathrm{H}} &= k_{x,1} + k_{x,2}, \\ k_z^{\mathrm{H}} &= k_{z,1} + k_{z,2}. \end{aligned}$$

Obviously, the interacted harmonic is allowed if

$$\mathcal{D}\left(\omega^{\mathrm{H}}, k_x^{\mathrm{H}}, k_z^{\mathrm{H}}\right) = 0,$$

and is forbidden if

$$\mathcal{D}\left(\omega^{\mathrm{H}}, k_x^{\mathrm{H}}, k_z^{\mathrm{H}}\right) \neq 0.$$

In general, there is probably no explicit rule to avoid applying the above procedures to every pair of interacting plane waves.

Suppose a family of dispersion relation can be expressed in the following form:

$$\mathcal{D}\left(\omega, k_x, k_z\right) \equiv k_x^{2n} - F(\omega; G_1, G_2, \ldots, G_s)\, k_z^{2n} = 0,$$

where G_1 to G_s are s parameters independent of $\omega, \mathbf{k}$ and F is non-dimensional. Thus, the dispersion relations for both interacting waves can be expressed as follows,

$$\begin{aligned} k_{x,1}^{2n} &= F(\omega_1; G_1, G_2, \ldots, G_s)\, k_{z,1}^{2n}, \\ k_{x,2}^{2n} &= F(\omega_2; G_1, G_2, \ldots, G_s)\, k_{z,2}^{2n}. \end{aligned}$$

The dispersion relation for interacted harmonic in terms of $k_{z,1}$ and $k_{z,2}$ reduces to either

$$\begin{aligned} \left[F^{1/(2n)}(\omega_1; G_1, G_2, \ldots, G_s)\, k_{z,1} + F^{1/(2n)}(\omega_2; G_1, G_2, \ldots, G_s)\, k_{z,2}\right] = \\ \pm F^{1/(2n)}(\omega_1 + \omega_2; G_1, G_2, \ldots, G_s)\, (k_{z,1} + k_{z,2}), \end{aligned}$$

or

$$\begin{aligned} \left[F^{1/(2n)}(\omega_1; G_1, G_2, \ldots, G_s)\, k_{z,1} - F^{1/(2n)}(\omega_2; G_1, G_2, \ldots, G_s)\, k_{z,2}\right] = \\ \pm F^{1/(2n)}(\omega_1 + \omega_2; G_1, G_2, \ldots, G_s)\, (k_{z,1} + k_{z,2}), \end{aligned}$$

a total of four variations. Therefore, this family of dispersion relation alone is not enough to determine the existence of harmonics.

If n is equal to 1, G_1 is the Brunt-Väisälä frequency, N, and G_2 is the Coriolis parameter, f, the dispersion relation for inertia-gravity wave is recovered:

$$k_x^2 = F(\omega; N, f)\, k_z^2, \;\; F(\omega; N, f) = \frac{\omega^2 - f^2}{N^2 - \omega^2} = \tan^2\theta,$$

and

$$k_x = \pm\sqrt{\frac{\omega^2 - f^2}{N^2 - \omega^2}}\, k_z.$$

In chapter 3 and 4, one more constraint is introduced to resolve this ambiguity: the radiation conditions of incoming beams. The radiation condition helps decide the direction of group velocity and phase velocity of the incoming beams. Consequently, one could distinguish which configuration out of the four variation is correct. In the thought experiments performed in chapter 3 and 4, the radiation condition contains the least geometric information needed from the two wave sources because the setup cleverly guarantees the interaction would always happen. Hence, some sort of geometric information about the two wave sources is needed to make sure that the two waves can interact somewhere for this family of dispersion relation. For interaction among IGW beams, radiation condition is enough. But for interaction between inertia-gravity conical waves, the determination of intersection points is necessary to retrieve the geometric information needed to obtain the relation between group velocity and phase velocity.

Therefore, the interaction of IGWs has several properties which are good for explaining selection rules: 1. It is easy to identify the interaction area. As a result, the extra geometric information needed is obtained easily. 2. The wave beam is a wave packet contains infinite number of wave vectors. Thus, there are infinite number of $\mathbf{k}_1, \mathbf{k}_2$ pairs interacting in the

interaction area and some of them would produce harmonics that satisfy quadratic nonlinearities and dispersion relation at the same time. 3. The phenomenon is distinguishable even by inspection: the internal wave beams with different frequencies propagate at different polar angles. 4. It has real physical applications, such as reflection from a slope and the interference pattern of the internal tide.

The selection rules derived in Chapter 3 and 4 are sufficient because no harmonic beams allowed by Tables 4.6 and 4.7 are missing from numerical simulations (all the possibilities have been tested). The selection rules derived in Chapter 5 are most probably also sufficient because no harmonic beams allowed are missing from numerical simulations (but not all the possibilities have been tested). The verification of all selection rules by numeric experiments will be addressed as part of future work.

Bibliography

M. H. Alford. Redistribution of energy available for ocean mixing by long-range propagation of internal waves. *Nature*, 423:159–162, 2003.

C. Chavanne, P. Flament, G. Carter, M. Merrifield, D. Luther, E. Zaron, and K-W. Gurgel. The surface expression of semidiurnal internal tides near a strong source at hawaii. part i: Observations and numerical predictions. *Journal of Physical Oceanography*, 40(6):1155–1179, 2010.

T. Gerkema and E. Exarchou. Internal-wave properties in weakly stratified layers. *Journal of Marine Research*, 66:617–644, 2008.

T. Gerkema, C. Staquet, and P. Bouruet-Aubertot. Non-linear effects in internal-tide beams, and mixing. *Ocean Modelling*, 12:302–318, 2006.

C.-H. Jiang and P. S. Marcus. Selection rules for the nonlinear interaction of internal gravity waves. *Physical Review Letters*, 102(12):124502, Mar 2009.

P. K. Kundu and I. M. Cohen. *Fluid Mechanics*. Elsevier Academic Press, 2004.

K. G. Lamb. Nonlinear interaction among internal wave beams generated by tidal flow over supercritical topography. *Geophysical Research Letters*, 31(9):L09313, doi:10.1029/2003GL019393, May 2004.

A. E. H. Love. Wave-motion in a heterogeneous heavy liquid. *Proceedings of the London Mathematical Society*, 22(9):307–316, May 1891.

D. E. Mowbray and B. S. H. Rarity. A theoretical and experimental investigation of the phase configuration of internal waves of small amplitude in a density stratified liquid. *Journal Of Fluid Mechanics*, 28:1–16, 1967.

T. Peacock and A. Tabaei. Visualization of nonlinear effects in reflecting internal wave beams. *Physics of Fluids*, 17:061702, 2005.

O. M. Phillips. Theoretical and experimental studies of gravity wave interactions. *Proceedings of the Royal Society of London. Series A, Mathematical and Physical Sciences*, 299(1456): 104–119, 1967.

L. Rainville, T. M. Shaun Johnston, G. S. Carter, M. A. Merrifield, R. Pinkel, P. F. Worcester, and B. D. Dushaw. Interference pattern and propagation of the M_2 internal tide south of the hawaiian ridge. *Journal of Physical Oceanography*, 40:311, 2010.

A. Tabaei, T. R. Akylas, and K. G. Lamb. Nonlinear effects in reflecting and colliding internal wave beams. *Journal Of Fluid Mechanics*, 526:217–243, 2005.

S. G. Teoh, G. N. Ivey, and J Imberger. Laboratory study of the interaction between two

internal wave rays. *Journal Of Fluid Mechanics*, 336:91–122, 1997.

H. van Haren. Tidal and near-inertial peak variations around the diurnal critical latitude. *Geophysical Research Letters*, 32:L23611, doi:10.1029/2005GL024160, 2005.

H. van Haren. Asymmetric vertical internal wave propagation. *Geophysical Research Letters*, 33:L06618, doi:10.1029/2005GL025499, 2006.

H. van Haren and C. Millot. Rectilinear and circular inertial motions in the western mediterranean sea. *Deep Sea Research Part I: Oceanographic Research Papers*, 51(11):1441 – 1455, 2004.

H. P. Zhang, B. King, and H. L. Swinney. Resonant generation of internal waves on a model continental slope. *Physical Review Letters*, 100:244504, 2008.

Z. Zhao and M. H. Alford. New altimetric estimates of mode-1 M_2 internal tides in the central north pacific ocean. *Journal of Physical Oceanography*, 39:1669, 2009.

Appendix A

Determine $2\tan^2\theta^{\mathrm{S}}/\tan^2\theta$ for $\Psi = -1$

The range of $\tan^2\theta^{\mathrm{S}}/\tan^2\theta$ for $\Psi = -1$ provides important information to determine necessary (not sufficient) conditions in Case II and III to distinguish intersection points which are capable to generate harmonics or not.

Based on [Eq. (5.2c)], the ratio between $\tan^2\theta^{\mathrm{S}}$ and $\tan^2\theta$ is

$$\frac{\tan^2\theta^{\mathrm{S}}}{\tan^2\theta} = \frac{f^2-4\omega^2}{4\omega^2-N^2}\,\frac{\omega^2-N^2}{f^2-\omega^2},$$

and is subjected to the constraint $N^2 < \omega^2 < (f/2)^2$ such that $N^2 < (2\omega)^2 < f^2$ is still valid. Taking derivative with respect to ω^2 of the ratio leads to

$$\frac{d}{d\omega^2}\left(\frac{\tan^2\theta^{\mathrm{S}}}{\tan^2\theta}\right) = \frac{-12(f^2-N^2)(\omega^4-N^2f^2/4)}{(4\omega^2-N^2)^2(f^2-\omega^2)^2}.$$

The derivative equals to zero while $\omega^2 = Nf/2$ and

$$\frac{d}{d\omega^2}\left(\frac{\tan^2\theta^{\mathrm{S}}}{\tan^2\theta}\right)\begin{cases} >0 & \text{if } \omega^2 < Nf/2 \\ <0 & \text{if } \omega^2 > Nf/2 \end{cases}.$$

Thus the maximum of $\tan^2\theta^{\mathrm{S}}/\tan^2\theta$ is located at $\omega^2 = Nf/2$ and the value is

$$\max\left(\frac{\tan^2\theta^{\mathrm{S}}}{\tan^2\theta}\right) = \left.\frac{\tan^2\theta^{\mathrm{S}}}{\tan^2\theta}\right|_{\omega^2=Nf/2} = \left(\frac{f-2N}{2f-N}\right)^2.$$

This maximum is bounded in between 0 while $N \to (f/2)$ and 1/4 while $N \to 0$, i.e.

$$0 < \max\left(\frac{\tan^2\theta^{\mathrm{S}}}{\tan^2\theta}\right) < \frac{1}{4}.$$

Therefore, a very conservative estimate is obtained:

$$0 < \frac{2\,\tan^2\theta^{\mathrm{S}}}{\tan^2\theta} < \frac{1}{2}. \tag{A.1}$$

Appendix B

Determine $\cos\Theta$ in Case VI?

The range of $\cos\Theta$ is crucial in deriving the selection rules. Since Θ is the angle enclosed by r_1 and r_2 in the triangle with sides of lengths r_1, r_2 and $2H$, see (Fig. 5.1(a)), (Fig. 5.1(b)) and (Fig. 5.1(c)) for illustrations. The famous law of cosines gives,

$$\cos\Theta = \frac{r_1^2 + r_2^2 - (2H)^2}{2r_1 r_2} = \frac{\tilde{r}_1^2 + \tilde{r}_2^2 - 1}{2\tilde{r}_1\tilde{r}_2} = \frac{(\tilde{r}_1 + \tilde{r}_2)^2 - 1}{2\tilde{r}_1\tilde{r}_2} - 1, \tag{B.1}$$

where nondimensional $\tilde{r_1}$ and $\tilde{r_2}$ are defined as,

$$\tilde{r}_1(\eta) \equiv \frac{r_1}{2H} = \frac{|z_I \cot\theta_1|}{2H} = \alpha_1|\eta|,$$

and

$$\tilde{r}_2(\eta) \equiv \frac{r_2}{2H} = \frac{|(z_I - V)\cot\theta_2|}{2H} = \alpha_2|\eta - 1|.$$

In the following derivation, it is also useful to work on $\tilde{r}_{\text{sum}} \equiv \tilde{r}_1 + \tilde{r}_2$ and $\tilde{r}_{\text{diff}} \equiv \tilde{r}_1 - \tilde{r}_2$ instead of r_1 and r_2. The nondimensional x-coordinate of intersection point, ξ, therefore can be rewritten as,

$$\xi - 1 = \tilde{r}_{\text{sum}}\,\tilde{r}_{\text{diff}},$$

and $2\tilde{r}_1\tilde{r}_2$ can also be expressed in terms of $\tilde{r}_{\text{sum}}$ and $\tilde{r}_{\text{diff}}$:

$$2\tilde{r}_1\tilde{r}_2 = (\tilde{r}_{\text{sum}}^2 - \tilde{r}_{\text{diff}}^2)/2.$$

Therefore, $\cos\Theta$ in terms of $\tilde{r}_{\text{sum}}$ and $\tilde{r}_{\text{diff}}$ is

$$\cos\Theta = \frac{\tilde{r}_{\text{sum}}^2 - 1}{2\tilde{r}_1\tilde{r}_2} - 1 = \frac{\tilde{r}_{\text{sum}}^2 + \tilde{r}_{\text{diff}}^2 - 2}{\tilde{r}_{\text{sum}}^2 - \tilde{r}_{\text{diff}}^2}. \tag{B.2}$$

Also, from the fundamental triangular inequality and inverse triangular inequality, the relation between $\tilde{r}_{\text{sum}}$ and $\tilde{r}_{\text{diff}}$ is

$$|\tilde{r}_{\text{diff}}| < 1 < \tilde{r}_{\text{sum}}.$$

When $\xi = 0$ or $\xi = 2$, the formula reduces to

$$0 < \cos\Theta = \frac{\tilde{r}_{\rm sum}^2 - 1}{\tilde{r}_{\rm sum}^2 + 1} < 1. \tag{B.3}$$

since $\tilde{r}_{\rm sum}^2 = \tilde{r}_{\rm diff}^{-2}$. Thus, $\cos\Theta(\xi = 0, 2)$ are always greater than zero and less than unity.

Substituting the definitions of $\tilde{r}_1(\eta)$ and $\tilde{r}_2(\eta)$ to rewrite $\cos\Theta$ in terms of η, the formula becomes:

$$\cos\Theta = \begin{cases} \frac{[(\alpha_1-\alpha_2)\eta+\alpha_2]^2-1}{2\alpha_1\alpha_2\eta(1-\eta)} - 1, & 0 < \eta < 1 \\ \frac{[(\alpha_1+\alpha_2)\eta-\alpha_2]^2-1}{2\alpha_1\alpha_2\eta(\eta-1)} - 1, & \eta > 1 \text{ or } \eta < 0 \end{cases}, \tag{B.4}$$

and the derivative of $\cos\Theta$ can be determined in terms of η, too:

$$\frac{d\cos\Theta}{d\eta} = \begin{cases} \frac{(\alpha_1^2-1)\eta^2-(\alpha_2^2-1)(\eta-1)^2}{2\alpha_1\alpha_2\eta^2(1-\eta)^2}, & 0 < \eta < 1 \\ \frac{(\alpha_2^2-1)(\eta-1)^2-(\alpha_1^2-1)\eta^2}{2\alpha_1\alpha_2\eta^2(1-\eta)^2}, & \eta > 1 \text{ or } \eta < 0 \end{cases}. \tag{B.5}$$

The denominators of $d\cos\Theta/d\eta$ are always positive so the signs are determined by their numerators. The numerators are parabolae in η. If the parabolae never cross the η-axis in the intersection range of two conical waves, $\cos\Theta$ is monotonically increasing or decreasing with respect to η for sure. Otherwise, it is complicated to determine the range of $\cos\Theta$. $d\cos\Theta/d\eta$ cross η-axis at $\eta_{\rm c}^{\pm}$,

$$\eta_{\rm c}^{\pm} \equiv \begin{cases} \frac{(\alpha_2^2-1)\pm\sqrt{(\alpha_2^2-1)(\alpha_1^2-1)}}{\alpha_2^2-\alpha_1^2}, & \text{Case VI (A)} \\ \text{No solutions}, & \text{Case VI (B)} \\ \frac{(\alpha_2^2-1)\pm\sqrt{(1-\alpha_2^2)(1-\alpha_1^2)}}{\alpha_2^2-\alpha_1^2}, & \text{Case VI (C)} \end{cases},$$

and

$$\cos\Theta(\eta = \eta_{\rm c}^{\pm}) = \frac{\pm 1 + \sqrt{(\alpha_2^2-1)(\alpha_1^2-1)}}{\alpha_1\alpha_2}, \text{ Case VI (A)}. \tag{B.6}$$

The ranges of $\cos\Theta$ are summarized as follows.

For $\Psi = +1$, in region (A1):

$$\begin{cases} 1 < \eta_4 \le \eta \le \eta^+(\xi = 2), & 1 = \cos\Theta(\eta_4) \ge \cos\Theta \ge \cos\Theta(\eta_{\rm c}^+) > {\rm Sr} \\ \eta^+(\xi = 2) \le \eta \le \eta^+(\xi = 0), & \cos\Theta(\eta^+(\xi = 0)) \ge \cos\Theta \ge \cos\Theta(\eta^+(\xi = 2)) > {\rm Sr} \\ 1 < \eta^+(\xi = 0) \le \eta \le \eta_1, & 1 = \cos\Theta(\eta_1) \ge \cos\Theta \ge \cos\Theta(\eta^+(\xi = 0)) > {\rm Sr}, \end{cases} \tag{B.7}$$

since $\eta_4 < \eta_{\rm c}^+ < \eta^+(\xi = 2)$. In region (A2):

$$\begin{cases} 0 < \eta_2 \le \eta \le \eta^-(\xi = 0), & 1 = \cos\Theta(\eta_2) \ge \cos\Theta \ge \cos\Theta(\eta^-(\xi = 0)) > 0 \\ \eta^-(\xi = 0) \le \eta \le \eta^-(\xi = 2), & \cos\Theta \ge \cos\Theta(\eta_{\rm c}^-) > -{\rm Sr} \\ \eta^-(\xi = 2) \le \eta \le \eta_3 < 1, & 1 = \cos\Theta(\eta_3) \ge \cos\Theta \ge \cos\Theta(\eta^-(\xi = 2)) > 0, \end{cases} \tag{B.8}$$

since $\eta^-(\xi = 0) < \eta_{\rm c}^- < \eta^-(\xi = 2)$.

In region (B1) or (C1) if $\alpha_1^2 < 1 - \mathrm{Sr}^2$:

$$\begin{cases} 1 < \eta_3 \le \eta \le \eta^+(\xi = 0), & \cos\Theta(\eta^+(\xi = 0)) \ge \cos\Theta \ge \cos\Theta(\eta_3) = -1 \\ 1 < \eta^+(\xi = 0) \le \eta \le \eta_1, & 1 = \cos\Theta(\eta_1) \ge \cos\Theta \ge \cos\Theta(\eta^+(\xi = 0)) > 0. \end{cases} \tag{B.9}$$

In region (B1) or (C1) if $\alpha_1^2 \ge 1 - \mathrm{Sr}^2$:

$$\begin{cases} 1 < \eta_3 \le \eta \le \eta^-(\xi = 2), & \cos\Theta(\eta^-(\xi = 2)) \ge \cos\Theta \ge \cos\Theta(\eta_3) = -1 \\ \eta^-(\xi = 2) \le \eta \le \eta^+(\xi = 2), & \cos\Theta(\eta^+(\xi = 2)) \ge \cos\Theta \ge \cos\Theta(\eta^-(\xi = 2)) > 0 \\ \eta^+(\xi = 2) \le \eta \le \eta^+(\xi = 0), & \cos\Theta(\eta^+(\xi = 0)) \ge \cos\Theta \ge \cos\Theta(\eta^+(\xi = 2)) > 0 \\ 1 < \eta^+(\xi = 0) \le \eta \le \eta_1, & 1 = \cos\Theta(\eta_1) \ge \cos\Theta \ge \cos\Theta(\eta^+(\xi = 0)) > 0. \end{cases} \tag{B.10}$$

In region (B2):

$$\begin{cases} 0 < \eta_2 \le \eta \le \eta^-(\xi = 0), & 1 = \cos\Theta(\eta_2) \ge \cos\Theta \ge \cos\Theta(\eta^-(\xi = 0)) > 0 \\ \eta^-(\xi = 0) \le \eta \le \eta_4 < 1, & \cos\Theta(\eta^-(\xi = 0)) \ge \cos\Theta \ge \cos\Theta(\eta_4) = -1. \end{cases} \tag{B.11}$$

In region (C2):

$$\begin{cases} \eta_4 \le \eta \le \eta^-(\xi = 0) < 0, & 1 = \cos\Theta(\eta_4) \ge \cos\Theta \ge \cos\Theta(\eta^-(\xi = 0)) > 0 \\ \eta^-(\xi = 0) \le \eta \le \eta_2 < 0, & \cos\Theta(\eta^-(\xi = 0)) \ge \cos\Theta \ge \cos\Theta(\eta_2) = -1. \end{cases} \tag{B.12}$$

Since $0 < \eta_c^+ < 1$ and $\eta_c^- < \eta_4$, $\eta_c^\pm$ are not in region (C1) or (C2).
For $\Psi = -1$, in region (A1):

$$\begin{cases} \eta_1 \le \eta \le \eta^-(\xi = 2) < 0, & 1 = \cos\Theta(\eta_1) \ge \cos\Theta \ge \cos\Theta(\eta^-(\xi = 2)) \\ \eta^-(\xi = 2) \le \eta \le \eta^-(\xi = 0), & \cos\Theta(\eta^-(\xi = 2)) \ge \cos\Theta \ge \cos\Theta(\eta^-(\xi = 0)) \\ \eta^-(\xi = 0) \le \eta \le \eta_4 < 0, & 1 = \cos\Theta(\eta_4) \ge \cos\Theta \ge \cos\Theta(\eta_c^+), \end{cases} \tag{B.13}$$

since $\eta_4 > \eta_c^+ > \eta^-(\xi = 0)$. Also, $\cos\Theta > \mathrm{Sr}^{-1}$. In region (A2):

$$\begin{cases} 0 < \eta_2 \le \eta \le \eta^+(\xi = 0), & 1 = \cos\Theta(\eta_2) \ge \cos\Theta \ge \cos\Theta(\eta^+(\xi = 0)) > 0 \\ \eta^+(\xi = 0) \le \eta \le \eta^+(\xi = 2), & \cos\Theta \ge \cos\Theta(\eta_c^-) > -\mathrm{Sr}^{-1} \\ \eta^+(\xi = 2) \le \eta \le \eta_3 < 1, & 1 = \cos\Theta(\eta_3) \ge \cos\Theta \ge \cos\Theta(\eta^+(\xi = 2)) > 0, \end{cases} \tag{B.14}$$

since $\eta^+(\xi = 0) < \eta_c^- < \eta^+(\xi = 2)$.
In region (B1) or (C1) if $\alpha_1^2 < \mathrm{Sr}^2 - 1$:

$$\begin{cases} \eta_1 \le \eta \le \eta^-(\xi = 2) < 0, & 1 = \cos\Theta(\eta_1) \ge \cos\Theta \ge \cos\Theta(\eta^-(\xi = 2)) > 0 \\ \eta^-(\xi = 2) \le \eta \le \eta_2 < 0, & \cos\Theta(\eta^-(\xi = 2)) \ge \cos\Theta \ge \cos\Theta(\eta_2) = -1. \end{cases} \tag{B.15}$$

In region (B1) or (C1) if $\alpha_1^2 \ge \mathrm{Sr}^2 - 1$:

$$\begin{cases} \eta_1 \le \eta \le \eta^-(\xi = 2) < 0, & 1 = \cos\Theta(\eta_1) \ge \cos\Theta \ge \cos\Theta(\eta^-(\xi = 2)) > 0 \\ \eta^-(\xi = 2) \le \eta \le \eta^-(\xi = 0), & \cos\Theta(\eta^-(\xi = 2)) \ge \cos\Theta \ge \cos\Theta(\eta^-(\xi = 0)) > 0 \\ \eta^-(\xi = 0) \le \eta \le \eta^+(\xi = 0), & \cos\Theta(\eta^-(\xi = 0)) \ge \cos\Theta \ge \cos\Theta(\eta^+(\xi = 0)) > 0 \\ \eta^+(\xi = 0) \le \eta \le \eta_2 < 0, & \cos\Theta(\eta^+(\xi = 0)) \ge \cos\Theta \ge \cos\Theta(\eta_2) = -1. \end{cases} \tag{B.16}$$

In region (B2):

$$\begin{cases} 0 < \eta_4 \le \eta \le \eta^+(\xi = 2), & \cos\Theta(\eta^+(\xi = 2)) \ge \cos\Theta \ge \cos\Theta(\eta_4) = -1 \\ \eta^+(\xi = 2) \le \eta \le \eta_3 < 1, & 1 = \cos\Theta(\eta_3) \ge \cos\Theta \ge \cos\Theta(\eta^+(\xi = 2)) > 0. \end{cases} \tag{B.17}$$

In region (C2):

$$\begin{cases} 1 < \eta_3 \le \eta \le \eta^+(\xi = 2), & \cos\Theta(\eta^+(\xi = 2)) \ge \cos\Theta \ge \cos\Theta(\eta_3) = -1 \\ 1 < \eta^+(\xi = 2) \le \eta \le \eta_4, & 1 = \cos\Theta(\eta_4) \ge \cos\Theta \ge \cos\Theta(\eta^+(\xi = 2)) > 0. \end{cases} \tag{B.18}$$

Since $0 < \eta_c^+ < 1$ and $\eta_c^- > \eta_4$, $\eta_c^\pm$ are not in region (C1) or (C2).

Appendix C

Determine the Relation Between $\cos\Theta(\eta=\eta_{\rm c}^{\pm})$ and $\cos\Theta^{\rm S,\pm}, \cos\Theta^{\rm D,\pm}$ in Case VI

In the region (A1), [Eq. (B.6)] can be rewritten as follows,

$$\begin{aligned}\cos\Theta(\eta_{\rm c}^{+}) &= {\rm Sr}\left\{\alpha_1^{-2}+\sqrt{\left({\rm Sr}^{-2}-\alpha_1^{-2}\right)\left(1-\alpha_1^{-2}\right)}\right\}\\ &= {\rm Sr}^{-1}\left\{\alpha_2^{-2}+\sqrt{\left({\rm Sr}^{2}-\alpha_2^{-2}\right)\left(1-\alpha_2^{-2}\right)}\right\}.\end{aligned}$$

In the case that $\Psi=+1$, $|\chi|>1/2$ and $\theta^{\rm D}<\theta_2<\theta_1$, recall

$$\cos\Theta^{\rm D,+}={\rm Sr}\left\{\frac{\tan^2\theta^{\rm D}}{\tan^2\theta_2}+\sqrt{\left({\rm Sr}^{-2}-\frac{\tan^2\theta^{\rm D}}{\tan^2\theta_2}\right)\left(1-\frac{\tan^2\theta^{\rm D}}{\tan^2\theta_2}\right)}\right\},$$

and in the case $\Psi=-1$, $\theta^{\rm S}<\theta_1<\theta_2$,

$$\cos\Theta^{\rm S,+}={\rm Sr}^{-1}\left\{\frac{\tan^2\theta^{\rm S}}{\tan^2\theta_1}+\sqrt{\left({\rm Sr}^{2}-\frac{\tan^2\theta^{\rm S}}{\tan^2\theta_1}\right)\left(1-\frac{\tan^2\theta^{\rm S}}{\tan^2\theta_1}\right)}\right\}.$$

Define utility functions $F(P)$ and $G(P)$ in the following ways,

$$\begin{aligned}F(P) &\equiv P+\sqrt{\left({\rm Sr}^{-2}-P\right)(1-P)}\ \text{for}\ {\rm Sr}<1, 0<P<1,\\ G(P) &\equiv P+\sqrt{\left({\rm Sr}^{2}-P\right)(1-P)}\ \text{for}\ {\rm Sr}>1, 0<P<1.\end{aligned}$$

Obviously, $\cos\Theta(\eta_{\rm c}^{+})$, $\cos\Theta^{\rm D,+}$ and $\cos\Theta^{\rm S,+}$ can be expressed in terms of $F(P)$ or $G(P)$:

$$\cos\Theta(\eta_{\rm c}^{+})={\rm Sr}\,F(P=\alpha_1^{-2})={\rm Sr}^{-1}\,G(P=\alpha_2^{-2}),$$

and

$$\begin{aligned}\cos\Theta^{\mathrm{D},+} &= \mathrm{Sr}\, F\left(P=\frac{\tan^2\theta^{\mathrm{D}}}{\tan^2\theta_2}\right),\\ \cos\Theta^{\mathrm{S},+} &= \mathrm{Sr}^{-1}\, G\left(P=\frac{\tan^2\theta^{\mathrm{S}}}{\tan^2\theta_1}\right).\end{aligned}$$

It can be shown that $dF(P)/dP < 0$ and $dG(P)/dP < 0$ if $0 < P < 1$. Putting every piece together, the relations between $\cos\Theta(\eta = \eta_{\mathrm{c}}^{+})$ and $\cos\Theta^{\mathrm{S},+}, \cos\Theta^{\mathrm{D},+}$ in region (A1) are

$$\text{if } \alpha_1^{-2} > \frac{\tan^2\theta^{\mathrm{D}}}{\tan^2\theta_2} \;\Rightarrow\; \cos\Theta(\eta_{\mathrm{c}}^{+}) < \cos\Theta^{\mathrm{D},+}, \tag{C.1a}$$

$$\text{if } \alpha_1^{-2} < \frac{\tan^2\theta^{\mathrm{D}}}{\tan^2\theta_2} \;\Rightarrow\; \cos\Theta(\eta_{\mathrm{c}}^{+}) > \cos\Theta^{\mathrm{D},+}, \tag{C.1b}$$

$$\text{if } \alpha_2^{-2} > \frac{\tan^2\theta^{\mathrm{S}}}{\tan^2\theta_1} \;\Rightarrow\; \cos\Theta(\eta_{\mathrm{c}}^{+}) < \cos\Theta^{\mathrm{S},+}, \tag{C.1c}$$

$$\text{if } \alpha_2^{-2} < \frac{\tan^2\theta^{\mathrm{S}}}{\tan^2\theta_1} \;\Rightarrow\; \cos\Theta(\eta_{\mathrm{c}}^{+}) > \cos\Theta^{\mathrm{S},+}. \tag{C.1d}$$

Similarly, in the region (A2):

$$\text{if } \alpha_1^{-2} > \frac{\tan^2\theta^{\mathrm{D}}}{\tan^2\theta_2} \;\Rightarrow\; \cos\Theta^{\mathrm{D},-} < \cos\Theta(\eta_{\mathrm{c}}^{-}) < \cos\Theta^{\mathrm{D},+}, \tag{C.2a}$$

$$\text{if } \alpha_1^{-2} < \frac{\tan^2\theta^{\mathrm{D}}}{\tan^2\theta_2} \;\Rightarrow\; \cos\Theta^{\mathrm{D},-} < \cos\Theta^{\mathrm{D},+} < \cos\Theta(\eta_{\mathrm{c}}^{-}), \tag{C.2b}$$

$$\text{if } \alpha_2^{-2} > \frac{\tan^2\theta^{\mathrm{S}}}{\tan^2\theta_1} \;\Rightarrow\; \cos\Theta^{\mathrm{S},-} < \cos\Theta(\eta_{\mathrm{c}}^{-}) < \cos\Theta^{\mathrm{S},+}, \tag{C.2c}$$

$$\text{if } \alpha_2^{-2} < \frac{\tan^2\theta^{\mathrm{S}}}{\tan^2\theta_1} \;\Rightarrow\; \cos\Theta^{\mathrm{S},-} < \cos\Theta^{\mathrm{S},+} < \cos\Theta(\eta_{\mathrm{c}}^{-}). \tag{C.2d}$$